Development of a Microbial Fuel Cell Cocatalyst with *Propionibacterium freudenreichii* ssp. *shermanii*

By Jessica Virginia Johnson

Thesis submitted to the Faculty of Graduate and Postdoctoral Studies In partial fulfillment of the requirements For the Degree of Master of Applied Science in Chemical Engineering

Department of Chemical and Biological Engineering
Faculty of Engineering University of Ottawa

Abstract

Addressing the low power generation of anodic biocatalysts is pertinent to the advancement of microbial fuel cell technology. While *Propionibacterium freudenreichii* ssp. *shermanii* has shown potential as a biocatalyst, its incomplete consumption of the anodic substrate is a persistent issue. This research aims to optimize substrate consumption to increase power generation using *Propionibacterium freudenreichii* ssp. *shermanii* as a biocatalyst.

The effect of coculturing *Geobacter sulfurreducens* with *Propionibacterium freudenreichii* ssp. *shermanii* was investigated. The cocatalyst and pure culture performance was tested in an air-cathode microbial fuel cell. *Geobacter sulfurreducens* produced the highest maximum power density among the experimental cases. Power density produced by *Propionibacterium freudenreichii* ssp. *shermanii* was improved in the air-cathode design compared to previous experiments performed in an H-type design. The novel cocatalyst was shown to produce electricity, however a full characterization to elucidate the contribution to power generation by each microbe would be desirable to investigate.

Resumé

Pour addresser les puissances faibles qui sont caractéristiques des piles à combustible microbienne, ce project met l'accent sur l'amélioration de la biocatalyseur anodique. *Propionibacterium freudenreichii* ssp. *shermanii* est prometteuse comme biocatalyseur, toutefois sa consommation incomplète de substrat glucidique rest un question à traiter. Cette recherche vise à optimiser la consommation deu substrat pour augmenter la production d'énergie en utilisant *Propionibacterium freudenreichii* ssp. *shermanii* comme biocatalyseur.

L'éffet de coculturer *Geobacter sulfurreducens* avec *Propionibacteria freudenreichii* ssp. *shermanii* a été étudiée. Le performance du cocatalyseur et des cultures pures a été testé dans un pile à combustible microbienne avec une cathode à air. *Geobacter sulfurreducens* a produit la plus haute densité de puissance des cas expérimentaux. La densité de puissance produit par *Propionibacterium freudenreichii* ssp. *shermanii a été* amélioré en utilisant la modèle de cathode à air comparé au expériences conduit dans le modèle de genre H. Le cocatalyseur inédit a été montrer pour produire de courant, cependant plus de caractérisation du contribution complet de chaque microbe serait souhaitable d'enquêter.

Statement of Contributions of Collaborators

I hereby declare that I am the sole author of this thesis. I conducted all of the experimental work, performed all of the data analysis and wrote all the chapters presented in this work. The air-cathode MFC design used in this work was principally created by Izcoatl Rafael Garduño Ibarra.

Dr. Kathlyn Kirkwood supervised this thesis project and provided continual guidance throughout. She also made editorial contributions to the written work presented.

Acknowledgments

I would first like to thank my supervisor Dr. Kathlyn Kirkwood for the opportunity to work on this interesting project. She allowed my research to take form as my own work, while dependably guiding and steering me in the right direction when needed.

I would also like to thank Izcoatl Rafael Garduño Ibarra for being my partner in the lab, willing to listen and work through roadblocks with me. Also, the technical staff for the Department of Chemical and Biological Engineering (Franco Ziroldo, James Macdermid, Gérard Nina and Louis Tremblay) were always available to help with laboratory resources and equipment.

Finally, I must express gratitude to my friends and family for providing me with unfailing support. I would like to give a special note of appreciation to Jen Lissemore and Jenn Barrow for their continuous encouragement and reassurance throughout this process. This accomplishment would not have been possible without them. Thank you.

Table of Contents

List of Tables

List of Figures

Nomenclature

μ	Electrochemical efficiency
A_{An}	Area of the anode (m^2)
E	Potential achieved by a fuel cell (V)
E^0	Standard cell potential (V)
E_{an}	Open circuit potential observed at anode
E_{cat}	Open circuit potential observed at cathode
F	Faraday's constant
G^0	Gibbs free energy at standard conditions ($Jmol^{-1}$)
g_1	Initial concentration of glucose (g/L)
g_2	Final concentration of glucose (g/L)
Hf°	Standard enthalpy of formation
I_{An}	Current (A)
I_{An}	Current density (mA/m^2)
n	Number of electrons transferred with complete oxidation of substrate
OCP	Open circuit potential
OD_{600}	Optical density observed at a wavelength of 600 nm
P	power
p_1	Initial concentration of the fermentation product of interest (g/L)
p_2	Final concentration of the fermentation product of interest (g/L)
P_{An}	Power
R	Gas constant
rcf	Relative centrifugal force

R_{ext}	External resistance
R_{int}	Internal resistance
$S_f°$	Standard entropy of formation (J/molK)
T	Temperature (K)
$Y_{p/g}$	Yield of product per gram of glucose fermented (g/g)
v	Volume of the anode

List of Abbreviations

CAC	Citric acid cycle
COD	Chemical oxygen demand
DAD	Diode array detector
DET	Direct electron transfer
DIET	Direct interspecies electron transfer
HPLC	High pressure liquid chromatograph
IET	Interspecies electron transfer
MET	Mediated electron transfer
MFC	Microbial fuel cell
PEM	Proton exchange membrane
PTFE	Polytetrafluoroethylene
RCM	Reinforced clostridial medium
RID	Refractive index detector
SMFC	Sediment microbial fuel cells

Metabolites

AQDS	Anthraquinone-2,6-disulfonate
PEP	Phosphenolpyruvate

Chapter 1 Research Background and Motivation

There is no simple solution to the climate change crisis. Global concerns regarding noxious emissions contributing to global warming as well as the impending depletion of finite energy resources have propelled research in the clean energy field. In contrast to conventional methods of generating electricity which involve the combustion of fuels and proliferation of greenhouse gas emissions, fuel cells are a clean technology that converts the chemical energy of hydrocarbon fuels directly into electrical energy thereby avoiding the combustion step (Edwards et al. 2008). Microbial fuel cells (MFCs) take this technology one step further by employing bacteria as the catalyst to generate electricity through oxidation of organic waste or renewable biomass. MFCs have the potential to use various organic substrates as fuel, which has ignited research in widespread applications of the technology (Pant et al. 2010).

While the world's most affluent countries have benefitted immensely from emitting greenhouse gases to drive economic growth, the effects of climate change are experienced globally with highly variable impacts from country to country (Althor, et al. 2016). As a result, the burden of global warming may disproportionately fall on countries that are more vulnerable to the effects of global warming while having scarcely contributed to its origin (Althor, et al. 2016). I have a strong desire to help address some of these imbalances with the ultimate goal of working to develop innovative solutions to address the issue of global climate change.

This project aims to advance MFC research and tackles the complex issue of climate change by identifying an area of waste that can be used for energy production. While MFCs are not likely to completely reform how electricity is produced, they are a step towards reforming how industries treat waste by recognizing the potential to recover energy from it. I believe that MFCs are one of many incremental advancements in the clean technology field that collectively, will result in a diminished dependence on non-renewable fuels and ultimately steer the world in a sustainable direction.

1.1 Objectives and thesis overview

The main objective of this thesis is to improve the bioconversion of a carbohydrate substrate (glucose) to electrical current in the MFC environment for the promising novel biocatalyst *Propionibacteria freudenreichii* ssp. *shermanii*. Detailed objectives to achieve this ultimate goal are listed below and are described in detail in sections 1.1.1-5:

- Medium optimization (Chapter 4)
- Cocatalyst development (Chapter 5)
- Evaluation of pure culture MFC performance (Chapter 6)
- Evaluation of cocatalyst MFC performance (Chapter 7)
- Experimental design optimization (Chapter 8)

1.1.1 Medium optimization (Chapter 4)

Results from batch fermentations of *P. shermanii* grown using glycerol versus glucose are presented to illustrate each substrate's effect on acetate and propionate yield. The fermentation environment of *P. shermanii* was then improved by developing a defined medium tailored to its growth requirements.

Chapter 4 outlines the development and analysis of culturing *P. shermanii* in the previously used M9 media (Loginova, Manuilova, and Tolstikov 1974) in contrast with a medium used in *P. shermanii* experiments (Zhang and Yang 2009). Specific experimental objectives included:

1. Illustrate effect of carbon source (glucose versus glycerol) on *P. shermanii* fermentation behaviour
2. Change the substrate from glycerol to glucose to alleviate consumption issues that were previously encountered and to encourage total consumption of the substrate throughout the duration of the experiments.
3. Formulate a new medium for *P. shermanii* growth requirements.

Batch fermentation experiments were performed anaerobically comparing glucose and glycerol as carbon sources in otherwise identical medium formulations. Carbon source consumption and conversion products were monitored using High Pressure Liquid Chromatography (HPLC). Based on these results it was determined that glucose would be used in further experiments to ensure carbon source consumption and encourage consistency within triplicates.

Batch fermentation experiments were then performed anaerobically using glucose as the sole carbon source for two different media. Glucose consumption was monitored using HPLC, and bacterial growth was observed using spectrophotometry. Based on these results, it was determined that the peptone media does not provide a significant advantage for increased glucose consumption for *P. shermanii* and alternative optimization methods were examined in Chapter 5.

1.1.2 Cocatalyst development (Chapter 5)

A pure bacterial strain was selected to coculture with *P. shermanii*. Chapter 5 outlines the selection strategy, which was primarily based on the strain's ability to consume organic acids which accumulate in the MFC environment upon consumption of glucose by *P. shermanii*. Additional exoelectrogenic activity of the strain through consumption of *P. shermanii's* byproducts was also considered during selection. *Geobacter metallireducens* and *Geobacter sulfurreducens* were investigated as potential cocatalysts. Specific experimental objectives included:

1. Design a medium to support growth of cocatalyst
2. Develop a bacterial quantification method for coculture
3. Establish the acetate threshold needed for *G. sulfurreducens* growth from *P. shermanii* by-products

Batch fermentations of the new cocatalyst medium were performed and were shown to support the coculture of *Geobacter* with *Propionibacteria*. The coculture fermentation process was analyzed for cell growth using a gram stain and microscopy protocol.

1.1.3 Pure culture MFC performance (Chapter 6)

A newly designed air-cathode MFC was tested with the new MFC medium outlined in Chapter 5. Chapter 6 served to compare the electrogenic activity of the pure cultures. Specific experimental objectives included:

1. Test the design of the single chamber, air-cathode MFC using pure biocatalysts.
2. Compare biocatalyst performance in mediatorless air-cathode MFC
    a. *P. shermanii* with glucose
    b. *G. sulfurreducens* with glucose

c. *G. sulfurreducens* with acetate

Voltage and power generation were used as performance indicators. Polarization and power density curves were created and compared.

1.1.4 Coculture MFC performance (Chapter 7)

The cocatalyst performance in the air cathode MFC design was tested. Specific experimental objectives of Chapter 7 included:

1. Test viability of cocatalyst performance in mediatorless air-cathode MFC
2. Macroscopically confirm coculture viability in MFC and fermentation environment

Electrogenic activity of the cocatalyst was confirmed using voltage and power generation performance indicators. Polarization and power density curves were created and compared. Simultaneous fermentation experiments provided further evidence of delayed but viable coculture growth.

1.1.5 Experimental design optimization (Chapter 8)

The necessary tools needed to further characterize the coculture and fully optimize the fermentative interactions for increased substrate consumption and power generation are discussed in Chapter 8. Plans for future experimentation are also outlined

1.2 Hypotheses

Carbohydrate conversion to electricity is expected to increase with the addition of a secondary cocatalyst with *P. shermanii*. The pure biocatalyst *P. shermanii* rapidly acidifies the anode environment due to the production of organic acids. By employing *G. sulfurreducens* as a secondary exoelectrogenic cocatalyst, its ability to consume one of the organic acids produced by *P. shermanii* (acetic acid) should result in more neutral growth conditions in the MFC environment.

In addition to pH control, *G. sulfurreducens* is expected to sustain growth and contribute to power generation once *P. shermanii* produces sufficient acetate concentrations from glucose consumption. The coculture is expected to result in prolonged power generation due to continued anabolism of the original carbohydrate substrate.

Chapter 2 Literature Review

2.1 MFC background

2.1.1 Overview

In contrast to conventional methods of generating electricity, which involve the combustion of fuels and proliferation of greenhouse gas emissions, fuel cells convert chemical energy of hydrocarbon fuels directly into electrical energy thereby avoiding the combustion step. MFCs take this technology one step further by employing microorganisms as a biocatalyst to generate electricity through oxidation of organic waste or renewable biomass (Javed et al. 2018). Traditional fuel cells may always produce higher power densities than MFCs, however the applications pertaining to each technology are unique (Hu et al. 2018). Traditional fuel cells are more functional in large scale applications, most notably in vehicular transportation (Ehsani et al. 2018). Alternatively, MFCs exhibit efficacy in small scale operations such as remote biosensors and in their ability to facilitate energy recovery from waste (Li and Sheng 2011).

Similar to conventional fuel cells, MFCs are comprised of four essential components; an anode, cathode, electrolyte and catalyst. In MFCs, the anode chamber contains the microbial catalyst which is separated from the cathode by the electrolyte - a proton exchange membrane (PEM) (Logan et al. 2006). It is imperative that the anode is kept anaerobic to ensure that the biocatalyst reaction takes place at the electrode to facilitate the transfer of electrons and diffusion of protons through the PEM (Logan 2008). As electrons are created by the biocatalyst, they flow along an external circuit, where electrical current is

captured or measured. The circuit is completed at the oxygenated cathode once protons have diffused through the PEM.

MFCs can be either single or double-chambered systems. In a double-chambered MFC, the cathode is filled with water and is aerated using dissolved oxygen as the electron acceptor (Logan 2008). The energy intensive process of aeration of this configuration is considered disadvantageous due to the decrease in overall efficiency of the system (Liu and Logan 2004). Ferricyanide can also be used as an electron acceptor in double-chambered systems which has shown to significantly improve power outputs (Oh et al. 2004). However, oxygen remains the more sustainable option due to its ambient availability (Logan et al. 2006).

Single chambered systems, illustrated by the schematic in Figure 2-1, are assembled with one side of the cathode open to the air with the other attached to the PEM. This allows for oxygen from the air to react directly with the electrode therefore eliminating the liquid buffer and the energy requirement of aeration. Single chamber designs have also been constructed without a PEM as an attempt to increase the economic viability of the system. While the PEM is not essential for power production, its absence leads to a loss of substrate due to oxygen diffusion into the anode chamber resulting in aerobic oxidation by the biocatalyst, which in turn decreased power generation (Liu and Logan 2004). The scale up of MFCs which has yet to be solved, is essential to support the practical applications of MFCs. The stability, cost and manufacturing process of the cathode becomes a greater issue as the size of an air-cathode MFC increases (Dong et al. 2012). Progress is being made to lessen the labour required to manufacture air-cathodes and use less expensive materials without compromising the electrochemical efficiency of the design (Dong et al. 2012).

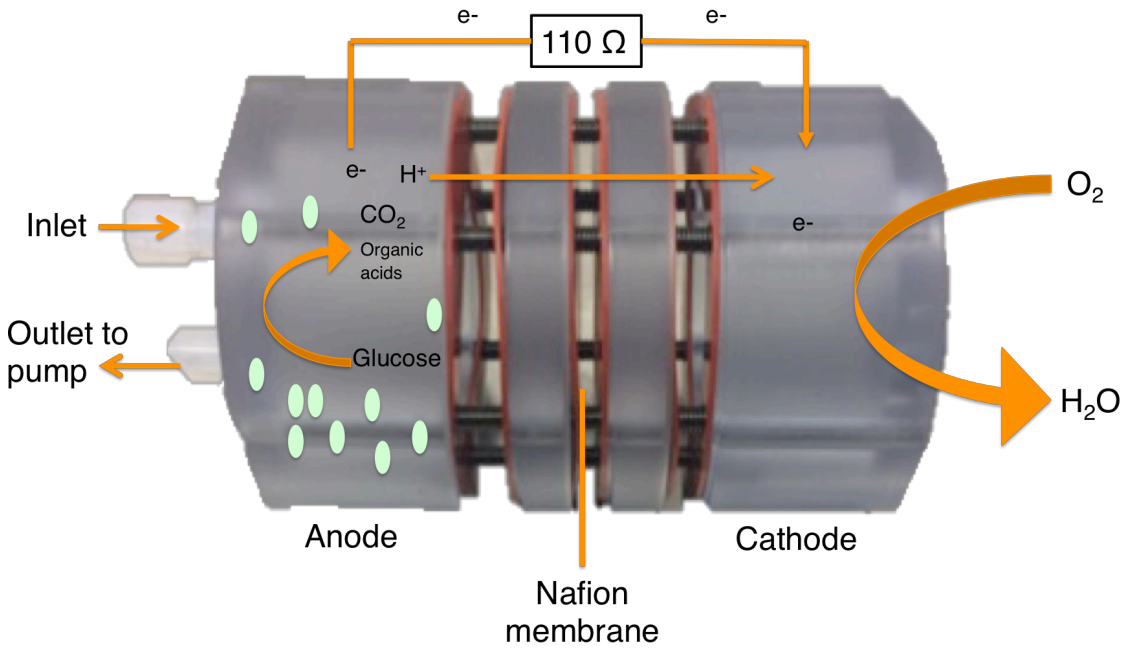

Figure 2-1 General MFC configuration showing the pathway of electrons and protons. Electrons generated in the anode are transported externally to the cathode while protons pass through the Nafion membrane. The oxygen at the air-cathode combines with protons and electrons to form water.

The materials selected for an MFC design play a critical role in the power generated from the system. The anode must be conductive, non-toxic to the biocatalyst and noncorrosive in the fermentation broth. Carbon is the most widely used material for anodes as it is inexpensive and can be manufactured in many different forms with rigid or flexible structures, including plates, rods, paper and felt (Logan et al. 2006). Many studies have achieved an increase in anode performance through chemical enhancements to reduce the resistance of charge transfer or through direct oxidation of microbial metabolites. The conductive polymer polyaniline is one example of an anode enhancing material that can be inexpensively deposited on carbon electrodes to improve power generation (Mehdinia et al. 2013). Optimization of the surface area available for

the biocatalyst reaction is also an important consideration when choosing the anode material (Logan et al. 2006).

Although materials that are used for the anode may also be used for the cathode, enhancing the cathode's catalytic activity can greatly improve the kinetics of the reduction of oxygen reaction taking place. While it is expensive and relatively unstable over time, platinum is commonly added to carbon-based cathodes to increase the rate of oxygen reduction (Logan 2008). More recently, cathode enhancement using metal-nitrogen-carbon catalysts involving transition metals associated with nitrogen-rich organic molecules have shown promise as an inexpensive design with catalytic activity comparable to Pt-based cathodes (Santoro et al. 2015).

MFCs that require separation of the anode and cathode most commonly use Nafion as the cation exchange membrane however more cost-effective and readily available materials such as j-cloth, nylon fibers and biodegradable shopping bags are being investigated (Santoro et al. 2017).

2.1.2 Biocatalysts

Many different pure and mixed cultures of microorganisms have been considered for use in MFCs as biocatalysts. Biocatalyst selection and optimization is an important consideration in MFC design since the metabolic activity of the biocatalyst governs the electricity generation. To produce a current, electrons must be transferred from inside the microorganism to the anode surface. Biocatalysts that do not have an inherent mechanism to transport electrons extracellularly can employ artificial chemical mediators such as 9,10-

anthra-quinone-2,6-disulfonic acid disodium salt (AQDS), resazurin, methylene blue, and humic acids to shuttle electrons from the bacteria to the anode (Sund et al. 2007). However, mediators can be expensive additives, may be toxic to microbes and tend to limit current generation based on the rate of mass transport of the selected mediator (Sund et al. 2007).

Electrochemically active microorganisms (exoelectrogens) are capable of transferring electrons that are released during degradation of the substrate to the anode without the addition of exogenous mediators (Zhou et al. 2017). The method by which electrons are transferred to the anode varies among microbes and may be direct or indirect. Direct contact with the anode surface can be made via c-type cytochromes or by conductive pili (Kumar et al. 2016). Indirect electron transfer occurs via electron shuttles secreted by the organism itself such as flavins as with *Shewanella oneidensis* (Kotloski and Gralnick 2013). In the anaerobic anode environment it can actually be advantageous for obligate anaerobes to donate their electrons to the anode as they are able to indirectly use oxygen while remaining in an anoxic environment (Sund et al. 2007).

2.1.3 Applications

Practical applications of MFCs require the use of economical materials and process operation requirements while achieving high power outputs. The optimization of MFC technology is still in developmental stages and has yet to be readily employed throughout the industrial market, however the possibilities are abundant.

Electricity generation is the primary motivation of MFCs, but power densities are often insufficient for practical energy supply. Despite this shortcoming, MFC technology has a unique advantage of recovering energy from the waste and can certainly be added to more robust technologies to increase output.

Common biological wastewater treatment processes such as the activated sludge process consume large amounts of energy therefore MFCs have been studied as a means of sustainable wastewater treatment. It is possible to lower the chemical oxygen demand (COD) of wastewater while simultaneously using it as a fuel to produce electricity in MFCs (Zhang et al. 2015). In 2004, Liu et al. demonstrated that domestic wastewater from a primary clarifier effluent could be used to generate electricity in a microbial fuel cell using only the mixed microbial culture present in the wastewater. Since then, studies have been done to characterize factors that affect microbial fuel cell performance using various wastewater sources. A sample of these studies and their respective results are summarized in Table 2-1.

Table 2-1 Lab scale MFC studies with different wastewater feedstocks.

Substrate	MFC Type	Power Density	COD removal	Reference
		Fed-batch Operation		
Domestic Wastewater	Single-chamber	334 mW/ m^2	>88%	(Ahn and Logan 2010)
Brewery Wastewater	Single chamber	205 mW/m^2	87%	(Feng et al. 2008)
Paper plant Wastewater	Single chamber	144 mW/m^2	29%	(Huang and Logan 2008)
		Continuous Operation		
Domestic Wastewater	Two single chamber MFCs in series,	422 mW/m^2	25.8%	(Ahn and Logan 2010)
Dairy Wastewater	Two chamber	621 mW/m^2	90.46%	(Mansoorian et al. 2016)

In addition to wastewater, energy production using industrial waste co-products is another practical application for MFCs. The biodiesel manufacturing process produces crude glycerol as a co-product, which is considered to be a waste stream due to the surplus that is produced and the high cost of purification needed to bring the raw material to the refined glycerol market (Yazdani and Gonzalez 2007). Direct oxidation of crude glycerol using an MFC coupled to the biodiesel process could increase the economic viability of biodiesel industrialization through energy cost recovery while also making use of the waste product (Sivell 2014).

The degradation of hydrocarbon compounds at the anode of an MFC has motivated research into using the technology for simultaneous electricity generation and bioremediation. Sediment microbial fuel cells (SMFCs) can be

used for this purpose and they typically consist of an anode buried in sediment with the cathode in an overlaying, oxidized water layer. For example, (Sherafatmand and Ng 2015) demonstrated SMFC's ability to remove polycyclic hydrocarbons from contaminated soil while generating consistent power of 3.63 mW/m^2 under anaerobic conditions. The distinctive low but consistent power generation of SMFCs has lead to their use as practical alternatives to batteries which can be placed in remote locations such as marine environments without the need for maintenance. Preliminary studies also show the potential to use flexible and biocompatible MFCs to power implanted medical devices which can be fuelled by microbes found in the body (Dong et al. 2013).

Additionally, due to the fact that the ambient environment at the anode within an MFC has an effect on the proliferation and metabolism of microorganisms, this elicits an effect on the observed power generation. The presence of organic substrates, toxic substances, pH level and temperature are examples of environmental conditions that affect power generation within an MFC allowing them to be calibrated to work as sensitive, self-sustaining biosensors for various substances (Yang et al. 2015). For example, MFC performance will be inhibited by the presence of toxins as they negatively affect electrogenic activity of the biocatalyst (Yang et al. 2015). A decline in current output can be standardized to yield quantitative results about the amount of toxic substance present in the MFC feed (Yang et al. 2015).

2.1.4 Performance measures

Evaluating the performance of different MFC designs is necessary to optimize this technology. With energy production in mind, power density is an important parameter to measure and compare, while electrochemical efficiency, coulombic

efficiency and polarization curves can provide a more in depth understanding of the successes and losses associated with each design.

The potential (E) is a standard measurement in fuel cells and is the product of the current (I) and external resistance (R_{ex}) connected to the circuit.

$$E = IR_{ex} \qquad \textbf{Equation 1}$$

The overall cell potential is defined by the potential difference between the anode and the cathode and can be determined with the fuel cell operating in open circuit.

The maximum potential that can be achieved by a fuel cell is governed by thermodynamics and based in the free energy change in the two half reactions occurring at the anode and cathode. The standard cell potential can be calculated using Equation 2 where ΔG is the Gibbs free energy under standard conditions (defined as 298.15 K, 1 bar pressure), n is the number of electrons per reaction mol and F is Faraday's constant (Logan 2008).

$$E^0 = -\frac{\Delta G^0}{nF} \qquad \textbf{Equation 2}$$

The upper limit of cell potentials for cells operating at non-standard conditions can be calculated by way of the Nernst equation (Equation 3). The symbol E represents the theoretical cell potential, R represents the universal gas constant and T represents the temperature in Kelvin.

$$E = E^0 - \frac{RT}{nF} \ln \left[\frac{products^p}{reactants^r}\right] \quad \textbf{Equation 3}$$

The equilibrium reduction potential associated with different half-reactions is accounted for in the final quotient of Equation 3. Here, the activity of the products and reactants raised to the number of electrons that are associated with each reaction is included. While this equation provides a valuable estimate, the thermodynamics of the half-reactions occurring in MFCs are much more complex than in standard fuel cells due to fluctuating biochemical processes at play in the anode (Zielke, n.d.).

The open circuit potential (OCP) represents the maximum experimental potential achieved by the cell at zero current and infinite resistance. The OCP should reflect the theoretically calculated maximum potential however, losses inherent to the MFC design and its operation result in a lower experimental value. Electrochemical efficiency represents this difference and is calculated from the OCP divided by the standard cell potential (Equation 4).

$$\mu = \frac{OCP}{E^0} \quad \textbf{Equation 4}$$

2.1.5 Polarization and power curves

To visualize the voltage as a function of current density, polarization curves are employed as a tool to analyze and characterize MFC operation. The energy losses can be identified in distinct areas of a polarization curve (Figure 2-2). The losses are generally dependant on current flow in the MFC and can be characterized into three categories spanning a range of operational currents. Activation losses

(Figure 2-2A) are the first class of losses, occurring at low currents and are incurred based on the activation energy required for an oxidation/reduction reaction to take place at the anode (Logan et al. 2006). In MFCs these losses are associated with the transfer of electrons from the biocatalyst to the electrode surface. Secondly, ohmic losses (Figure 2-2B) occur in the mid range of operational currents and are due to resistance to the flow of electrons and ions within the MFC (Logan et al. 2006). The materials used as well as the organization of the electrodes, interconnections and proton exchange membrane of the MFC govern these losses (Logan et al. 2006). Finally, mass transfer losses (Figure 2-2C) dominate at high currents due to the limited mass transfer of chemical species to the electrode surface. These losses can be further defined as the limited diffusion of oxidized species from the anode or reduced species towards the anode and vice versa at the cathode (Logan et al. 2006).

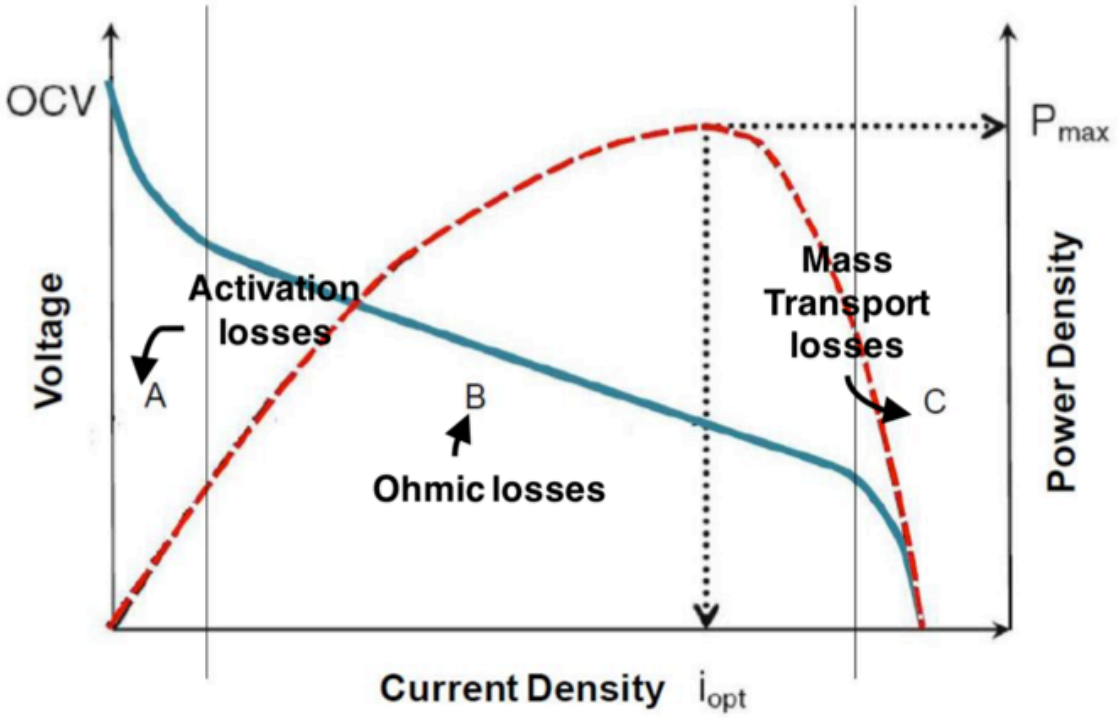

Figure 2-2 Polarization and power density curves with associated operational losses. Figure from Sivell 2014, modified from Logan, 2008.

A power curve (also shown in Figure 2-2) can then be calculated from the polarization curve to describe power density as a function of current density. Equation 5 can be used to calculate power, which defines the amount of electrical energy produced by the fuel cell, where I represents current.

$$P = IE_{MFC}$$ **Equation 5**

To allow for easy comparison of energy output between different designs, Equation 6 uses the surface area of the anode (A_{An}) to normalize power generation to the area available for microbial growth to determine power density (P_{An}).

$$P_{An} = \frac{IE}{A_{An}}$$ **Equation 6**

Using the calculations in this section to evaluate MFC designs, modifications geared towards diminishing losses and optimizing certain parameters are possible.

2.2 *Propionibacteria freudenreichii* ssp. *shermanii* as a biocatalyst

Propionibacteria are gram positive, non-motile, non-pathogenic bacteria commonly found in milk and dairy products. Previous work done by (Reiche et al. 2015) demonstrated the electrogenic activity of both *P. freudenreichii* ssp. *freudenreichii* and ssp. *shermanii*. Within this work, glycerol was used as a substrate in a double chamber MFC with *P. shermanii* achieving the highest power density of 31 mW/m^2 and a maximum OCV of 500 mV. Only 50% of glycerol was consumed during these trials suggesting that there is opportunity to enhance the glycerol conversion to achieve more power generation through medium optimization or by ensuring that the pre-culture of *P. shermanii* is sufficiently active.

Subsequent work by Sivell 2014 further investigated the metabolic activity of P. *shermanii* in an MFC and fermentation environment using pure analytical glycerol, analytical glycerol supplemented with NaCl and KCl and crude glycerol with various salt concentrations as experimental substrates. In the MFC environment, the most significant results were achieved using analytical glycerol with the addition of NaCl to a final concentration of 1.25 g/L. In this trial, approximately 6 g/L of 10 g/L glycerol was consumed after 225 h of operation. Trials with pure analytical glycerol, crude glycerol and glycerol supplemented with KCl did not produce significant results due to lack of substrate

consumption and negligible power generation. Furthermore, these results were uncharacteristic of what was observed in previous studies by Reiche et al. in 2015 suggesting that further optimization of the P. *shermanii* could be pursued.

In addition to being an exoelectrogen, *P. shermanii* produces propionic acid (propionate in solution) as a fermentation product. Propionate is used commercially as a preservative in foods and its biosynthesis is of interest as a sustainable alternative to the current standard of synthesizing propionic acid through petrochemical processes (Gonzalez-Garcia et al. 2017). This value-added co-product could potentially increase the economic feasibility of using *P. shermanii* as a biocatalyst. Considering both glucose, glycerol and a mixture of both substrates, it was found that glycerol alone produced a higher propionate yield than glucose alone, however the mixture of two produced the highest yield and selectivity of propionate among the three fermentation conditions (Wang and Yang 2013). Acetate and succinate are also produced as by-products in the fermentation of both glucose and glycerol (Wang and Yang 2013).

2.2.1 Growth limitations

pH levels of growth medium greatly affects the production of end products, specifically propionate which is increased at lower pH levels due to the formation of non-growth associated propionate (Piveteau 1999). This suggests an inherent change in metabolic activity of *P. shermanii* based on the pH of the growth medium. In general the accumulation of organic acids in microbial fermentations, inhibits the proliferation of microbial growth as the acidity in the growth medium becomes toxic to microbes at a certain level. Furthermore, in *Propionibacteria* it has been shown that propionic acid is an end product inhibitor to both specific growth and further production of the product (Rehberger 1996).

This inhibition caused by the accumulation of acids therefore elicits a negative effect on current generation in MFCs due to the decrease in metabolic rate.

2.2.2 Anaerobic fermentation of glucose by *P. shermanii*

The pathway by which P. shermanii is believed to ferment glucose in shown in Figure 2-3.

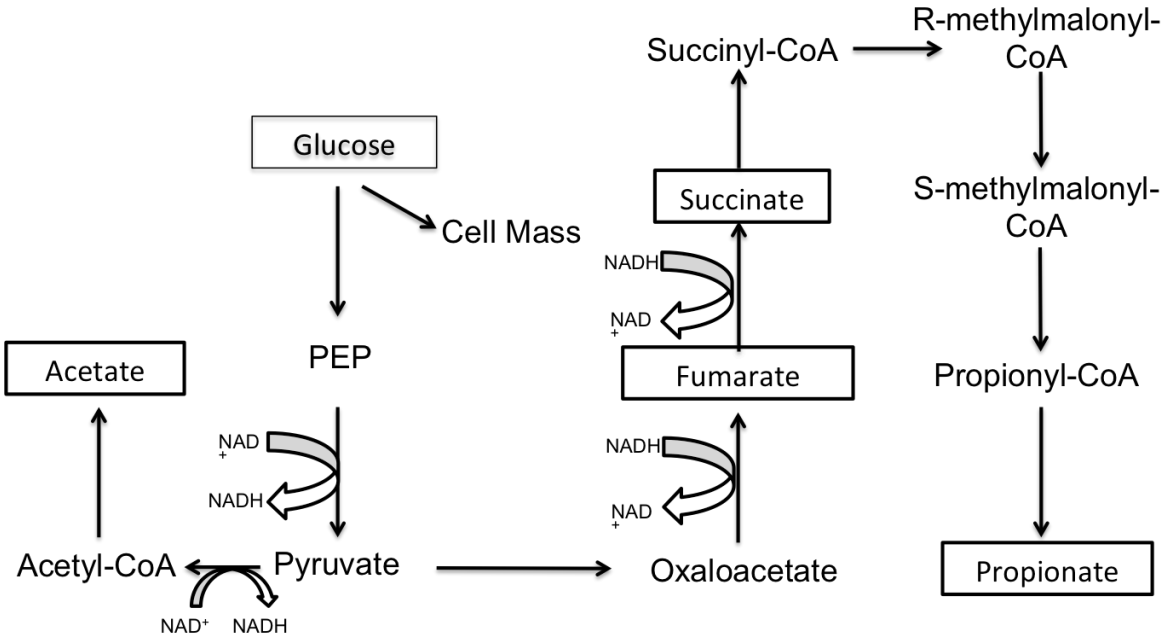

Figure 2-3 Anaerobic fermentation of glucose by *P. shermanii*. Adapted from (Piveteau 1999).

While reactions are reversible, they are directed towards the formation of propionate and acetate. Beginning with glucose, glycolysis generates pyruvate by way of phosphenolpyruvate (PEP). Propionate is the main product from the reduction of pyruvate by *P. shermanii* and is produced via the Wood-Werkman cycle (Thierry et al. 2011). The formation of oxaloacetate is followed by two NADH consuming steps to form fumarate and subsequently succinate. Succinate is then converted to propionate via methylmalonyl-CoA intermediates. In order to maintain redox potential, pyruvate is also oxidized to form acetate and CO_2 via the citric acid cycle (Thierry et al. 2011).

2.3 *Geobacter* as a biocatalyst

Microbes from the *Geobacteraceae* are typically found in subsurface environments such as aquatic sediments (Lovley et al. 2011). Their ability to couple the oxidation of organic substrates with the oxidation of metal oxides commonly found in soils (eg. Fe(III) and Mn(IV) oxides) and in contaminated soils (eg. uranium related contaminants) illustrate their biogeological significance especially in connection with bioremediation efforts (Akob et al. 2008). They are particularly renowned for their ability to make direct contact with external electron acceptors using highly conductive pili, rendering them ideal for employment in MFC applications (D. R. Bond and Lovley 2003). In fact, among the consortium of bacteria that exist in subsurface anaerobic sediments, microbes from the *Geobacteraceae* family will naturally colonize the surface of an energy harvesting anode when placed in the natural environment (Bond 2002). *Geobacter*'s affinity to couple the oxidation of organic matter with the reduction of stationary surfaces can therefore be exploited in an MFC environment.

2.3.1 Electron transfer mechanisms and biofilm formation

Bond and Lovely 2003 confirmed that *G. sulfurreducens* can fully oxidize electron donors in an MFC setting by attaching to the electrode without the addition of electron mediators. In MFCs, electrodes act as the insoluble extracellular electron acceptor which ignites a different mechanism within the bacteria than that seen in nature where mobile insoluble electron acceptors such as Fe (III) oxide are present (Lovley et al. 2011). The stationary nature of the electrode allows for the growth of multilayered microbe biofilms (>50 μm) that attach to the electrode

surface and remain viable to oxidize the substrate (Snider et al. 2012). This allows for a continuous process to be developed as stationary bacteria can be maintained by replenishing the feed substrate. In contrast, these biofilms do not form when *Geobacter* is grown in with Fe (III) oxide as the acceptor as Fe (III) is depleted as it reduced by the bacteria.

Although there are a variety of microorganisms that have filaments referred to as nanowires (eg. *Shewanella oneidensis*), the pili characteristic of *G. sulfurreducens* and *G. metallireducens* are the only filaments that are essential for their extracellular electron transport and conduction within biofilms (Malvankar and Lovley 2012). The direct electron transfer (DET) mechanism performed by nanowires has been well studied due to *Geobacter* having the most conductive pili of any known bacteria. The pili facilitate the extracellular electron transfer without mediation by cytochromes and are conductive across their diameter, which allows for biological electron transfer to be carried out over a distance (Reguera et al. 2005). PilA monomers join together to form these type IV pili, which are mediated by nanowire associated c-type cytochromes to perform the DET (Malvankar and Lovley 2012, Alves et al. 2016). The precise electron transfer mechanism role carried out by the nanowire chromosome is not fully understood however details regarding the thermodynamic and kinetic properties of the protein have recently been revealed (Alves et al. 2016). In an effort to harness the unique metallic-like conductivity of type IV pili, they have even been genetically expressed in other species to successfully improve conductivity (Tan et al. 2017).

Mediated electron transfer (MET) mechanisms are also present and engaged in *Geobacter*. In MET, the mediator acts as a reversible terminal electron acceptor that transfers electrons from the bacterial cell to its final destination

(Schröder 2007). *G. sulfurreducens* also secretes riboflavin as a natural mediator that interacts as a co-factor bound to outer membrane c-type cytochromes and consequently plays a key role in MET mechanism (Okamoto et al. 2014).

In the MFC environment, *Geobacter* cells adhere to the anode surface and multiply into a persistent multilayer conductive biofilm in which the monomer PilA plays a key role in this adhesive ability (Malvankar et al. 2014). While monolayer biofilms that form on electrodes allow for the majority of cells to be in close proximity to the electrode surface and to contribute to current generation, multilayer biofilms require the passage of charge throughout the biofilm to preserve conductivity. This is achieved through long-range electron transfer enabled by charge propagation along the pili in *Geobacter* (Kumar et al. 2016). Electricity production through long-range electron transfer has been accepted as the most efficient method for electron transfer in MFCs, particularly with *Geobacter* where the rate of transfer of electrons to the anode is comparable to the rate of respiration of soluble oxidants (Bond et al. 2012). The biofilm formed by *G. sulfurreducens* has been shown to be at its highest electrochemical activity when it reaches a thickness of 20 μm (Sun et al. 2016).

2.3.2 *Geobacter sulfurreducens* and *Geobacter metallireducens* in MFCs

G. sulfurreducens and *G. metallireducens* are two well-characterized gram-negative species of *Geobacter* that both produce the aforementioned electrochemically active pili called nanowires. They also share several metabolic abilities however G. *metallireducens* is capable of oxidizing a much wider range of substrates than *G. sulfurreducens* as seen in Table 2-2.

Table 2-2 Natural environment and growth requirements for *G. sulfurreducens* and *G. metallireducens* (Lovley et al. 2011;Trinh et al. 2009; Speers and Reguera 2012).

Geobacter species	***sulfurreducens***	***metallireducens***
Source	Aquatic sediments	Contaminated ditch
Electron donors	acetate, H_2, formate, lactate	acetate, benzaldehyde, benzene, butanol, butyrate, benzoate, benzylalcohol , p-hydroxybenzaldehyde, p-hydroxybenzoate, p-hydroxybenzylalcohol, isobutyrate, isovalerate, phenol, propionate, propanol, pyruvate, toluene, valerate , acetate, hydrogen gas
Electron acceptors	Tc(VII), Co(III), U(VI), AQDS, fumarate, malate, O_2	Mn(IV), Tc(VII), U(VI), AQDS, humics, nitrate
Optimal growth temperature	30 – 35 °C	30 °C

2.4 Geobacter sulfurreducens

Although *Geobacter* species optimally grow under anaerobic conditions, *G. sulfurreducens* can tolerate exposure to oxygen at low (10%) atmospheric levels using oxygen as a terminal electron acceptor (Lin et al. 2004). This allows the microbe to survive in subsurface environments and is applicable in air-cathode configurations where there is potential for small amounts of oxygen to be present

at the cathode interface (He et al. 2016). *G. sulfurreducens* has a limited metabolic range only able to use acetate, formate, lactate and pyruvate as organic acid substrates (Speers and Reguera 2012).

In a study using acetate as the electron donor in a mediator-less double chamber MFC with carbon paper electrodes the maximum power achieved in this MFC was 7 mW/m^2 under a 5000 Ω resistance (Kim and Lee 2010). Kim and Lee were able to produce a stable current over 60 d with the repeated addition of 20 mM acetate, with coulombic yields of approximately 24.0 – 26.2 electrons per mole of acetate consumed.

Alternatively, G. *metallireducens* has more versatile respiratory pathways than *G. sulfurreducens* with the ability to oxidize benzaldehyde, butanol, ethanol, phenol, propionate and propanol in addition to the substrates oxidized by *G. sulfurreducens* (Aklujkar et al. 2009). *G. metallireducens* can also reduce inorganic compounds which adds to its potential for more broad use in biotechnological applications (Aklujkar et al. 2009).

To date, the potential of *G. metallireducens* has yet to be fully realized with a limited number of studies involving its use in MFCs however a power density of 40 mW/m^2 was produced by a pure culture in a double chamber MFC (Min et al. 2005). The importance of minimizing internal resistance and dissolved oxygen concentrations for *G. metallireducens* as a pure biocatalyst was also illustrated in this study.

2.4.1 Anaerobic fermentation of acetate in *Geobacter*

The pathway by which *Geobacter* is believed to ferment acetate is shown in Figure 2-4.

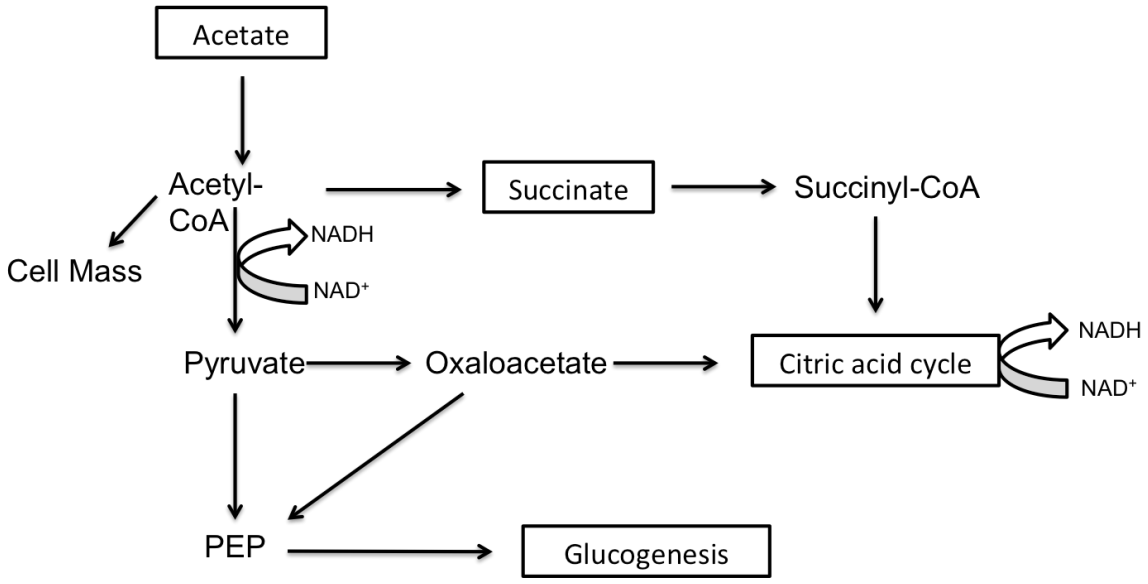

Figure 2-4 Central metabolism of *G. sulfurreducens* when acetate is available. Figure adapted from (Shrestha et al. 2013).

Acetate is the preferred electron donor for *Geobacter* and can be oxidized in the CAC producing ATP for cell growth and electrons for electrogenesis. Acetate is also converted to pyruvate and subsequently PEP which contributes to glucogenesis and biomass synthesis (Shrestha et al. 2013). A flux between the CAC and glucogenesis pathways exists and varies with the presence of certain electron donors and acceptors (T. H. Yang et al. 2010). While the acetate metabolism pathway exists in both *G. sulfurreducens* and *G. metallireducens,* only the latter possesses the propionate fermentation pathway. The proposed pathway for fermentation of propionate by *G. metallireducens* is shown in Figure 2-5.

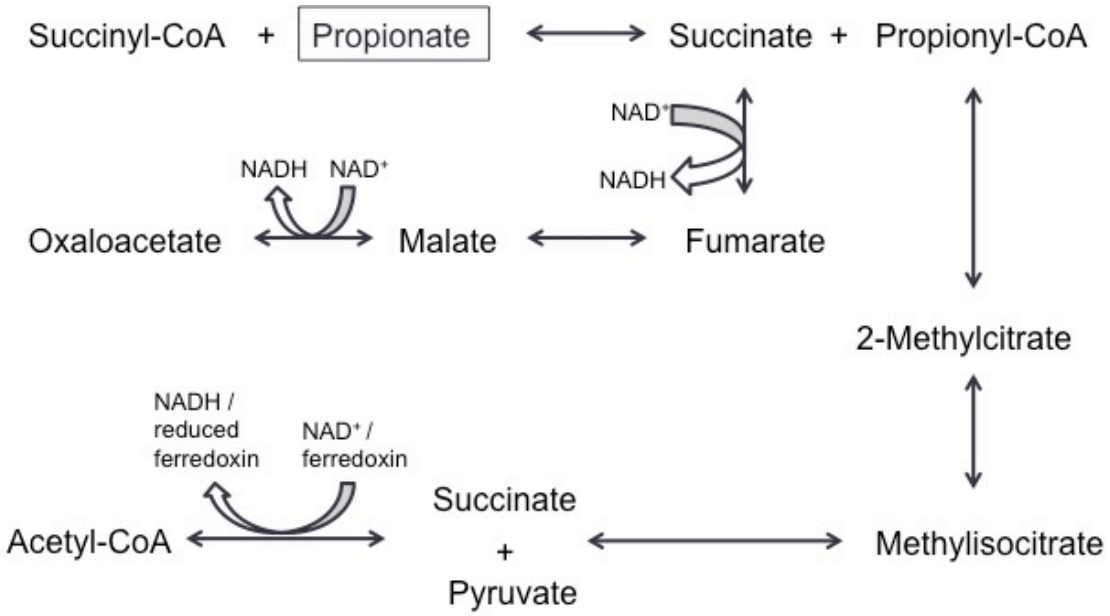

Figure 2-5 Proposed propionate metabolism pathways in *G. metallireducens*. Image adapted from Aklujkar et al., 2009.

G. metallireducens contains a gene able to convert propionate to succinate and propionyl-CoA, which allows it to subsequently produce activity to complete the CAC pathway (Aklujkar et al. 2009). Propionyl-CoA continues on to produce succinate and pyruvate and finally acetyl-CoA which are all metabolites seen in the fermentation of glucose by *P. shermanii.*

2.5 Use of cocultures in MFCs

Microbial consortia and cocultures have been used industrially for food and beverage production and more recently in waste water treatment and biogas production resulting in advantages such as increased product yield or improvement in process control (Bader et al. 2010). The motivation for developing cocultures in a lab environment may be for a multitude of reasons including to study natural interactions or to establish synthetic interactions between species (Goers et al. 2014). Relevant to this project, synthetic cocultures

may also be designed to improve culturing success of a monoculture (Goers et al. 2014). Interactions between populations of cells in microbiology are commonly achieved through material compounds such as signalling molecules or metabolites (Goers et al. 2014). These interactions can enable the coupling of redox reactions that occur inside bacterial cells during metabolism for growth and maintenance. This cascade of redox reactions may be accomplished by two or more species through interspecies electron transfer (IET) which occurs through diffusion via electron carriers. IET has been well documented between fermentative bacteria and methanogenic archaea which transfer hydrogen and formate between each other to complete the transformation of volatile fatty acids to methane (Kouzuma et al. 2015).

Similarly, direct interspecies electron transfer (DIET) is a mechanism of exchange through biological electrical connections and has been characterized in the *Geobacter* species. Evidence of DIET was demonstrated in a coculture of *G. sulfurreducens* and *Clostridium pasteurianum* where *G. sulfurreducens* grew with *Clostridium pasteurianum* acting as the only available electron acceptor present in the medium (Moscoviz et al. 2017). More commonly in electron flux studies between exoelectrogens such as *Geobacter* and a fermentative species, the fermenter is responsible for the break down of organic matter into organic acids which can then be used by the exoelectrogen to generate electricity in an MFC environment.

Designing cocatalysts for use in MFCs comes from the need to improve the environment for known exoelectrogens or to fulfill a metabolic role that the pure exoelectrogen is unable to complete on its own. Cocatalysts have been used to degrade complex substrates that would otherwise not be a viable feedstock for the exoelectrogen. In the search for an alternate transformation of cellulosic

biomass to electricity, a coculture of *Clostridium cellulolyticum* and *G. sulfurreducens* simultaneously degraded cellulose and generated a maximum power density of 143 mW/m^2 in a double chamber MFC (Ren et al. 2007). There is no singular microbe that is capable of completing the full cascade of reactions therefore the synergistic coculture resulted in cellulose degradation by *C. cellulolyticum* producing acetate, ethanol and hydrogen as fermentation products; all of which can be oxidized by the well-known exoelectrogen *G. sulfurreducens* (Ren et al. 2007).

Cocatalysts can also improve the MFC environment to provide optimal conditions for the exoelectrogen. This concept was carried out by coculture of a non-exoelectrogenic strain of *E. coli* that served to scavenge oxygen in a single chambered air-cathode MFC using *G. sulfurreducens* as the biocatalyst (Qu et al. 2012). A significant improvement of current generation was observed in the coculture compared to the pure culture due to decreased levels of dissolved oxygen (Qu et al. 2012). A similar study was done, however using an exoelectrogenic strain of *E. coli* to both help with oxygen removal in coculture with *G. sulfurreducens* and also to further the understanding of the interactions that occur in the complex microbial community of wastewater-fed MFCs (Bourdakos et al. 2014). The coculture did not improve power generation compared to the pure *G. sulfurreducens* MFC, however a stable pH was attained with the coculture, which is beneficial for prolonged microbial viability in the anode chamber (Bourdakos et al. 2014).

It was proposed that *G. sulfurreducens* successfully reduced acidification of the MFC environment through consumption of metabolites and proton depletion at the cathode following the redox reaction at the anode and cathode seen in Equation 7 and Equation 8 respectively (Bourdakos et al. 2014).

$$CH_3COO^- + 2H_2O \rightarrow 2CO_2 + 8e^- + 7H^+$$ **Equation 7**

$$2O_2 + 8H^+ + 8e^- \rightarrow 4H_2O$$ **Equation 8**

Despite the above study, in many cases, multispecies cultures are able to convert organic substrates into electrical power more efficiently than single species cultures however the reasons behind this phenomenon are largely unknown. Prokhorova et al. 2017 investigated the community composition and metabolic dynamics of a biofilm formed by *S. oneidensis*, *G. sulfurreducens*, and *G. metallireducens* with all three microbes contributing to the stable biofilm over seven d. The individual cultures all produced less current than when in coculture with each other and genomic analysis revealed an upregulation in the expression of genes involved with the central metabolism in all three microbes signifying a positive interaction within the coculture (Prokhorova et al. 2017).

Chapter 3 Materials and Methods

3.1 Chemicals

Chemicals used and their suppliers are shown in Table 3-1.

Table 3-1 Purity of chemicals as supplied.

Chemical	Purity	Supplier
Acetic acid	99%	Fisher Scientific
D-Glucose	99%	Fisher Scientific
Ethanol	98%	Fisher Scientific
Gram decolourizer	100%	BD
Gram safranin	100%	BD
Gram crystal violet	100%	BD
Hydrogen peroxide	3%	Fisher Scientific
Iodine (stabilized)	100%	BD
Methanol	99.80%	Fisher Scientific
Propionic acid	99%	Fisher Scientific
Sodium thioglycolate	>96.5 %	Sigma Aldrich
Succinic acid	99.50%	Fisher Scientific
Sulfuric acid	1N	Fisher Scientific

3.2 Growth media

Many different formulas of growth medium were used throughout this project. All media and stock solutions used throughout the project are shown in Table 3-2 through Table 3-9.

Table 3-2 Commercially available rich media.

Medium	Supplier
Bacto agar	BD
Bacto yeast extract	BD
Reinforced clostridial medium	Oxoid

Table 3-3 Defined M9 Media, enriched with 2.5 g/L yeast extract.

Component	amount per 500 mL
Na_2 HPO_4-7H_20	6.4 g
KH_2PO_4	1.5 g
NaCl	0.25 g
NH_4Cl	0.5 g
Yeast extract	2.5 g
500 g/L glucose	10 mL
1M Mg SO_4	1 mL
1M $CaCl_2$	50 uL
100g/L Sodium thioglycolate	5 mL
Deionized H_20	to 500 mL

Table 3-4 peptone media (10g/L glucose).

Component	amount per 500mL
500 g/L glucose	10 mL
12.5 g/L KH_2PO_4	10 mL
2.5 g/L $MnSO_4$	10 mL
Yeast Extract	2.5 g
Trypticase	2.5 g
100 g/L Sodium thioglycolate	5 mL
Deionized H_20	to 500 mL

Table 3-5 *G. metallireducens* (ATCC 1768 media).

Component	Amount per 500mL
Ferric citrate	6.85 g
Wolfe's vitamin solution	5 mL
Wolfe's mineral solution	5 mL
$NaHCO_3$	1.25 g
NaH_2PO_4	0.261 g
KCl	0.05 g
Sodium acetate	3.4 g
10N NaOH	3.5 mL
Deionized H_20	to 500 mL
Sparge with 80% N_2- 20% CO_2 gas mix	

Table 3-6 *G. sulfurreducens* (ATCC 1957 media).

Component	Amount per 500mL
NH_4Cl	0.75 g
Wolfe's vitamin solution	5 mL
Wolfe's mineral solution	5 mL
$NaHCO_3$	1.25 g
NaH_2PO_4	0.3 g
KCl	0.05 g
Sodium acetate	0.41 g
Sodium fumarate	4 g
Deionized H_20	to 500 mL
5% coenzyme M	5 mL
Sparge with 80% N_2- 20% CO_2 gas mix	

Table 3-7 Wolfe's Vitamin solution as supplied by ATCC.

Component	Amount per 1L
Biotin	2 mg
Folic acid	2 mg
Pyridoxine hydrochloride	10 mg
Thiamine . HCl	5 mg
Riboflavin	5 mg
Nicotinic acid	5 mg
Calcium D-(+)-pantothenate	5 mg
Vitamin B12	0.1 mg
p-Aminobenzoic acid	5 mg
Thioctic acid	5 mg
Deionized H_20	to 1 L

Table 3-8 Wolfe's mineral solution as supplied by ATCC.

Component	Amount per 1L
Nitrilotriacetic acid	1.5 g
$MgSO_4 . 7H_2O$	3 g
$MnSO_4 . H_2O$	0.5 g
NaCl	1 g
$FeSO_4 . 7H_2O$	0.1 g
$CoCl_2 . 6H_2O$	0.1 g
$CaCl_2$	0.1 g
$ZnSO_4 . 7H2O$	0.1 g
$CuSO_4 . 5H2O$	0.01 g
$AlK(SO_4)_2 . 12H_2O$	0.01 g
H_3BO_3	0.01 g
$Na2MoO_4 . 2H_2O.$	0.01 g
Deionized H_20	to 1 L

Table 3-9 Modified MFC media with 2.5 g/L yeast extract, 10 g/L glucose and additional buffer.

Component	amount per 500mL
500g/L glucose	10 mL
Wolfe's vitamin solution	5 mL
Wolfe's mineral solution	5 mL
$NaHCO_3$	1.25 g
NaH_2PO_4	1.83 g
Na_2HPO_4	1.38 g
NH_4Cl	0.75 g
KCl	0.05 g
Yeast extract	2.5 g
Deionized H_20	to 500 mL
(100 g/L) Sodium thioglycolate	0.5 mL
Sparge with 80% N_2- 20% CO_2 gas mix	

Commercially available Reinforced Clostridial Medium (RCM) was used for *P. shermanii* pre-cultures which were subsequently cultured in enriched M9 medium, peptone medium and the defined MFC medium according to the experimental conditions. *G. metallireducens* was initially cultured in the media designed by ATCC (ATCC medium 1768) while *G. metallireducens* was initially grown on its respective medium from ATCC (ATCC medium 1957). Both ATCC media required Wolfe's Vitamin Solution and Wolfe's mineral solution outlined in Table 3-7 and Table 3-8.

RCM (Oxoid) was prepared using deionized water according to manufacturer's instructions. The formulation of enriched M9 medium, shown in Table 3-3, was derived from the basic M9 medium outlined by(Sambrook, Fritsch, and Maniatis 1989). Based on the experimental plan, the formula included Bacto yeast extract (BD) and either glucose or glycerol as a carbon source.

The defined MFC medium was derived from ATCC medium 1768 however glucose was used as the carbon source in place of acetate. Additional phosphate buffer was also included. Finally, sodium thioglycolate, an oxygen scavenger, was included to a concentration of 0.5g/L to maintain anaerobic conditions in fermentations and MFC trials.

In general, media were prepared by boiling water, adding salts, sparging with N_2 or 80% N_2- 20% CO_2 gas mix while the solution cooled to help maintain low oxygen content. Aliquots were dispensed into sparged bottles and crimped with butyl rubber stoppers before autoclaving at 121°C and 15 PSI for 20 min. The stock glucose and sodium thioglycolate solutions were sterilized separately by autoclaving and subsequently added to the complete media.

3.3 Cultures

Propionibacteria freudenreichii ssp. *shermanii* (ATCC 9614) was stored at -80°C in 30% glycerol solutions in RCM. Freezer stocks were grown on RCM agar plates at 30°C in an anaerobic jar containing a CO_2 gas generating kit with an anaerobic indicator.

Geobacter metallireducens (ATCC 53774) and *Geobacter sulfurreducens* (ATCC 51573) were obtained from the American Type Culture Collection. *Geobacter* strains were stored at -80°C in 30% glycerol solutions in their respective ATCC media formulations. Strains were grown anaerobically at 30°C in Hungate tubes containing liquid media. Strains were transferred weekly into fresh liquid medium.

3.4 Microbial fuel cell design

A new modular MFC design was designed by Izcoatl Rafael Garduño Ibarra[1] for use as a double chamber or single chamber MFC to test the anodic catalysts. The single chamber air-cathode MFCs were used to run all experiments. The body of the MFC was machined from polycarbonate with an anodic chamber working capacity of 140mL. The three-piece, cylindrical design pictured in Figure 3-1 contained two silicone gaskets between each section, which were tightened with washers, nuts and bolts which secured screws that ran through the length of the cylinder.

The MFC was specifically designed to be adaptable to different experimental configurations. By making material, spatial and operational changes the H-type MFC was improved upon.

The body of the MFC was machined from polycarbonate, which is a cost effective, durable, non-corrosive alternative to glass. The anode was made of

[1] Izcoatl Rafael Garduño Ibarra developed the design. Preliminary assembly and testing of the design and minor modifications to improve the final model were performed as a team.

carbon felt 0.5 mg/cm^2 60% Pt on Vulcan (Fuel Cell Store) with a surface area of 36 cm^2 and was rolled up inside the anode chamber. The new anode material served to increase the surface roughness of the anode over carbon cloth while maintaining the same biocompatibility. Surface roughness of an anode affects the attachment and electron transfer of biofilm forming exoelectrogens such as *G. sulfurreducens* (Champigneux et al. 2018). The cathode was also modified to be open to air with a surface area of 19.65 cm^2 and was made from 0.2 mg/cm^2 20% platinum on Vulcan (Fuel Cell Store). The air-cathode material was made of carbon cloth at the microbial interface consistent with the previous design while the surface that was open to air was coated with polytetrafluoroethylene (PTFE) for its waterproofing properties. A view of the cathode open to air can be seen in Figure 1A. A Nafion membrane (Fuel Cell Store) had the same projected surface area as the cathode and was secured between the electrodes. Nickel wire was used to connect the anode and cathode externally and to the resistor.

To improve mass transfer within the anode chamber, the new MFC design included several spatial and mechanical improvements. Firstly, the electrodes were designed to be in close proximity to the membrane as opposed to having the electrodes suspended in the media such as in the H-type design. This served bring the membrane in closer proximity to the electrode surface to improve the mass transfer of protons through the membrane once they evolve from the site of the reaction. Two outlets in addition to the butyl rubber sampling port were added to the anode, which fed to a peristaltic pump (Figure 3-1B). The pump enabled slow mixing of the anode to improve mass transport phenomena in the anodic fermentation. In addition, a port was introduced into the top of the anode chamber to allow for the release of gas into a water trap.

To improve the ease of use, assembly and prolonged operation of the MFC, the new design employed screws and nuts and silicon gaskets between each section of the MFC to reduce the occurrence of leakage. The modular tube design permits reorganization of the two identically sized chambers as necessary. The design is functional as a single chamber and provides the option of connecting a second chamber, or multiple units to create a stacked MFC. The addition of feed ports connecting to the peristaltic pump also permit including an anode reservoir, which could ultimately develop into a continuous mode of operation.

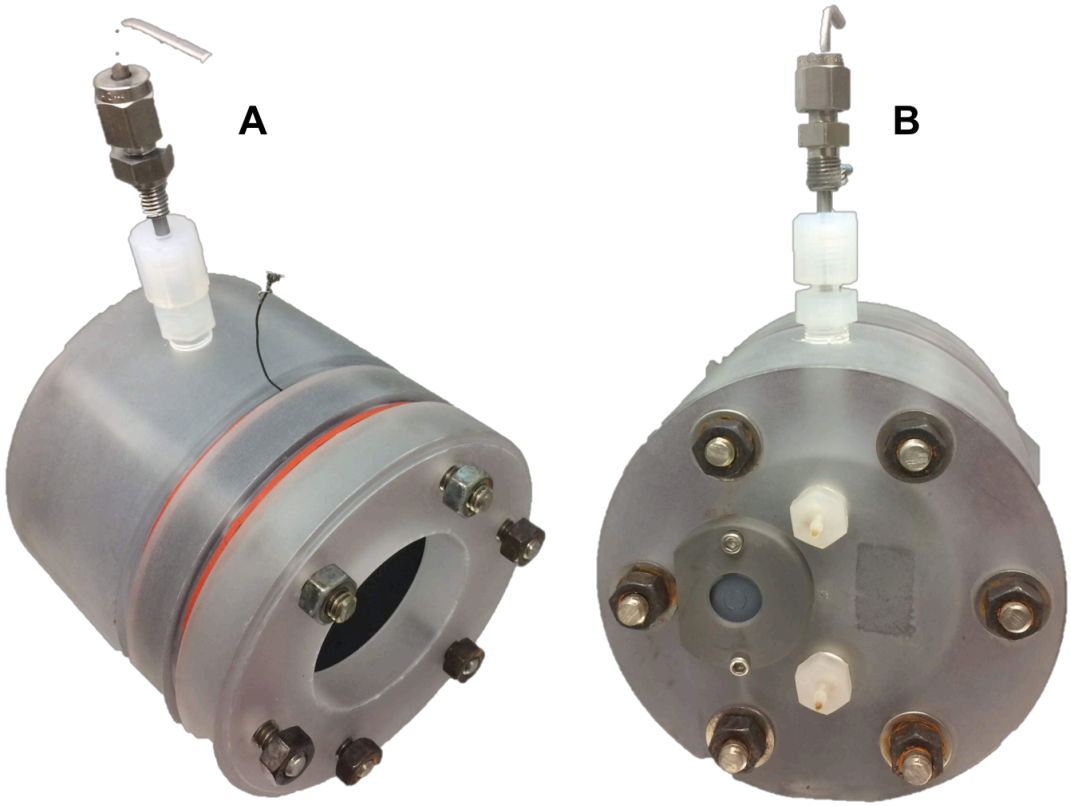

Figure 3-1 Air cathode MFC design. Image A shows the air cathode side with the PTFE coated side exposed to air. Image B shows the anode side with the butyl rubber stopper for inoculation and two ports leading which led to the pump.

3.5 MFC assembly and operation

The membranes were activated before use by sequentially boiling them in 3% hydrogen peroxide, deionized water, 0.5 M sulfuric acid and again with deionized water for 1 h in each solution. Nickel wire was woven through the anode and used to connect the circuit to the resistor and cathode. The anode chamber was sealed with butyl rubber plug seal caps and sparged with a gas mix of 80% N_2 and 20% CO_2 prior to inoculation. A headspace of approximately 10 mL was left in the anodic chamber and connected to an external air trap to allow for gases to be expelled without affecting the pressure of the system. Anodic cultures were gently mixed using a peristaltic pump, which was connected to the MFC using tubing. A beaker of 100 mL of water was placed in the incubator to humidify the air inside the incubator and reduce dehydration of the cells.

All components of the fuel cell were autoclaved except for the air cathode due to its sensitivity to heat. The components were reassembled in a biosafety cabinet and inoculated with 133 mL MFC media and 7 mL preculture to reach a final volume of 140 mL with a 5% v/v biocatalyst. Once inoculated, cells were connected to a peristaltic pump and incubated at 30°C. After 48 h of operation 20 mL of media was added to each cell to aid in maintaining an anaerobic environment to offset the media lost due to evaporation. For the coculture trials, this additional medium included the *G. sulfurreducens* culture.

3.6 MFC and fermentation experiments

For both MFC and fermentations, a single *P. freudenreichii* ssp. *shermanii* colony was chosen from an RCM agar plate and transferred anaerobically to a hungate

tube containing 5 mL liquid RCM. After incubating at 30°C for 48 h, 0.5 mL of the culture was transferred to 50 mL of defined medium in a 125 mL serum bottle.

G. sulfurreducens was transferred using anoxic liquid ATCC media in 5 mL hungate tubes. As soon as red aggregates formed at the bottom of the culture after approximately seven d, cells were transferred to preculture 125 mL serum bottles containing the ATCC media.

Samples taken throughout MFC and fermentation trials were viewed under the microscope (Olympus BX40). Samples for HPLC were also taken periodically throughout operation, centrifuged at 13,400 rcf for 2 min and supernatants were stored at -20°C until analysis.

3.7 Electrochemical analysis

The MFC electrodes were hooked up to a 110 Ω resistor, and voltage was measured daily using a voltmeter (VWR). Polarization curves were generated for MFCs using a potentiostat (VSP BioLogic Science Instruments) once a stable maximum potential had been achieved. Fuel cells were arranged in open circuit operation for 30 min to allow the OCP to stabilize; polarization curves were generated using a scan rate of 5 mVs^{-1}.

3.8 Analytical methods

To quantify the consumption of glucose and production of metabolites, samples were analyzed with an Agilent 1200 series High Pressure Liquid Chromatograph (HPLC) using an Aminex HPX-87H column maintained at a temperature of 50°C.

Carbohydrate consumption was quantified using the Refractive Index Detector (RID) while metabolite production was quantified using the Diode Array Detector (DAD) at a wavelength of 210 nm. A 5 mM sulfuric acid solution was used as the eluant, which was vacuum filtered through a 0.45 μm pore size MF-Millipore mixed cellulose ester membrane prior to use at a flow rate of 0.6 mL min^{-1}. Samples were run for 25 min each. Carbohydrate and metabolite concentrations were quantified by comparison to a linear calibration using the integrated peaks of analytical grade standards. Standard curves for carbohydrates and organic acids are shown in Appendix B with retention times shown in Table 3-10.

Table 3-10 HPLC metabolite retention times.

Compound	Retention time (min)	Detector
Glucose	11.2	RID
Acetic acid	18.6	DAD
Propionic acid	22.3	DAD
Succinic acid	14.9	DAD

Identification of pure cultures was done through microscopy. Samples were vortexed to break up conglomerates of cells and diluted with distilled water to 1:10 and 1:100 before fixing to microscope slides. Cells were fixed chemically using methanol. BD gram stain was then used according to manufacturer's instructions.

Chapter 4 Medium Optimization

4.1 Introduction

Bacterial culture medium must contain the necessary nutrients and carbon sources to sustain the desired microbe's growth. In general, defined media will be organism-specific based on nutritional needs to propagate growth but will often include a source of energy, proteins and amino acids, essential minerals and a buffering agent. The proteins and amino acids allow the bacteria to build its proteins. A carbon source is required for bacterial growth and to maintain cellular functions within the cells. Many bacteria also require minerals that are essential to activate specific cellular pathways (eg. magnesium, iron) however these requirements vary widely among microorganisms. Finally, a buffering agent is needed to control the pH of the media as the bacteria produce acidic or basic metabolites (eg. phosphates , acetates).

4.2 Glycerol substrate

To further the goal of ultimately using glycerol as a substrate for the fuel cell, a study comparing consumption and metabolites of growth of *P. shermanii* on glucose compared to glycerol was performed. It has been a goal of the overarching project to use glycerol as the substrate as it is a co-product produced during biodiesel production. Glycerol's relevance as a value-added product has decreased due to the production in abundance of its demand (Yazdani and Gonzalez 2007). To retrieve some value from this waste product, direct use of crude glycerol from biodiesel production in an MFC would offer a sustainable waste treatment solution which would recover energy from the process. Product

yields of acetate and propionate from *P. shermanii* grown on glucose and glycerol in M9 are shown in Table 4-1.

Table 4-1 Product yield of *P. shermanii* grown on 5g/L glucose and 5g/L glycerol. ***Cell mass and the product are formed simultaneously therefore product yield does not account for substrate used for cell growth.***

	Average Yield (g/L)	
Product	**Glucose**	**Glycerol**
Acetate	0.0535 ± 0.0108	0.0536 ± 0.0203
Propionate	0.426 ± 0.0774	0.336 ± 0.0494

The augmented standard deviation among the glycerol cultures illustrates the variability in growth under these substrate conditions. This is consistent with the variable growth of *P. shermanii* growth on glycerol that was previously demonstrated by Reiche 2012 and Sivell 2014.

HPLC data illustrating the consumption of both substrates and the production of acetate, propionate and succinate over the length of the fermentation are shown in Figure 4-1 and Figure 4-2.

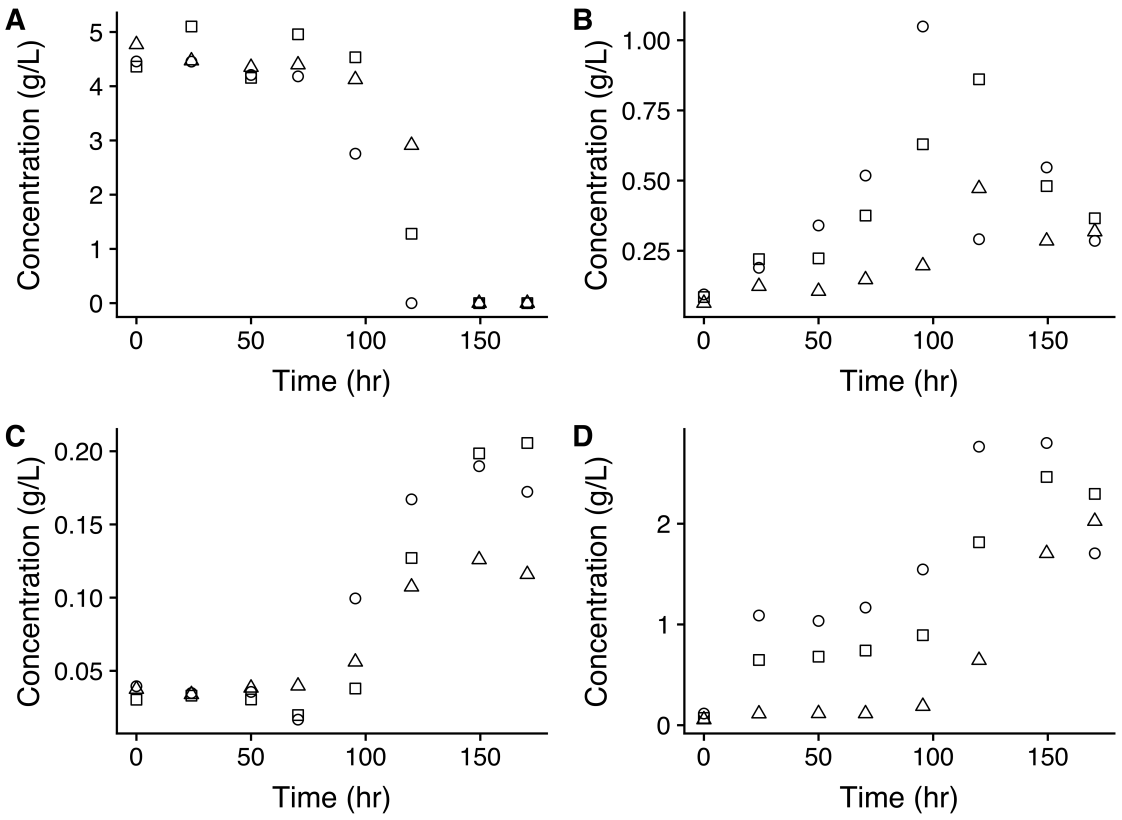

Figure 4-1 HPLC results for *P. shermanii* fermentation grown on 5 g/L glucose and triplicate experiments are shown. Figures A, B, C and D correspond to concentrations of glucose, acetate, succinate and propionate respectively.

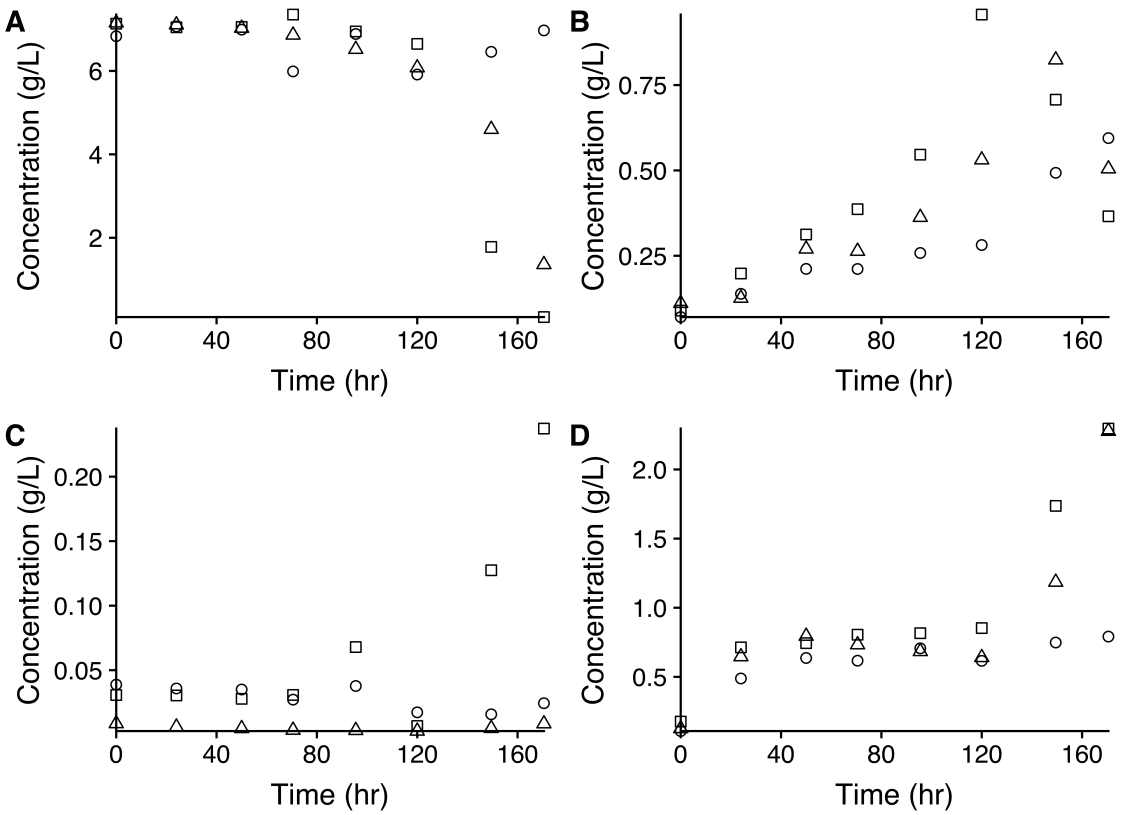

Figure 4-2 HPLC results for *P. shermanii* fermentation grown on 5 g/L glycerol and triplicate experiments are shown. Figures A, B, C and D correspond to concentrations of glycerol, acetate, succinate and propionate respectively.

Glucose as a substrate lends to more consistent growth with complete glucose consumption achieved at 150 h for all three runs. In contrast the glycerol fermentations exhibited more variation with one culture appearing not to consume any glycerol. This is also reflected in the metabolite concentrations that remain relatively constant throughout the glycerol trial. The slight increase in acetate shown in Figure 4-2B is likely due to consumption of the carbohydrate source (glucose) present in the media supplemented with yeast extract.

Despite the observed variability, the use of glycerol remains a beneficial option for economic reasons as the glycerol feedstock is readily available at a low

cost, and could make energy recovery of a biodiesel plant possible through directly applying the technology to the waste glycerol stream. Use of glycerol with the biocatalyst *P. shermanii* remains an overarching goal, however due to the observed inconsistency in growth, glucose was chosen as the carbon source in subsequent chapters in order to elucidate the behaviour of *P. shermanii* with more regularity.

4.3 *Propionibacteria freudenreichii* ssp. *shermanii* growth considerations

M9 medium was originally formulated for use with *Escherichia coli* and is commonly used as a defined minimal medium to culture a variety bacteria. *Propionibacteria* are known for having complex growth requirements. Certain vitamins, minerals and constituents in yeast extract have shown to be essential for growth while the supplementation of amino acids to traditional media has also produced an increase in growth (Prokhorova et al. 2017).

M9 medium enriched with 5 g/L yeast extract was determined to most significantly improve glycerol conversion for *Propionibacteria freudenreichii* ssp. *shermanii* in previous experiments (Reiche 2012). Reiche 2012 observed complete conversion of 10 g/L glycerol in the fermentation environment while in the MFC environment, only half of the available glycerol was consumed. When repeated under the same conditions, at most, approximately half of the available 10 g/L analytical glycerol was consumed in the fermentation and MFC environment with varying results (Sivell 2014). To alleviate these consumption issues and to

encourage total conversion of the substrate for analysis purposes, the carbon source was changed from glycerol to glucose throughout this project.

To further elucidate amino acid usage by *P. shermanii* Brendehaug and Langsrud 1985 investigated amino acid consumption during glucose fermentation. This study demonstrated that free amino acids were reduced in the flowing order under anaerobic conditions: Glu/Asn, Asp, Ala, Ser, Gly, Leu, Lys, Cys/2, Val, Pro, Thr, Ile, Arg, Phe, while the remaining 7 amino acids were minimally used. In contrast, in an aerobic environment, Ala and Gly were completely catabolized and Set was nearly reduced to zero demonstrating a shift in metabolic processes in the two environments (Brendehaug and Langsrud 1985).

Brendehaug and Langsrud 1985 illustrated a definitive use of free amino acids during *P. shermanii* growth therefore a comparative medium experiment was performed to evaluate whether increasing the amount of free amino acids in the culture broth would improve substrate conversion.

4.4 Peptone medium for *Propionibacteria*

In studies culturing *Propionibacteria*, a formula including trypticase peptone has been used (Zhang and Yang 2009). Trypticase peptone is a pancreatic digest of casein containing a high nitrogen content without any additional carbohydrates. Different forms of peptone illicit an effect on the metabolic activity of microorganisms (Loginova et al. 1974). The addition of addition trypticase peptone to growth medium increases the amount of free amino acids in solution

and it is recommended for use in applications where good bacterial growth is required (Biosciences 2018).

A medium optimization experiment was therefore performed using a medium formulation including trypticase peptone compared with enriched M9 medium. The medium found in Zhang and Yang 2009 was modified to match the yeast extract and glucose concentrations of the enriched M9 medium formula and sodium thioglycolate was also added to ensure that anaerobic conditions were maintained. Table 4-3 shows the medium formulations side by side to illustrated their similarities and differences.

Table 4-2 M9 medium compared to Peptone medium used in the media optimization study. Common medium components are in bold.

M9 Medium Components	Amount per 500 mL	Peptone Medium Components	Amount per 500 mL
$Na_2 HPO_4$-$7H_20$	6.4 g	$Mn SO_4$	0.025 g
KH_2PO_4	**1.5 g**	**KH_2PO_4**	**0.125 g**
NaCl	0.25 g	Trypticase	2.5 g
NH_4Cl	0.5 g		
Yeast extract	**2.5 g**	**Yeast Extract**	**2.5 g**
500 g/L glucose	**10 mL**	**500 g/L glucose**	**10 mL**
1M $Mg SO_4$	1 mL		
1M $CaCl_2$	50 uL		
100g/L Sodium thioglycolate	**5 mL**	**100 g/L Sodium thioglycolate**	**5 mL**
Deionized H_20	**to 500 mL**	**Deionized H_20**	**to 500 mL**

4.5 M9 compared with peptone medium

Triplicate anaerobic fermentations were performed and evaluated for both media. At this stage of experimentation, the HPLC was not in operation therefore testing for conversion products was not possible. Average glucose consumption and OD_{600} values for both media are presented in Figure 4-3. The triplicate results of glucose consumption on the enriched M9 medium and peptone medium are presented in Figure 4-4.

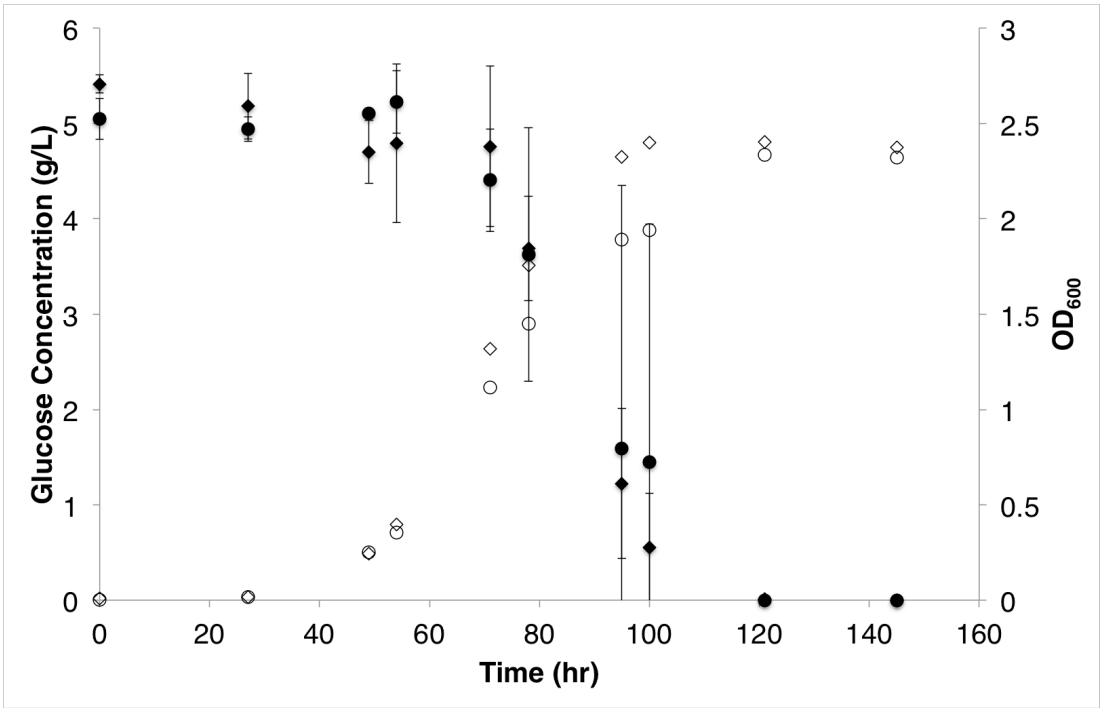

Figure 4-3 Average consumption of glucose with standard deviation (n=3) are shown for M9 medium and peptone medium by symbols ◆ and ● respectively. The OD_{600} values for M9 medium and peptone medium are shown by symbols ◇ and ○ respectively.

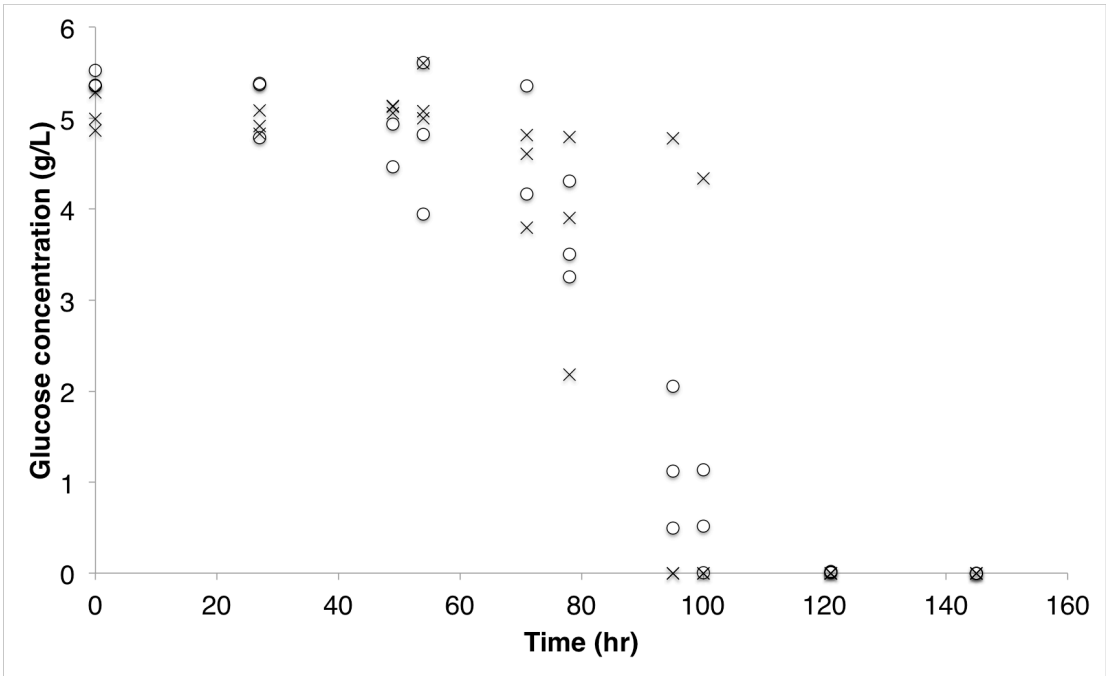

Figure 4-4 Consumption of glucose in triplicate comparative media fermentations are shown. Peptone medium trials are denoted by O and M9 medium trials are denoted by ×.

Figure 4-4 showing the triplicate runs illustrates the variation observed among the trials. Two of the three M9 culture were able to completely consume glucose between 78 and 95 h while the last fermentation lagged well behind the other two. Less variation was observed among the peptone media fermentations however all three required at least 121 h to completely consume glucose. Average values reported in Figure 4-3 reveal that as a whole, the M9 media fermentations exhibited a faster rate of glucose consumption. The difference between the two media however, is not statistically significant with a two-tailed p-value of 0.904. For this reason, an alternative route to improve *P. shermanii*'s efficacy as a biocatalyst was explored.

4.6 Conclusions

Fermentations of *P. shermanii* with 5 g/L glucose compared to 5 g/L glycerol produced significantly different consumption rates of each carbohydrate source.

The culture grown with glucose exhibited more consistency in consumption rates among the triplicates. Both fermentation cases produced similar yields of acetate, while the glucose fermentation produced a higher yield of propionate.

The addition of trypticase peptone to growth media increases the concentration of free amino acids and has shown to have a beneficial effect on bacterial growth. Batch fermentation experiments performed anaerobically using glucose as the sole carbon source for M9 and *Propionibacteria* specific medium including trypticase peptone did not exhibit a significant difference in glucose conversion. Based on the glucose conversion HPLC results, it was determined that the peptone media did not provide a significant advantage for increased glucose consumption for *P. shermanii* and alternative optimization methods are examined in Chapter 5.

Chapter 5 Development of Cocatalyst

5.1 Introduction

This chapter focuses on selecting a pure bacterial strain to culture with *Propionibacteria freudenreichii* ssp. *shermanii*. *Geobacter metallireducens* was chosen and grown anaerobically on its preferred medium in the lab. A modified medium based on the *G. metallireducens* ATCC formula was developed to concurrently support *P. shermanii* growth. Batch fermentations in the modified media of pure *P. shermanii*, pure *G. metallireducens* and of the coculture were performed to test the feasibility of the new formula. Gram stain of the coculture produced positive results showing growth of both strains.

After experiencing multiple setbacks including a notice of contamination from ATCC of the original *G. metallireducens* batch and the subsequent lack of consistent propagation of the *G. metallireducens* strain; confirmation was received from ATCC about the illegitimacy of the supplied batch of *G. metallireducens* and their inability to supply a new viable batch of *G. metallireducens*. A new *Geobacter* strain was therefore chosen. Development and testing of the cocatalyst resumed with *G. sulfurreducens* as the new strain.

5.2 Strain selection

After reviewing available electroactive microbes with similar growth conditions as *P. shermanii*, *G. metallireducens* was chosen as the coculture candidate primarily due to its ability to metabolize *P. shermanii* metabolites acetate and propionate. The summarized criteria in Table 5-1 outlines the main considerations used in the selection of *Geobacter* as a cocatalyst.

Table 5-1 Criteria used in the selection of cocatalyst.

Criteria	Question	Positive response
Growth conditions	Compatible with *P. shermanii*?	Yes
Metabolism	Able to consume *P. shermanii* by-products?	Yes
Electroactivity	Electrogenic?	Yes
Pathogenicity	Pathogenic?	No

G. metallireducens is non-pathogenic with optimal growth conditions similar to *P. shermanii* (anaerobic, 30°C, neutral pH) enabling a coculture to be created in the lab environment. Furthermore, *G. metallireducens* is known to produce nanowires but has rarely been employed in MFCs therefore its potential as a cocatalyst and also as a pure culture in the MFC environment should be explored.

5.3 *Geobacter metallireducens* experiments

Revival of the *G. metallireducens* strain from ATCC was performed in the suggested media outlined in Table 3-5, Chapter 3. ATCC 1768 media uses Fe (III) as the electron acceptor in the fermentation broth which has been shown to be favourable when preparing microbes for the MFC environment as Fe (III) is an insoluble electron acceptor similar to a cathode. Growth in this medium was monitored by the colour change from light brown to dark brown and to eventual fade in colour as shown in Figure 5-1. This colour change is due to the reduction of Fe (III) to Fe (II) therefore signifying growth. The progression of growth took 7 d for the initial culture and was reproduced via 5% anaerobic transfer into fresh

media. In the subsequent transfers, the full colour change progressed faster over approximately 4 d. Dark coloured cells were visible in the clear and colourless fermentations.

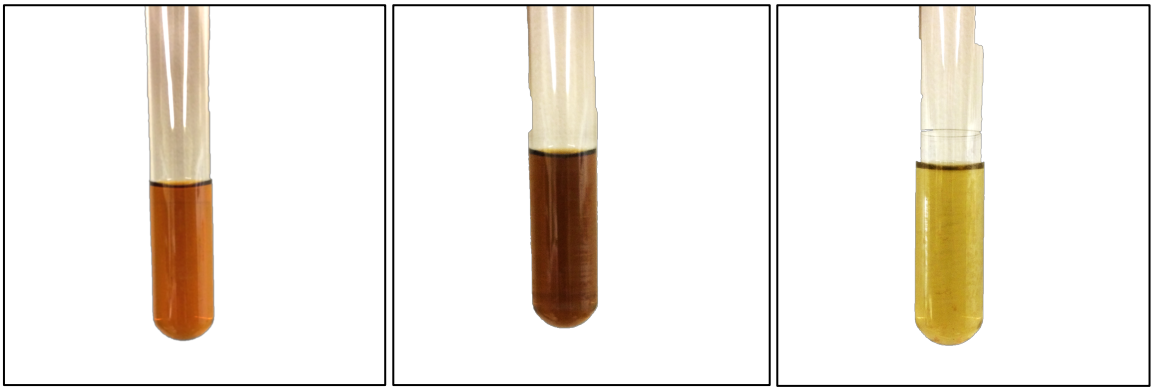

Figure 5-1 Progression of colour change resulting from to *G. metallireducens* growth in ATCC 1768 media. From left to right, appearance of hungate tube upon inoculation, after 72 h of growth, after 160 h of growth.

Literature from ATCC indicates that this strain is difficult to grow on plates, however a purity test was attempted using the ATCC media with 0.1% yeast extract added to 15% agar which produced dark brown colonies after approximately 10 d of growth in an anaerobic environment.

Four months after acquisition of the strain, ATCC sent a notice regarding this initial culture as it was contaminated. A new culture was received. Revival of the new culture was successful however subsequent propagation and transfer of the bacteria was unsuccessful. Freezer stocks of the initially received culture were made using 30% glycerol and were attempted to be grown in fresh media, on plates in various conditions without success. After inquiring with ATCC for potential solutions to the inability to propagate the bacteria, information was received that the ATCC labs were experiencing similar issues and they had yet to determine the root cause of the issue. As a viable strain of *G. metallireducens* was

currently unavailable, the use of *Geobacter sulfurreducens* was proposed as a potential candidate for coculture with *P. shermanii*.

5.4 Cocatalyst development with *Geobacter sulfurreducens*

Revival of the *G. metallireducens* strain from ATCC was performed in the suggested media outlined in Table 3-6, Chapter 3. ATCC 1957 media differs from that used to grow *G. metallireducens* with sodium fumarate used as the electron acceptor in fermentations instead of ferric citrate. As sodium fumarate is soluble in water, the resulting medium is clear and colourless. Growth is evident when slight turbidity occurs in the media and over time, bright red cell clusters flocculate and settle visibly at the bottom of the fermentation vessel.

Since, *G. metallireducens* was selected based on its ability to metabolize both of *P. shermanii*'s by-products, the consumption of the acetate and propionate by-products would help to alleviate the acidification of the anode environment while also contributing to electricity generation. The switch to *G. sulfurreducens* would follow this same hypothesis however only acetate would be consumed.

In the *P. shermanii*, *G. sulfurreducens* cocatalyst model, both strains of bacteria are exoelectrogens meaning they both supply electrons to the anode. It is common in MFC literature to coculture species together where one serves as the designated fermenter and the other as the designated exoelectrogen (Moscoviz et al. 2017, Qu et al. 2012). However, this model risks the advent of the fermenter adversely affecting electricity production by diverting energy away from electricity generation (Wang et al. 2016). This cocatalyst will therefore elucidate on the efficacy and performance of using two exoelectrogens.

5.5 Cocatalyst media

Coculture medium was designed using the ATCC 1957 medium as a basis due to the specific vitamin and mineral requirements of *G. sulfurreducens*. Furthermore, based on the results in Chapter 4, *P. shermanii* has demonstrated its ability to thrive in media not explicitly designed for its nutritional needs. Several modifications were made to the ATCC 1957 media to accommodate *P. shermanii* growth as shown in Table 5-2.

Table 5-2 Modifications made to ATCC 1957 media.

	ATCC 1957 media	**Cocatalyst media**
Carbon source	Sodium acetate	Glucose
Enrichment	N/A	2.5 g/L yeast extract
Buffer	0.6 g/L Na_2HPO_4	Additional: 2.75 g/L Na_2HPO_4 4.22g/L $NaH_2PO_4 \bullet H_2O$
Electron acceptor	Sodium fumarate	Anode

Firstly, the carbon source was changed to glucose and yeast extract was added to support *P. shermanii* growth. Next, the buffer capacity was increased in the cocatalyst media by adding additional phosphate buffer. This modification was motivated by a similar study, which employed *G. metallireducens* as a biocatalyst where the additional buffer served to reduce changes in pH in the MFC environment (Min et al. 2005). Finally, sodium fumarate was removed from the media to ensure use of the anode as the cocatalyst terminal electron acceptor.

Preliminary fermentations were performed to test *P. shermanii* growth in the coculture medium. Growth of *P. shermanii* was confirmed by turbidity in the fermentation serum bottle and by plating the culture anaerobically on RCM plates where morphologically characteristic pure colonies were observed. The HPLC was not operational at this time to analyze metabolite and end product formation.

5.6 Development of coculture quantification method

Growth of *P. shermanii* was initially monitored by measuring absorbance at 600 nm, however the culture coagulated together in the new cocatalyst media. This caused absorbance values to be highly inaccurate therefore alternative quantification methods were investigated.

PCR was entertained as a method to identify individual strains, however developing quantitative results using PCR proved to be too intensive and had questionable accuracy. Knowing that *P. shermanii* contains a peptidoglycan layer while *G. sulfurreducens* does not, gram staining could be used to differentiate between the two strains. Having access to all necessary resources played a significant role in choosing the gram stain and microscopy protocol.

5.6.1 Gram stain and microscopy

The following protocol was developed to identify and quantify the coculture:
A 0.5 mL sample was placed in a microcentrifuge tube and vortexed for 30 sec. Dilutions to 1:10 and 1:100 were prepared in in deionized water. A 10 μL sample of each dilution was placed on a slide, spread and fixed with methanol. The gram

stain protocol as directed by manufacturers was then performed on each slide. Five different fields of views were chosen at random to identify and enumerate cells under the microscope at 60X magnification.

This protocol was initially proven to work with fresh cultures where slides made after two d of coculture growth produced a clear distinction between red and violet cells. Limitations to this protocol arose during experimentation, which will be discussed in Chapter 6 and 7.

5.7 Conclusions

G. sulfurreducens was chosen to be cocultured with *P. shermanii* in part, due to the unavailability of *G. metallireducens*. Coculture medium was successfully developed to support the growth of both biocatalysts. Confirmation of *P. shermanii* growth in the newly developed medium was achieved in fermentation trials.

Chapter 6 Pure Culture Fermentations and Air-cathode MFC Performance

6.1 Introduction

The following chapter explores the use of pure cultures of *Propionibacteria freudenreichii* ssp. *shermanii* and *Geobacter sulfurreducens* as anodic biocatalysts in an air-cathode MFC. Glucose was used as the substrate for both pure cultures. An additional experiment using *G. sulfurreducens's* desired substrate acetate was then performed to confirm its electrochemical activity in the MFC environment.

The single chamber air-cathode was chosen as the experimental model. Power density curves were created to determine the maximum power density achieved by each catalyst. Maximum power density values of each experiment were used as the main performance indicator and source of comparison between the pure cultures. In addition to this, change in working potential, electrochemical efficiency, and identification of the nature of energy losses provided additional information regarding the performance of each MFC. Fermentations of the pure catalysts were also performed alongside the MFCs. Samples from the fermentations and MFCs were taken throughout each trial to analyze substrate consumption and metabolite evolution in both cases. Gram staining and microscopy was employed for identification and quantification of the catalysts, however the results were inconclusive.

6.2 MFC design test

An initial test was performed with the double chamber MFC design. Lack of sufficient pressure relief caused by the accumulation of carbon dioxide gas in the anode chamber caused the malleable membrane to protrude into the cathode chamber resulting in leakage between the two chambers. To avoid this issue, the air-cathode design was used for subsequent experiments. In addition to the ease of use of the air-cathode design, air-cathode MFCs are more feasible economically and are more efficient when considering energy requirements and scaling up operations (Dong et al. 2012). With future applications in mind, the air-cathode MFC is a more reliable design than the double chamber.

6.3 Pure culture experiments

MFCs were sterilized, filled with MFC media and inoculated with 10% v/v active cultures of either *P. shermanii* or *G. sulfurreducens* in triplicate. The anode and cathode were connected with an external load of 110 Ω and voltage was measured periodically throughout the trial. Once the measured voltage peaked, the circuit was disconnected to find the OCP value and to gather polarization data. The circuit was subsequently reconnected to resume the trial. Triplicate fermentations from identical pre-cultures were inoculated in the same medium alongside the MFCs. Samples were taken from the anode and fermentations to monitor glucose consumption and metabolite evolution.

6.4 *Propionibacteria freudenreichii* ssp. *shermanii*

6.4.1 Consumption of glucose and metabolite analysis of fermentation and MFC trials

HPLC data illustrating the consumption of glucose and evolution of metabolites and end products for the fermentation trial and MFC trial using *P. shermanii* as a catalyst are presented in Figure 6-1 and Figure 6-2 respectively.

For all fuel cell experiments, the concentration of glucose decreased throughout the trial and was fully consumed between 117 and 142 h as shown in Figure 6-2. The working potential from Figure 6-2 begins to decrease between 117 and 142 h in all 3 MFCs corresponding with the depletion of glucose within that same time frame. Glucose also decreased in the fermentations but was not fully consumed at the termination of the trial after 142 h.

The metabolite analysis established the presence and accumulation of the necessary acetate levels for *G. sulfurreducens* growth for the coculture. Both the fermentations and MFC HPLC data reveal that there are sufficient concentrations of acetate present in the medium to support *G. sulfurreducens* growth. In the MFC there is an average of 1.27 g/L in all 3 cultures after 47 h. The fermentations produced significantly less acetic acid (0.662 g/L) after 47 h however this amount is still able to support initial growth of *G. sulfurreducens* and continue to do so as the concentration of acetic acid rises with additional *P. shermanii* growth. Average yields of acetate, propionate and succinate normalized to glucose consumption are shown in Table 6-1.

Table 6-1 Average yeilds of acetate, propionate and succinate for P. shermanii fermentations and MFC trials. Standard deviation is also reported.

Average Yield	Fermentation	MFC
Acetate	0.187 ± 0.023	0.291 ± 0.056
Propionate	0.572 ± 0.041	0.616 ± 0.083
Succinate	-0.00308 ± 0.00034	0.00351 ± 0.00077

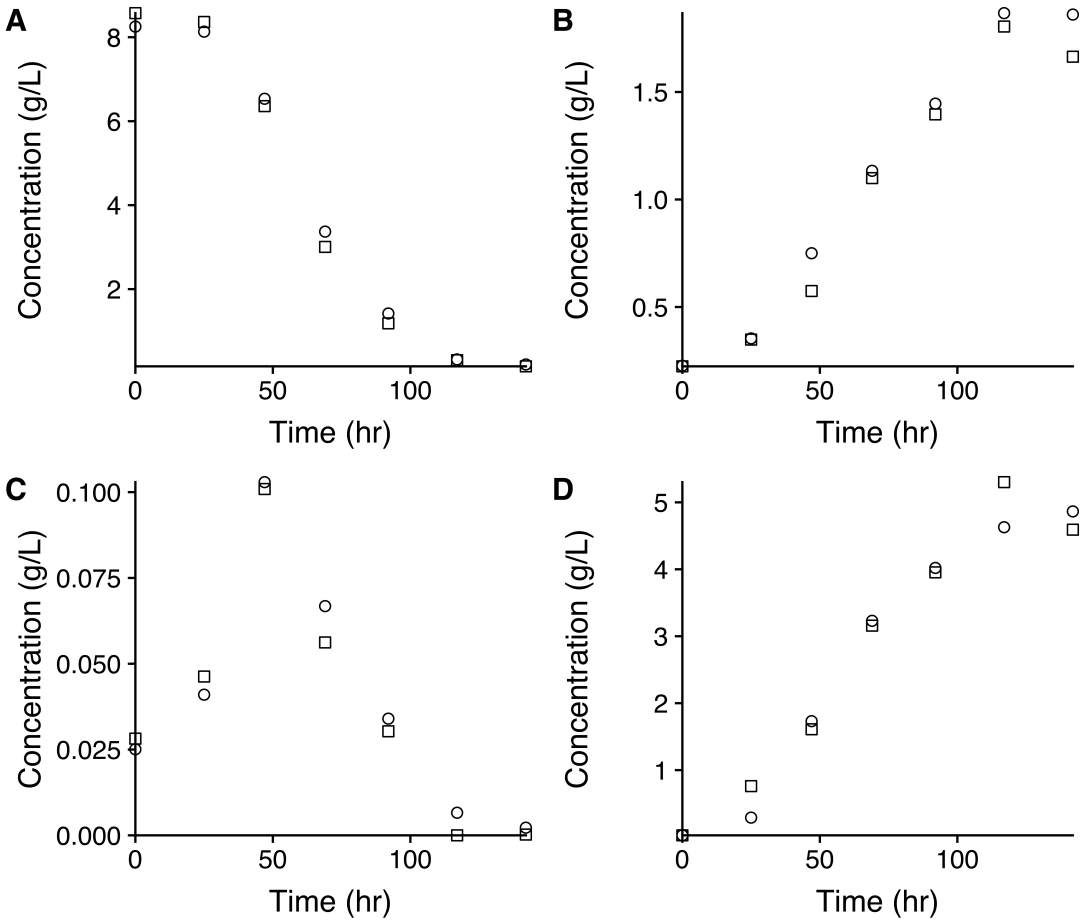

Figure 6-1 HPLC results for *P. shermanii* fermentation trials and duplicate experiments are shown. Figures A, B, C and D correspond to concentrations of glucose, acetate, succinate and propionate respectively.

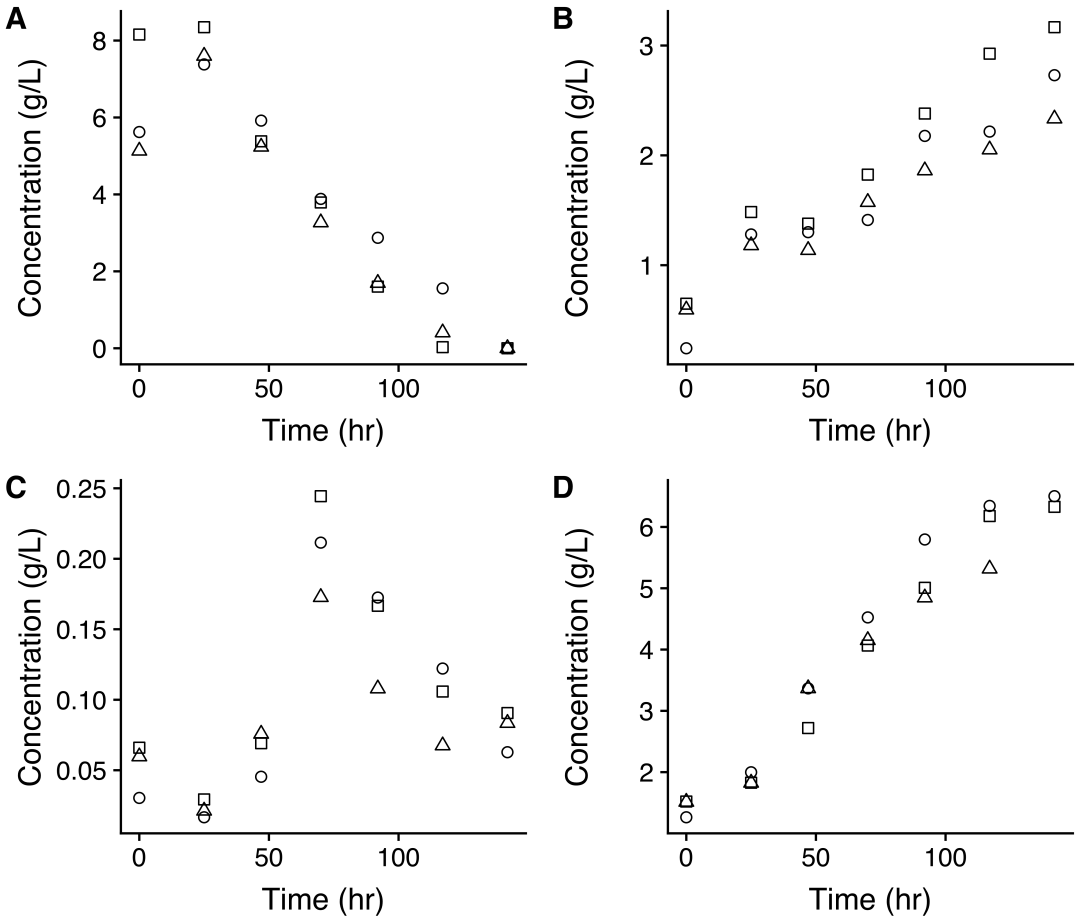

Figure 6-2 HPLC results for *P. shermanii* MFC trials and triplicate experiments are shown. Figures A, B, C and D correspond to concentrations of glucose, acetate, succinate and propionate respectively.

Yields of all three metabolites are higher in the MFC environment. The negative succinate yield in the fermentation is likely due to the presence of succinate in the inoculum. Succinic acid is an intermediary metabolite as shown in the anaerobic consumption of glucose for *P. shermanii* (Figure 2-3) which was likely introduced into the cell with the inoculum and later transformed into propionate. Data for both MFCs and fermentations exhibit a clear initial increase, peak and decrease in succinic acid concentrations illustrating the progression of *P. shermanii's* metabolic pathway.

The higher yields of end products propionate and acetate in the MFC suggest that their activity is altered in comparison to the fermentation bottle. This change in activity may be due to a multitude of factors including the available gas relief in the MFC set up. Carbon dioxide gas is able to escape via a gas trap in the MFC set up while it accumulates in the closed fermentation system. This would lead to an increase in carbonic acid in solution creating a more acidic, inhospitable environment for *P. shermanii* growth in the fermentations. The accumulation of acetic acid and propionic acid also contributes to growth inhibition due to the decrease in pH.

6.4.2 Power generation

Working potentials measured immediately after filling and inoculating the fuel cells were 296, 308 and 260 mV for cells A, B and C respectively. Recorded potential values begin once the cell equalized over a period of approximately 24 h and subsequent values were taken at various times throughout the study and are shown in Figure 6-3.

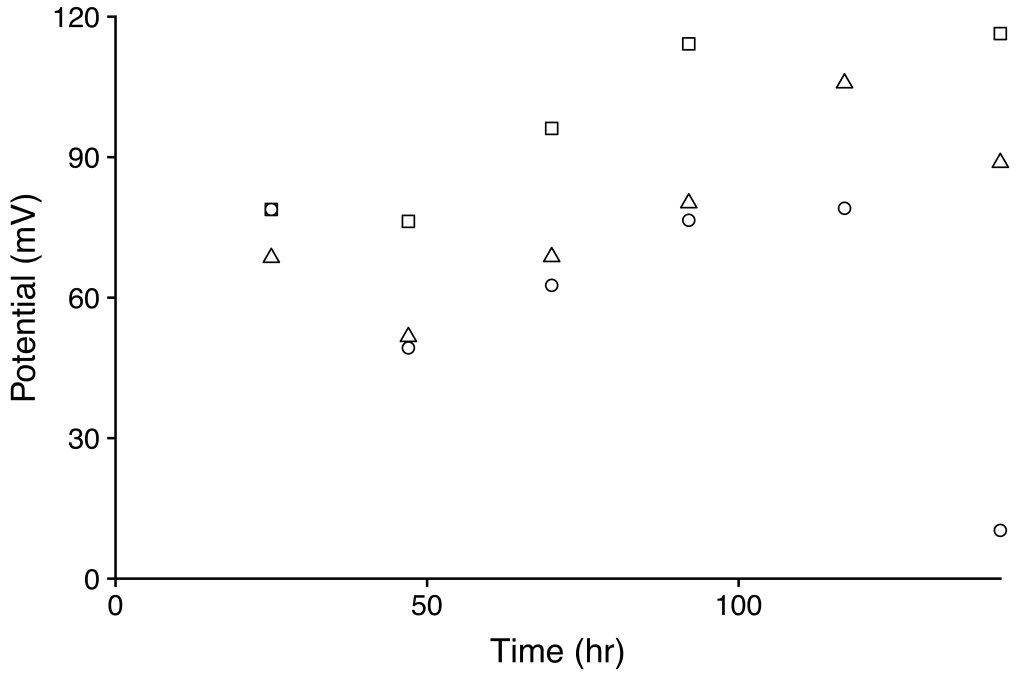

Figure 6-3 Potential achieved by *P. shermanii* grown on glucose in MFC trials. Potential was measured across a 110 Ω resistor. Triplicate experiments are shown.

A steady increase in potential occurs after 45 h with a clear peak at 117 h. The maximum potentials range from 79.1 and 131.5 mV. Cell B shows a large drop in potential at the end of the trial due to loss of liquid in the anode chamber which contributed to the lower potentials achieved by this cell.

Polarization curves were produced for each experiment to demonstrate the change of the MFC anode potential from its equilibrium state due to the flow of current. Polarization data are obtained with the use of working, counter and reference electrodes which together vary the circuit external resistance and measure the relationship between current and potential of the active MFC. The power density curve can subsequently be calculated from the same data. Polarization and power density curves generated for MFCs with *P. shermanii* as the anodic catalyst are shown in Figure 6-4.

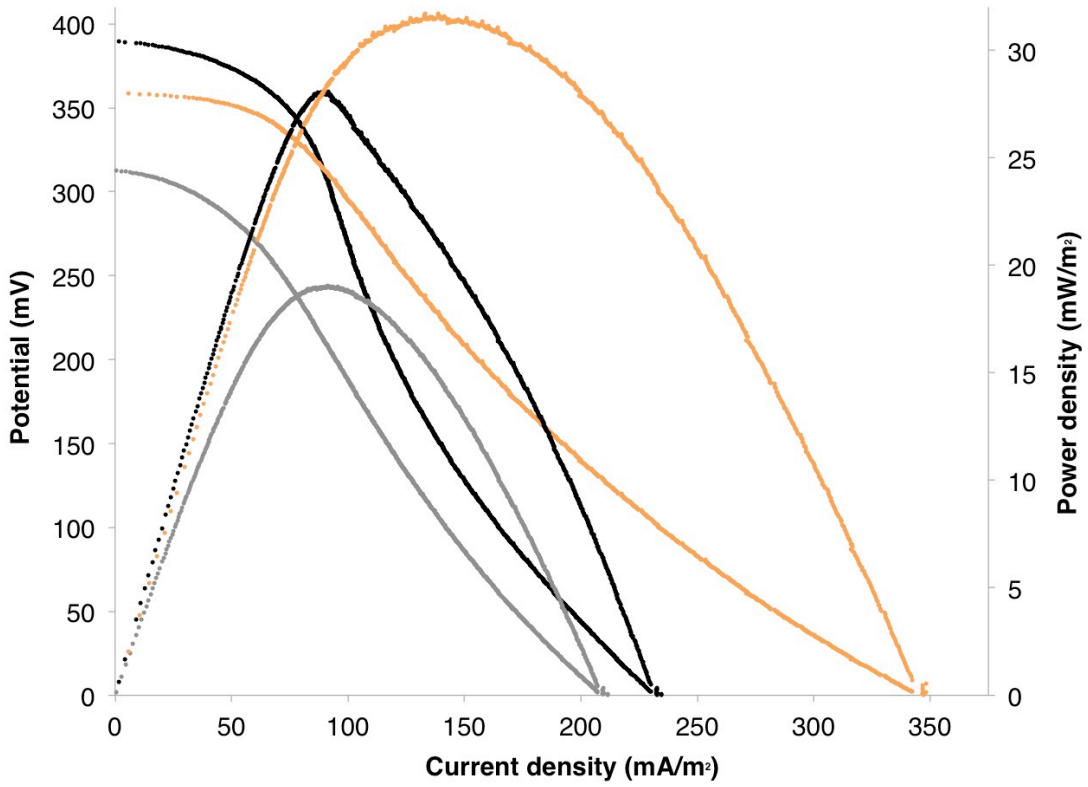

Figure 6-4 Polarization (left axis) and (right axis) power density curves observed with the use of *P. shermanii* as anodic catalyst grown on glucose. Triplicate experiments are shown and polarization and power density curves for each experiment correspond in colour. ***Current density and power density were normalized to the anode surface area. Curves were generated for each condition tested after the maximum potential was observed, which in this case occurred 95.5 h after inoculation.***

The maximum power density achieved among the MFCs run in triplicate during this trial ranged from 19.0 mW/m^2 to 31.7 mW/m^2 *P. shermanii* as a biocatalyst grown on analytical glycerol in the previous MFC design reached a maximum power density of 14.9 mW/m^2. This comparison is not equivalent due to the many differences between the two media used and the MFC designs however it is valuable to report the increase in power generation of over 100% using this biocatalyst under new conditions.

The polarization curves provide insight into the nature of the power losses during MFC operation. The initial change in potential exhibited in the range of low current densities indicates significant resistance due to activation losses. The extended period of activation losses evident in Figure 6-4 signifies that there is a slow reaction taking place at the anode. The new MFC design involved a modification of anode material from carbon cloth to carbon felt which inevitably altered the electrode microstructure. While this material is beneficial for power generation with biofilm forming bacteria, *P. shermanii* is not known to perform DET and likely produces endogenous mediating compounds to enable extracellular electron transfer like other *P. freudenreichii* strains (Wang et al. 2008). The change in material could have had a negative effect on the catalyst's exoelectrogenic activity. This change in electrode microstructure may reflect the increase in activation losses seen in this trial (Zhao et al. 2009).

The majority of the polarization data are dominated by Ohmic losses which are characteristic of the resistance to the flow of electrons throughout the circuit or resistance of ions through the membrane in MFC operation (Logan et al. 2006). Biofouling at the membrane cathode interface was observed to different extents in all three cells. The presence of this biofilm would have undoubtedly increased the resistance to ions passing through the membrane. Biofilm formation in air-cathodes occurs over long periods of operation due in part to the cation transport which concurrently transfers water molecules that are subsequently exposed to air (Pasternak et al. 2016). As a result, biofilm growth causes an increase in mass transport losses due to the reduced oxygen diffusion rates at the cathode (Pasternak et al. 2016). This phenomenon is likely the cause of the small region of mass transport losses evident in the *P. shermanii* polarization curves (Figure 6-4).

Due to the non-linear ohmic loss region of the polarization curves, an accurate estimation of the internal resistance is not possible in this trial without the implementation of electrochemical impedance spectroscopy (Zhao et al. 2009).

Electrochemical efficiencies were calculated as described by Equation 17 in Appendix A. Efficiency values found in Table 6-2 were determined assuming complete oxidation of glucose to carbon dioxide as shown in the reaction outlined in Appendix A. These values are a comparative performance indicator however the calculation assumes complete oxidation of the glucose and ignores its contribution to cell growth and other complexities intrinsic to bacterial metabolism. The theoretical maximum cell potential is therefore an overestimation of what is achievable by a living catalyst and results in lower calculated efficiencies. Nevertheless, the efficiencies are low, (<50%) and in fact lower than the maximum efficiency achieved with analytical glycerol in the previous design, which ranged from 0.23 - 0.41 (Sivell 2014).

Table 6-2 Performance indicators for MFC trials using *P. shermanii* as a catalyst and glucose as a substrate. A, B and C refer to triplicate experiments.

Trial	**A**	**B**	**C**
OCP (mV)	358	312	389
Max P_{den} (mW/m^2)	31.7	19.0	28.1
Max j (mA/m^2)	348.1	211.7	234.5
η	0.294	0.256	0.319

6.4.3 Comments on purity

MFC and fermentation cultures were streaked on RCM plates and grown aerobically and anaerobically to confirm purity of *P. shermanii.* Plates exhibited the characteristic morphology on anaerobically grown plates while an unidentified culture was observed on the aerobic plates from the MFC environment. As anaerobic conditions are necessary for power generation within the MFC, and with the inclusion of oxygen scavenger sodium thioglycolate, purity within the MFC is likely however additional analysis of the microbial community should be completed in the future.

6.4.4 Summary

Glucose consumption was achieved in all fermentations and MFCs inoculated with *P. shermanii*. Acetate concentrations were shown to be sufficient to support *G. sulfurreducens* growth after 47 h of operation. *P. shermanii* as the anodic catalyst appeared to successfully catabolize glucose and use the anode as the terminal electron acceptor to generate power. Cell A with the highest power generation had the fastest rate of glucose consumption rate among the three cells and produced the largest concentration of acetic acid. Cell C had the highest OCP resulting in the highest electrochemical efficiency.

6.5 *Geobacter sulfurreducens* with glucose

6.5.1 Consumption of glucose and metabolite analysis

HPLC data illustrating the consumption of glucose and evolution of metabolites and end products for the fermentation trial and MFC trial using *G. sulfurreducens* as a catalyst are presented in Figure 6-5 and Figure 6-6 respectively.

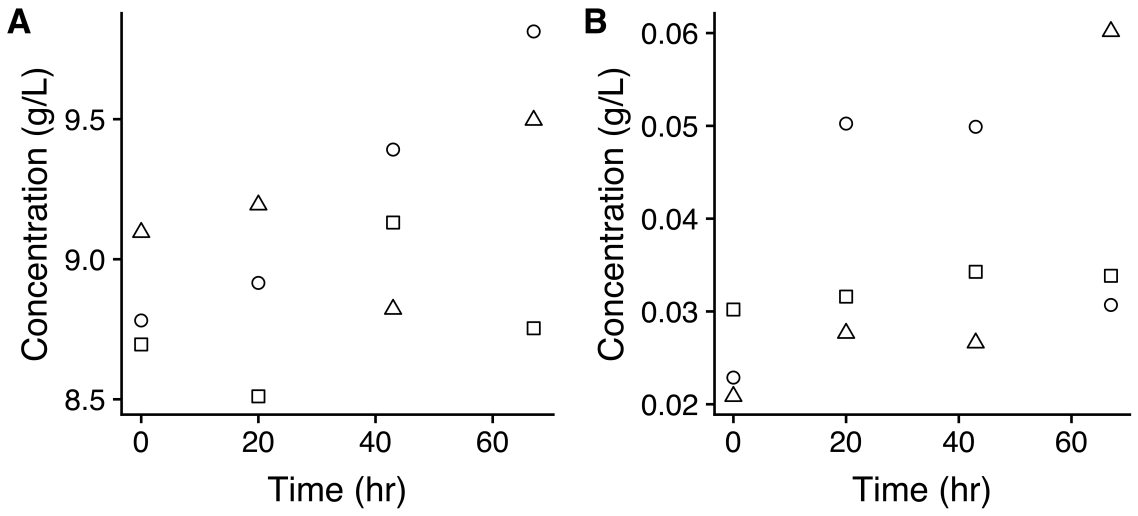

Figure 6-5 HPLC results for *G. sulfurreducens* fermentation trials and triplicate experiments are shown. Figures A and B correspond to concentrations of glucose and succinate respectively.

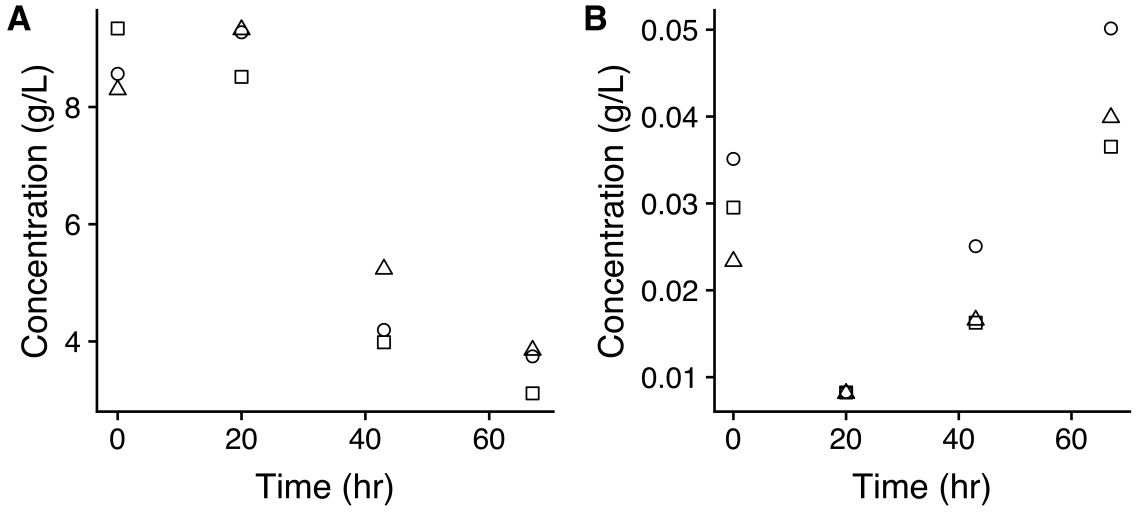

Figure 6-6 HPLC results for *G. sulfurreducens* MFC trials and triplicate experiments are shown. Figures A and B correspond to concentrations of glucose and succinate respectively.

Figure 6-6A shows that glucose was consumed in all three cells. Due to *G. sulfurreducen*'s inability to use this carbohydrate as an electron donor, consumption is likely due to the presence of a contaminant within the cell. The fuel cells are assembled in a biosafety cabinet after sterilization; therefore

contamination from bacteria in the surrounding environment is a concern in this step. Glucose is widely consumed by different bacteria, therefore as aforementioned, cultivation of the MFC media by another bacteria is not a surprising result especially if the desired bacteria are not able to use glucose as a substrate (Yang et al. 2010). The production of succinate, shown in Figure 6-6B, supports the idea that glucose is being consumed by an unidentified bacterium from the surrounding environment. As succinate is a common metabolite and part of the citric acid cycle, this metabolite could arise from a number of different bacteria.

Dissimilarly, in the fermentations a prolonged sterile environment is much easier to achieve as the fermentation bottles and medium are never exposed to air following sterilization. In this environment, consumption of glucose is not observed (Figure 6-5A). The variation shown over time is not significant as the change in glucose concentration is slight and likely due to HPLC variability. The variation in succinic acid shown in Figure 6-5B is also insignificant and likely due to variability in HPLC readings. From this, it can be deduced that there is no significant production of succinic acid in the fermentations.

6.5.2 Power generation

Working potential was taken at various times throughout the trial, values are shown in Figure 6-7.

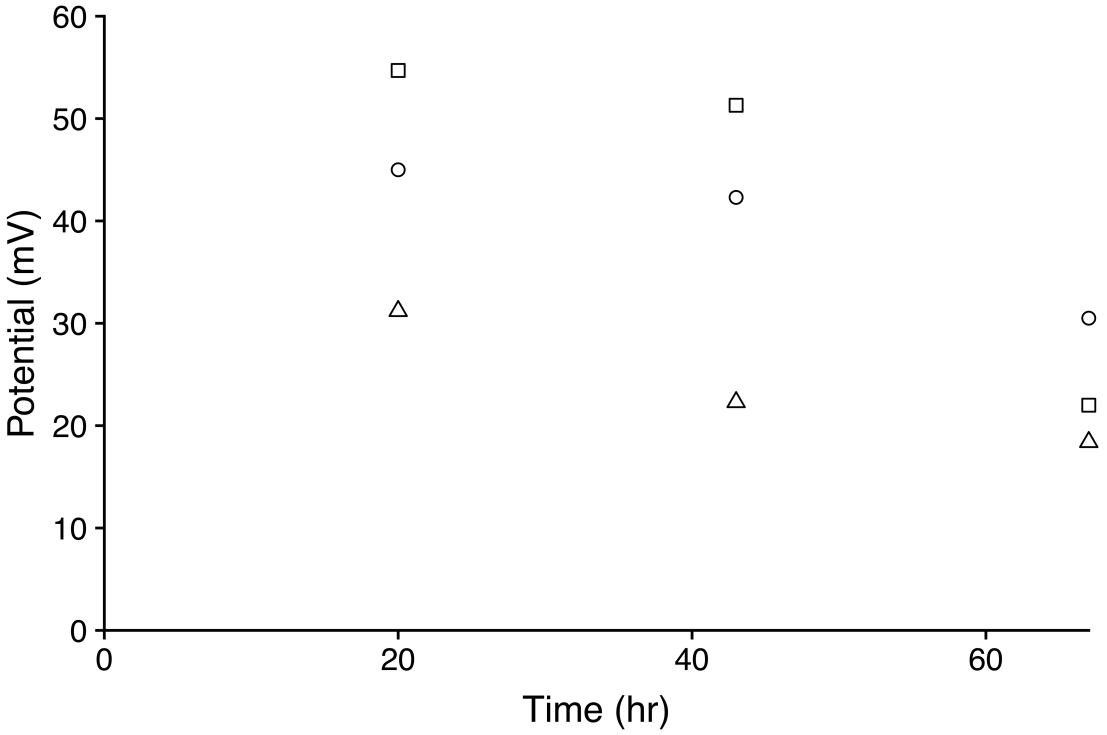

Figure 6-7 Potential achieved by *G. sulfurreducens* grown on glucose in MFC trials. Potential was measured across a 110 Ω resistor. Triplicate experiments are shown.

Initial working potentials were 110, 112 and 105 mV for cells A, B and C respectively and there was no stabilization or increase in working potential throughout the trial. Instead, a steady decrease in working potential was observed until the trial was terminated at 67 h.

G. sulfurreducens is not known to use glucose as an electron donor and therefore does not have a viable substrate to oxidize in this trial. Without an electron donor, *G. sulfurreducens* is unable to generate power through electron transfer to the anode. The steady decrease in potential after stabilization of the cell supports this hypothesis and the basal potential attained is likely only due to the difference in potential between the anode and cathode as a result of the conductivity of the salts present in the medium. With the presence of glucose in

the cell and without an inoculated bacterial culture to colonize the cell, the system is prone to contamination from surrounding bacteria. Despite the colonization from bacteria in the surrounding environment, this trial does provide an estimate of the basal working potential of the MFC system because there are no exoelectrogenic bacteria actively reducing the anode.

Polarization and power density curves generated for MFCs with *G. sulfurreducens* as the anodic catalyst are shown in Figure 6-8.

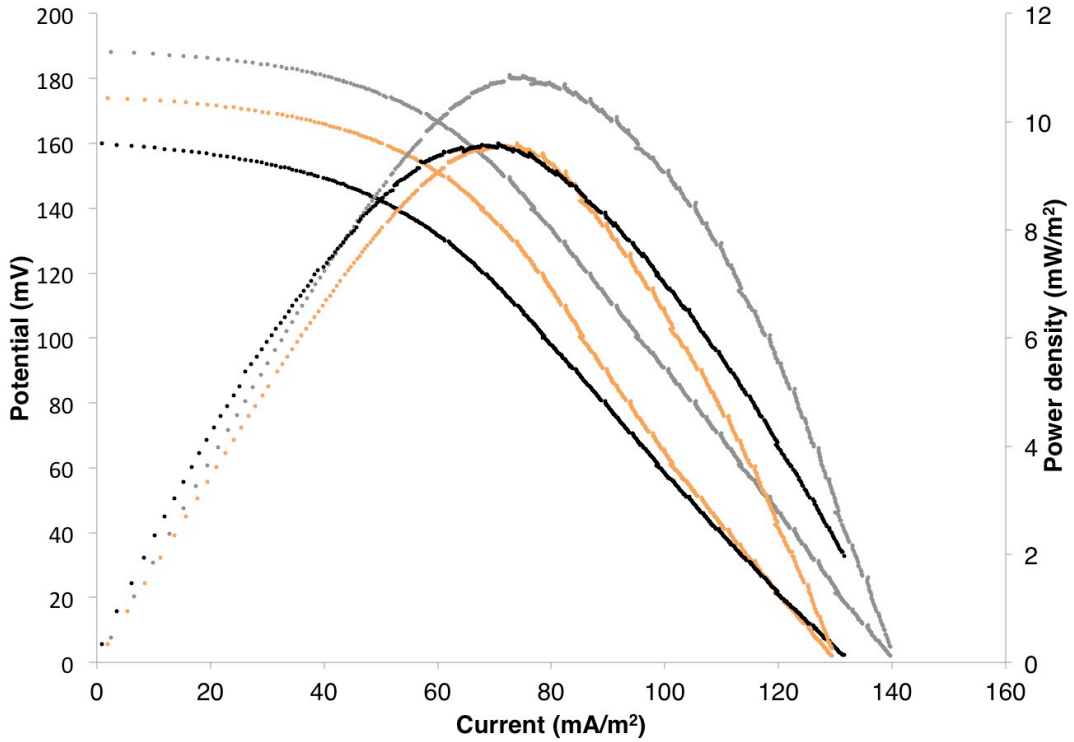

Figure 6-8 Polarization (left axis) and (right axis) power density curves observed with the use of *G. sulfurreducens* as anodic catalyst grown on acetate. Triplicate experiments are shown and polarization and power density curves for each experiment correspond in colour. *Current density and power density were normalized to the anode surface area. Curves were generated 67 h after inoculation.*

The maximum power density achieved among the MFCs run in triplicate during this trial ranged from 8.21 to 10.9 mW/m^2. The current produced during

this trial is likely a result of the conductive nature of the medium as opposed to the electrochemical activity of the bacterial. The shape of the polarization curve therefore demonstrates the inherent losses in the MFC design. The region of activation losses is pronounced in all three cells at low currents. Ohmic losses are shown to dominate the remainder of the polarization curve, indicative of the losses that can be attributed to the new air-cathode design. Due to the relatively linear nature of these polarization curves after the activation losses subside, a simplistic estimation of the internal resistance can be done. Using Equation 13 in Appendix A, the internal resistance for each cell is included in Table 6-3. These internal resistances are comparable to what was observed in the previous H-type MFC design.

Table 6-3 Performance indicators for MFC trials using *G. sulfurreducens* as a catalyst and glucose as a substrate. A, B and C refer to triplicate experiments.

Trial	**A**	**B**	**C**
OCP (mV)	188.1	174.1	159.9
Max j (mA/m^2)	139.6	129.4	131.5
Max P_{den} (mW/m^2)	10.9	9.60	8.21
η	0.179	0.184	0.083
R_{int} (Ω)	2216	2317	1904

6.5.3 Summary

Glucose consumption was observed in the MFCs but not the fermentations suggesting that a contaminant from the surrounding environment colonized the fuel cell. *G. sulfurreducens* as the anodic catalyst did not appear to catabolize glucose and use the anode as the terminal electron acceptor to generate power. This trial successfully provided an approximation of a negative control for the

MFC operation in the absence of any anodic exoelectrogenic activity by a biocatalyst.

6.6 *Geobacter sulfurreducens* with acetate

To confirm the activity of *G. sulfurreducens* in the air-cathode experimental set up, a trial was performed with acetate as the substrate. *G. sulfurreducens* is known to use acetate as a preferred electron donor, therefore this trial served to be a positive control for the biocatalyst. This experiment required the use of fumarate as the terminal electron acceptor to permit growth in the fermentations, while the anode served as the sole electron acceptor in the MFC.

6.6.1 Consumption of acetate and metabolite analysis

HPLC data illustrating the consumption of acetate and evolution of metabolites and end products for the MFC trial using *G. sulfurreducens* as a catalyst is presented in Figure 6-9.

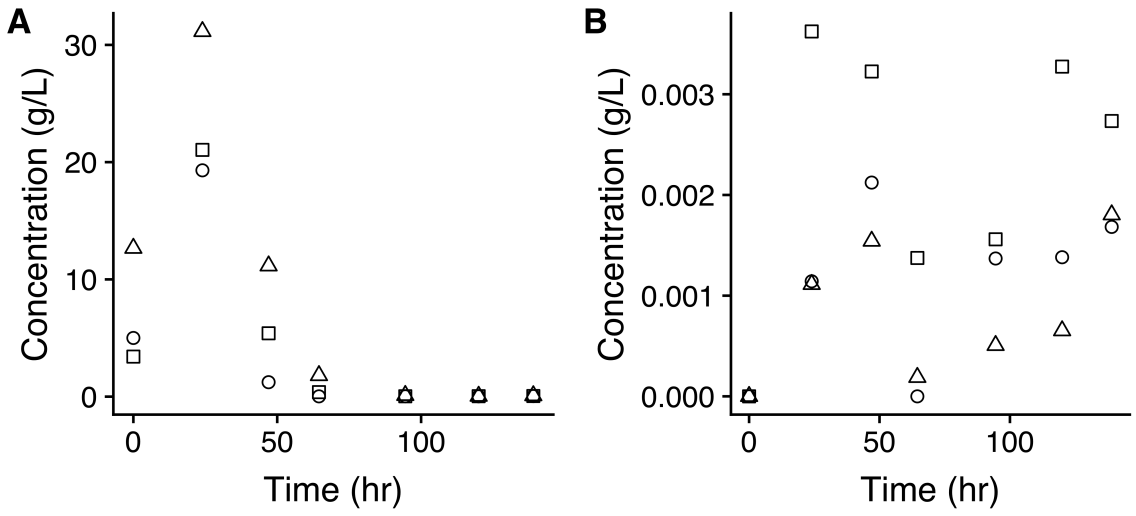

Figure 6-9 HPLC results for *G. sulfurreducens* MFC trials and triplicate experiments grown on acetate are shown. Figures A and B correspond to concentrations of acetate and succinate respectively.

Complete consumption of acetate is achieved in the MFC environment. Quantification of acetate values in MFC were challenging to extract due to an unidentified nearby peak in the HPLC results that was detected in this trial. Acetate concentrations reported at 24 h show a large increase in acetate, which is unfitting since no additional acetate was added at this time and acetate is not produced by *G. sulfurreducens*. Despite these uncertainties, the conclusion that acetate was fully consumed in all cells between 64 and 94 h is concrete as the peak at the standard retention time fully disappeared by the end of the trial. This depletion of acetate also corresponded with the drop in working potential shown in Figure 6-10. Galushko and Schink found that in a similar experimental setup, *G. sulfurreducens* consumed 1.1808 g/L (20mM) acetate in 60 h. This study exhibits comparable results. Additionally, there was no clear trend observed with succinate in the MFCs

HPLC analysis of the fermentations was not possible due to an overlap in peak activity at the acetate and succinate retention time. This could have been due to the abundance of fumarate in the media.

6.6.2 Power generation

Working potential was taken at various times throughout the trial, values are shown in Figure 6-10.

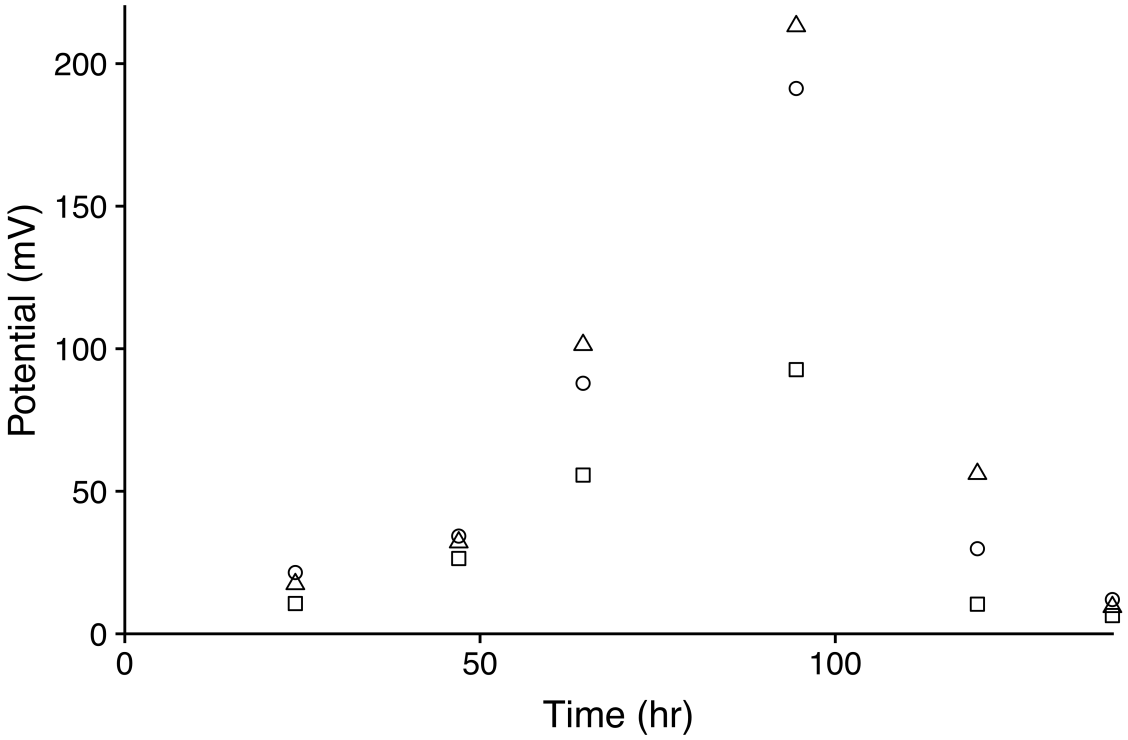

Figure 6-10 Potential achieved by *G. sulfurreducens* grown on acetate in MFC trials. Potential was measured across a 110 Ω resistor. Triplicate experiments are shown.

Initial potential started at 77.4, 108.1 and 90.3 mV for the cells A, B and C respectively and the plotted values were recorded once the cell equalized over a period of approximately 24 h. A steady increase in potential is shown with a clear peak at 94.5 h for all cells with maximum potentials in the range of 92.7 to 213.2 mV.

The low potential achieved by cell A is likely due to leak of air into the anode chamber upon inspection of the setup. The presence of oxygen may not have been significant enough to fully inhibit acetate consumption by G. *sulfurreducens*, however oxygen would have acted as the terminal electron acceptor inside the anode therefore decreasing the amount of electrons transferred to the anode for electricity production.

Polarization and power density curves generated for MFCs with *G. sulfurreducens* as the anodic catalyst are shown in Figure 6-11. The maximum power density achieved among the MFCs ranged from 22.7 to 51.9 mWm^2. Polarization curve of cell A exhibited the lowest OCP and power density which was consistent with the observed partially aerobic condition .The region of activation loss at low current densities in cells B and C was less pronounced than in the pure *P. shermanii* MFCs. Based on the new microstructure of the electrode that lends to biofilm formation and DET, this was likely a beneficial modification for *G. sulfurreducens* which is known for both phenomena.

The maximum power density was achieved by cell C while cell B had the highest OCP. The polarization curve for cell C clearly exhibited less activation loss compared to cell B which suggests a difference in catalyst behaviour at the anode. The presence of a more robust biofilm on the anode surface likely contributed to the superior power generation and lesser activation losses seen from Cell B.

Ohmic losses continue to dominate the remainder of the MFCs which pertain to the internal losses in the MFC design. Due to the non-linear ohmic loss

region of the polarization curves, an estimation of the internal resistance was not considered in this trial.

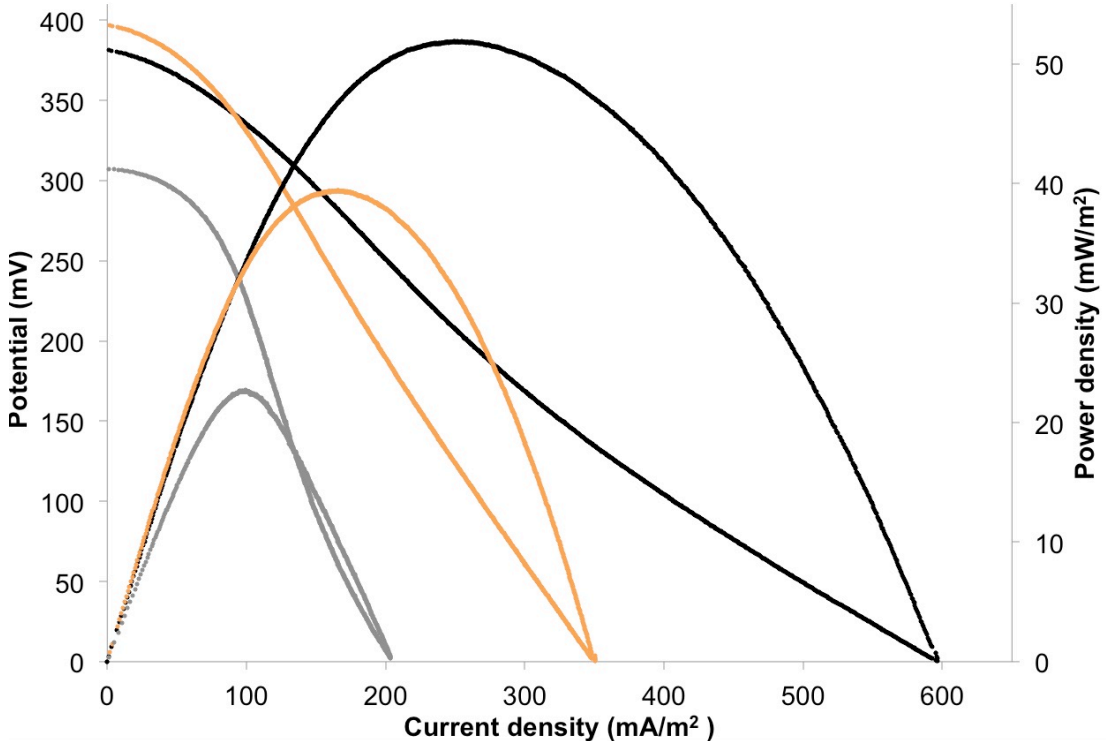

Figure 6-11 Polarization (left axis) and (right axis) power density curves observed with the use of *G. sulfurreducens* as anodic catalyst grown on acetate. Triplicate experiments are shown and polarization and power density curves for each experiment correspond in colour. *Current density and power density were normalized to the anode surface area. Curves were generated for catalyst after the maximum potential was observed, which in this case occurred 94.5 h after inoculation.*

Electrochemical efficiencies were calculated as described by Equation 17 in Appendix A. Efficiency values found in Table 6-4 were determined assuming complete oxidation of acetate to carbon dioxide as shown in the reaction outlined in Appendix A. As with the efficiencies calculated with glucose, the theoretical

maximum cell potential is also an overestimation of what is achievable in practice. Once again, the efficiencies are low, (<50%) ranging from 0.25 - 0.35.

Table 6-4 Performance indicators for MFC trials using *G. sulfurreducens* as a catalyst and acetate as a substrate. A, B and C refer to triplicate experiments.

Trial	**A**	**B**	**C**
OCP (mV)	307.3	396.7	381.2
Max j (mA/m^2)	203.6	350.5	596.7
Max P_{den} (mW/m^2)	22.7	39.4	51.9
η	0.252	0.325	0.312

6.6.3 Summary

Complete consumption of acetate was achieved in all three MFCs using *G. sulfurreducens* as a pure catalyst. Power generation was observed in all three cells and power densities were higher than that achieved by pure *P. shermanii*. This trial provided a successful positive control for *G. sulfurreducens* in the air-cathode design. Metabolite analyses for the fermentations were inconclusive.

6.7 Conclusions

The performance of pure biocatalysts *P. shermanii* and *G. sulfurreducens* was successfully evaluated in the air-cathode design. While equivalent conditions were designed for the triplicate runs, differences in reproducibility were observed in the pure culture MFCs. The maximum power density of *P. shermanii* was increased compared to previous experiments with the H-type MFC design. *G. sulfurreducens* was shown not to produce any electricity without its preferred substrate of acetate. When acetate was present as an electron donor, *G.*

sulfurrenducens produced a higher power density than pure *P. shermanii*. The bacterial quantification protocol using gram stain and microscopy did not produce useful results for the pure cultures therefore future experimentation should employ a new quantification method which will be discussed in Chapter 8.

Chapter 7 Coculture Fermentations and Air-cathode MFC Performance

7.1 Introduction

The following chapter presents the results of coculturing *Propionibacteria freudenreichii* ssp. *shermanii* with *Geobacter sulfurreducens* in batch fermentation and as a cocatalyst in an air-cathode MFC. Two trials for the coculture were performed. Due to the characteristic variability of anaerobic cultures, the two trials and their distinct issues and successes will be presented and discussed.

7.2 Coculture experiment

In the *G. sulfurreducens* preferred medium, it was provided with 0.82 g/L (13.9mM) acetate and as an active culture, has previously been shown to consume 20mM acetate in 60 h (Galushko and Schink 2000). From the metabolite analysis performed in Chapter 5, it was determined that after 48 h of growth there would be sufficient acetate produced by *P. shermanii* to support the growth of *G. sulfurreducens*.

MFCs were sterilized, filled with MFC media containing 10g/L glucose as the primary substrate and inoculated with 10% v/v (of the final working anode volume) of *P. shermanii* pre-culture in exponential growth. The anode and cathode were connected with an external load of 110 Ω and voltage was measured as with the pure cultures in Chapter 6. After 48 h of growth, 10% v/v *G. sulfurreducens* was introduced into the anode chamber. Polarization data was gathered at the height of voltage production. Triplicate fermentations in the same

medium were run alongside the MFCs following the same inoculation protocol. Samples were taken from the anode and fermentations to monitor glucose consumption and metabolite evolution.

7.3 *Propionibacteria freudenreichii* ssp. *shermanii* and *Geobacter sulfurreducens* as cocatalysts

7.3.1 Consumption of glucose and metabolite analysis in fermentation

Due to the variable nature of growth seen with anaerobic organisms, two different trials were conducted to encapsulate the cocatalyst's potential. The fermentation data gathered form the first trial exhibited concrete evidence of the ability for the two bacteria to coexist in the newly designed coculture medium. However, the cocatalyst inoculated from the same pre-culture did not appear to survive the MFC environment as power generation ceased abruptly after the addition of *G. sulfurreducens*. Despite this incongruity, valuable insight was gained from the fermentation through macroscopic observations and from HPLC analysis. Table 7-1 and Figure 7-1 display the macroscopic evidence that was gained in the lab.

Table 7-1 Macroscopic observations of coculture batch fermentations.

Trial	Macroscopic observation
1	- Slightly turbid prior to *G. sulfurreducens* inoculation - Red cultures first appear at 165 h time sample
2	- Most turbid prior to *G. sulfurreducens* inoculation - Red cultures first appear at 93.5 h time sample - Most red cultures, settled at bottom of vial at end of trial
3	- Least turbid - Red cultures only appear at final time sample of 235 h

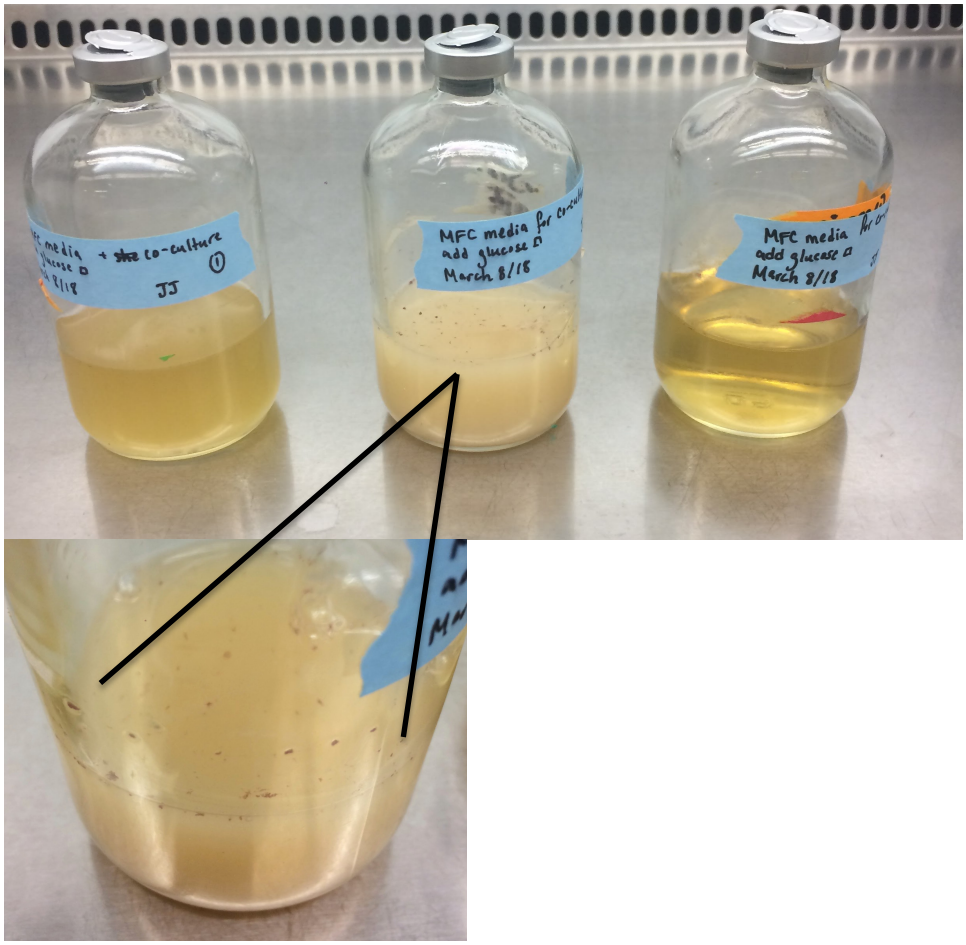

Figure 7-1 Macroscopic evidence of coculture growth in fermentation bottles. Image A shows the variation between the triplicate fermentations. Image B shows a close up view of characteristic red *G. sulfurreducens* culture.

HPLC data illustrating the consumption of glucose and evolution of metabolites and end products for the fermentation trial using *G. sulfurreducens* and *P. shermanii* as cocatalysts is presented in Figure 7-2.

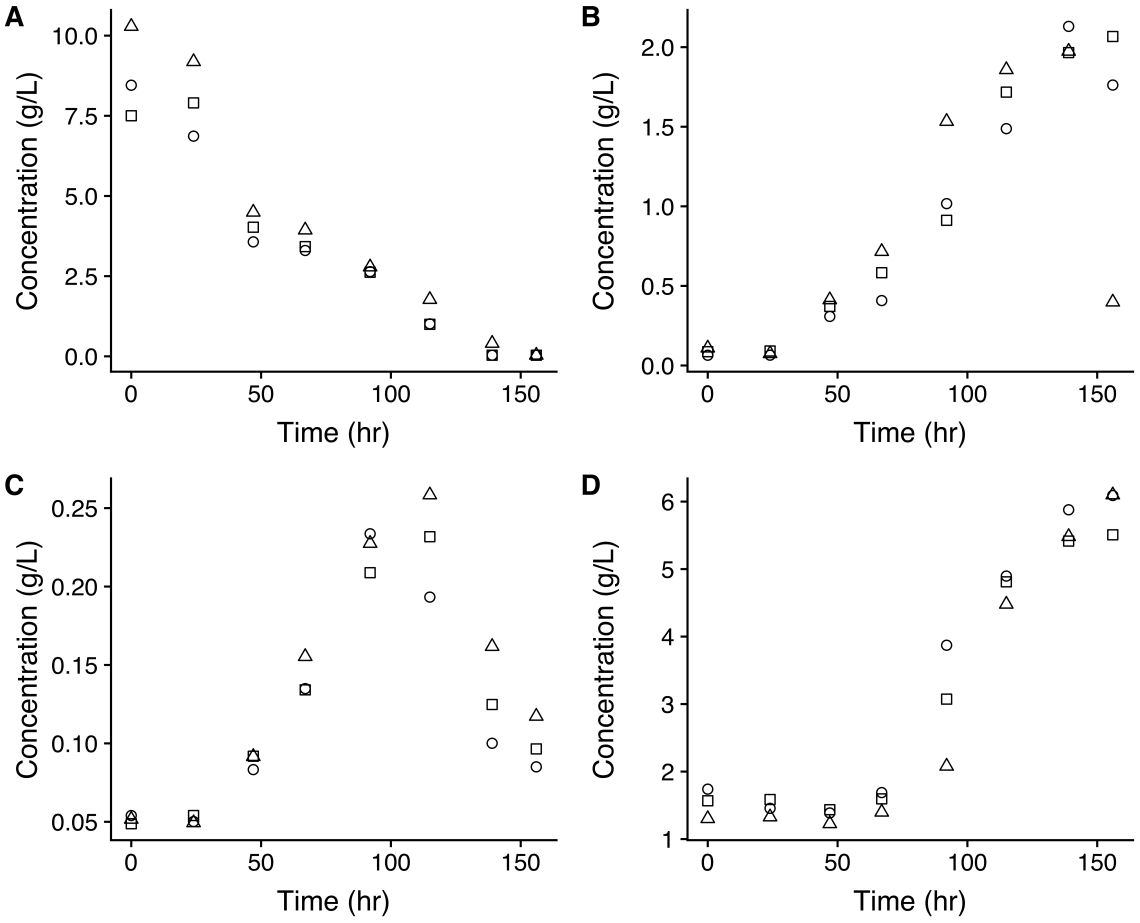

Figure 7-2 HPLC results for cocatalyst *P. shermanii* and *G. sulfurreducens* fermentation trials and triplicate experiments are shown. Figures A, B, C and D correspond to concentrations of glucose, acetate, succinate and propionate respectively.

Most notably from the fermentations, production of propionic acid and the characteristic appearance of a red culture in the liquid medium confirmed the presence and growth of both coculture strains. The propionate concentration reached an average of 5.60 ± 0.50 g/L with a slight plateau which is comparable to the concentration and trend seen in the pure *P. shermanii* culture.

In the fermentation medium, *G. sulfurreducens* did not have access to a viable electron acceptor, which must have facilitated an obligate syntropic relationship between the two species. While obligate syntropic relationships are

commonly found in anaerobic environments in nature, the pairing of *Geobacter* and *Propionibacteria* does not occur naturally. Furthermore, a thorough search of the relevant literature did not yield any indication of a comparable coculture being explored in synthetic environments in the lab. The coexistence of both species in this medium provided preliminary evidence of the obligate syntropic DIET between *G. sulfurreducens* and *P. shermanii*. Further characterization of the metabolic interactions are necessary to fully exploit the exoelectrogenic activity of both species. With this preliminary result, Chapter 8 will elaborate on the procedures needed to fully evaluate the viability of this novel cocatalyst.

The acetate levels reached in the pure culture of *P. shermanii* compared to the coculture provide insight into acetate use by *G. sulfurreducens*. From Chapter 6, the pure culture acetic acid concentrations (Figure 6-1B) form a plateau at the termination of the trial with an average concentration of 1.76 ± 0.139 g/L. In contrast, the coculture acetate concentrations converge at stable values in all three experiments, but with a reduced average concentration of 0.949 ± 0.02 g/L. This is the preferred metabolite to support the growth of *G. sulfurreducens* therefore this difference could be a result of consumption of acetate by *G. sulfurreducens*.

The average yield of succinic acid in the pure culture was negative ($-3.08 \times 10^{-3} \pm 3.4 \times 10^{-3}$) due to the final succinate concentration being less than that which was carried in with the inoculum medium. The average yield of succinic acid in the coculture was $34.7 \times 10^{-3} \pm 18.9 \times 10^{-3}$. Due to the difference in runtimes of both trials, yields were calculated for samples at the time closest to the termination of the pure culture run time of 142 h. For the coculture fermentation

this corresponded to the sample being taken at 141 h. The aforementioned lag time of glucose consumption by *P. shermanii* in the coculture is likely the cause of the elevated succinate concentrations at the comparable sample time of the pure culture. Otherwise, succinate progression follows a similar trend in both the pure and coculture.

7.3.2 Consumption of glucose and metabolite analysis in the MFC

HPLC data illustrating the consumption of glucose and evolution of metabolites and end products for the MFC trial using *G. sulfurreducens* and *P. shermanii* as cocatalysts is presented in Figure 7-3.

Glucose was fully consumed in all three MFCs after 139 h of operation. The deviation in metabolic rates seen in the batch fermentation of *P. shermanii* may have also occurred in the MFCs resulting in the reduced activity of the coculture in the MFC environment. As was discussed in Chapter 6, despite the observed consumption of glucose, the potential slow initial growth by *P. shermanii* leaves the MFC vulnerable to contamination.

Similar to the trend observed in the fermentations, the acetic acid levels reached in the pure *P. shermanii* MFC compared to the coculture MFC also reflected consumption by *G. sulfurreducens.* The pure culture of *P. shermanii* accumulated an average of 2.74 ± 0.41 g/L acetic acid at the termination of the study without fully exhibiting a plateau. In contrast, two of the three coculture MFCs reached a maximum concentration of acetic acid at 139 h and concentrations decreased in these cells towards the end of the study. The average concentration of acetic acid among all three cells was 1.41 ± 0.89 g/L. The large

standard deviation can be attributed to one cell in which the concentration of acetic acid reached 0.399 g/L. This outlier was Cell C which experienced a leak, however without inclusion of this data point the average acetic acid concentration in the remaining MFCs was 1.91 ± 0.21 g/L which was still considerably lower than the concentration found with pure *P. shermanii*. The reduced acetate concentrations of the coculture suggest that the metabolite is being consumed by *G. sulfurreducens* to support growth.

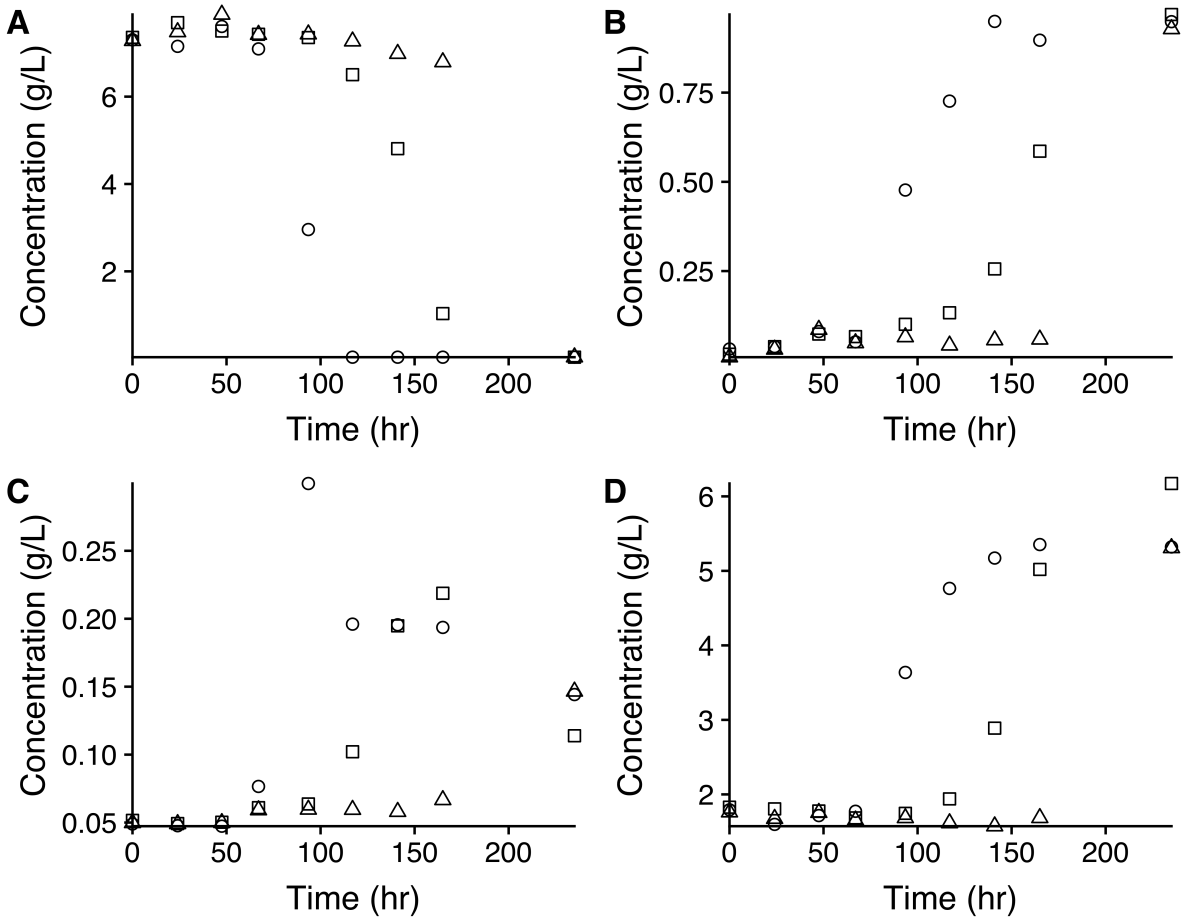

Figure 7-3 HPLC results for cocatalyst *P. shermanii* and *G. sulfurreducens* MFC trials and triplicate experiments are shown. Figures A, B, C and D correspond to concentrations of glucose, acetate, succinate and propionate respectively.

Propionate concentration reached an average of 5.80 ± 0.41 g/L without reaching a plateau. This observation suggests that the concentration of propionate was not yet inhibiting *P. shermanii* growth at the termination of the study. The decrease in acetate concentration likely resulted in a more habitable pH for *P. shermanii*. A pH analysis throughout and at the end of the fermentation would further elucidate its effect on growth.

Similar to what was observed in the pure *P. shermanii* MFC trial, the progression of succinate throughout the coculture trial follows the characteristic accumulation and consumption of the acid. The average yield of succinate in the pure culture and coculture was $3.51x10^{-3} \pm 0.76x10^{-3}$ and $8.93x10^{-3} \pm 3.0\ x10^{-3}$ respectively. To normalize the yields to time, the 139 h sample was used for the coculture MFC yield calculation. The increase in succinate yield may be a reflection of the lag time previously discussed to be associated with the coculture progression and growth. The yield calculated at the termination of the coculture was found to be $5.49x10^{-3} \pm 1.56x10^{-3}$ which is still more than that obtained at the end of the pure culture. Therefore the change in succinate levels can likely be attributed to the *G. sulfurreducens* growth in the coculture as *G. sulfurreducens* also transiently produces succinate in its central metabolism of acetate.

7.3.3 Power generation

The initial trial exhibited a steady decrease in cell potential, however the fermentations provided important insight into the cocatalyst behaviour which will be discussed below. Working potential was taken at various times throughout the subsequent trial for which values are shown in Figure 7-4.

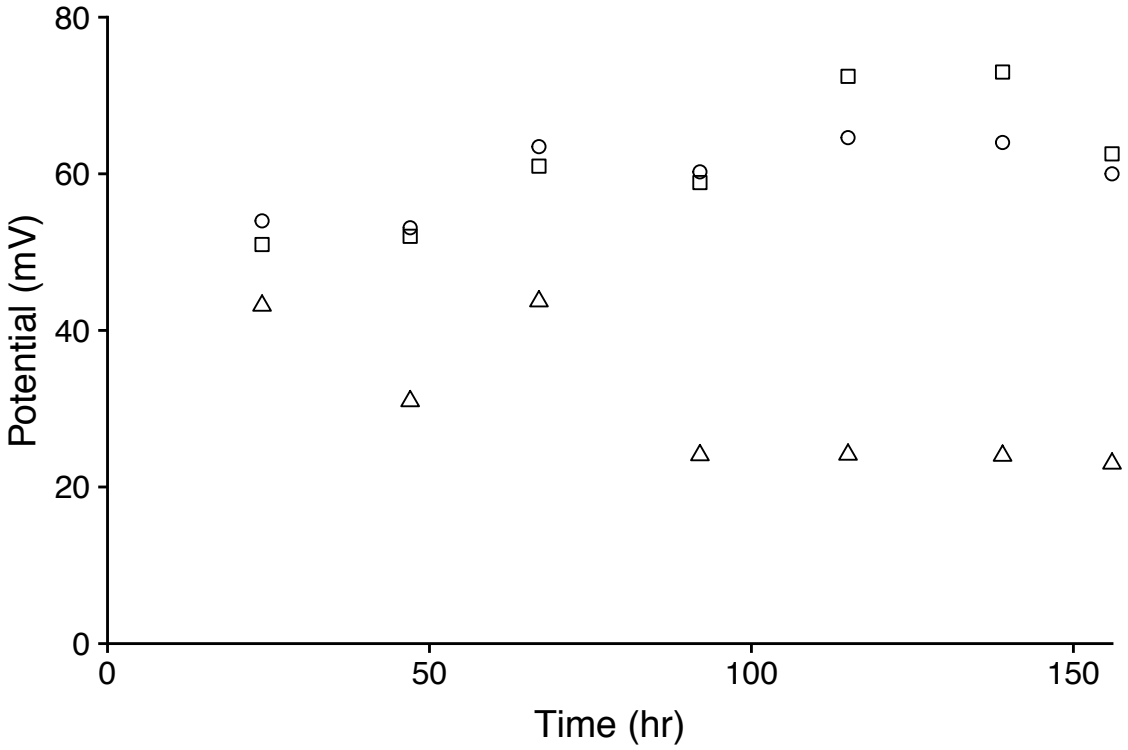

Figure 7-4 Potential achieved by the coctalyst of *P. shermanii* and *G. sulfurreducens* grown on glucose in MFC trials. Potential was measured across a 110 Ω resistor. Triplicate experiments are shown.

The second trial exhibited an increase in potential after the addition of *G. sulfurrenducens* in two of the three cells. Initial working potential started at 163, 161 and 93 mV for the cells A, B and C respectively. The exceptionally low potential exhibited by MFC C was attributed to a leak in the anode. While the power generated by the other two MFC experimental setups was low compared to the pure catalysts, the analytical data ascertains the successful coculture of this novel cocatalyst and establishes the foundation of the cooperative potential between these exoelectrogens. The trial was terminated once working potential began to decrease. Performance indicators for the triplicate experiments are provided in Table 7-2.

Table 7-2 Performance indicators for cocatalyst *P. shermanii* and *G. sulfurreducens* MFC trials with glucose as a substrate. A, B and C refer to triplicate experiments.

Trial 2	**A**	**B**	**C**
OCP (mV)	218.8	224.4	101.2
Max j (mA/m^2)	166.9	182.6	154.9
Max P_{den} (mW/m^2)	12.3	14.0	8.04
η	0.179	0.184	0.083

Polarization and power density curves generated for MFCs with the coculture of *P. shermanii* and *G. sulfurreducens* as the anodic catalyst are shown in Figure 7-5.

The maximum power density achieved among the MFCs run in triplicate during this trial ranged from 8.04 mW/m^2 to 14.0 mW/m^2.

While cell C generated the lowest power due to a leak, the polarization curve shape does provide some insight into the losses incurred by a malfunctioning MFC. The activation loss portion of the curve extends well past the low current density region which reveals that an unusually slow reaction is taking place at the anode. The activation loss in this case is even more pronounced than in the trial *G. sulfurreducens* grown without a viable substrate. This nonstandard polarization curve is likely a result of oxygen diffusing into the anode chamber. A loss in anaerobic anodic conditions would further hinder the microbe's activity and the availability and transfer of free hydrogen ions and electrons throughout the circuit. The polarization curve is therefore reflective of

the experimental condition in this case. The remaining two experiments exhibit similar losses as seen in the pure *G. sulfurreducens* and *P. shermanii* trials.

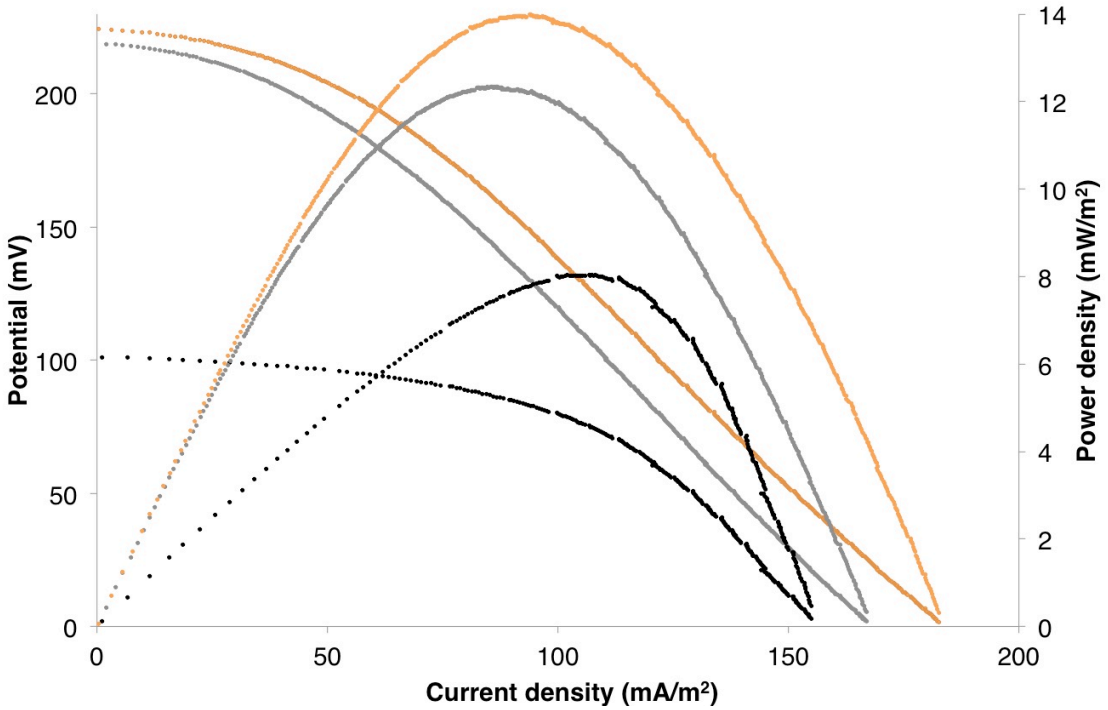

Figure 7-5 Polarization (left axis) and (right axis) power density curves observed with the use of *P. shermanii* and *G. sulfurreducens* as anodic cocatalyst grown on glucose. Triplicate experiments are shown and polarization and power density curves for each experiment correspond in colour. ***Current density and power density were normalized to the anode surface area. Curves were generated for each catalyst after the maximum potential was observed, which in this case occurred 115 h after inoculation.***

MFC B, which produced the maximum power density among the coculture trials had the greatest amount of red culture at the termination of the trial which is indicated in the macroscopic observations in Table 7-1. This observation adds credence to the hypothesis that there is a contribution of exoelectrogenic activity from *G. sulfurreducens* in this trial.

7.3.4 Evidence of syntropic interactions

Together, the two trials determine an initial picture of the cocatalyst viability. The trials exposed the extent of variability in anaerobic growth of *P. shermanii* which is an influential factor pertaining to the success of the cocatalyst. The prolonged fermentation demonstrated the progression of the coculture by way of macroscopic red culture which appeared in all three cultures as each fermentation progressed at different times. As discussed earlier, variation is characteristic of anaerobic growth however the delay in *P. shermanii* growth was exceptional to this trial. Nevertheless, this would have incurred a detrimental effect on the extent of power generation in the MFC environment. A timely in vivo determination of acetate concentrations would help to establish appropriate inoculation times for *G. sulfurreducens* based on the observed variations.

The observed growth of *G. sulfurreducens* without a terminal electron acceptor is crucial to note. With this preliminary finding, additional information regarding the DIET interactions with *P. shermanii* should be characterized to fully harness the exoelectrogenic activity of both catalysts. A similar relationship was investigated with *G. sulfurreducens* in coculture with *Clostridium pasteuraniumi* in which *G. sulfurreducens* was able to grow using *C. pasteuraniumi* as the sole terminal electron acceptor (Moscoviz et al. 2017). In turn, a shift in metabolic activity towards one end product and a decrease in biomass production was observed (Moscoviz et al. 2017). A shift towards more end product production and less biomass growth would be beneficial in the MFC setting as this would improve the coulombic efficiency as more electrons would be transferred to the anode as opposed to being used in the production of biomass (Logan et al. 2006).

The effect of the syntropic coculture relationship should therefore be thoroughly investigated.

In the aforementioned coculture studies, PCR is used to identify and distinguish the microbial growth. Due to the lack of information gained from microscopy, a preliminary protocol for PCR analysis was completed and is discussed in Chapter 8. Furthermore, the abundance of propionic acid produced in the MFC supports the original proposal to employ *G. metallireducens* as the cocatalyst. Hypotheses regarding the use of this strain of *Geobacter* will also be discussed in Chapter 8.

7.3.5 Comments on purity and quantification

MFC and fermentation cultures were streaked on RCM plates and grown both aerobically and anaerobically prior and after the addition of *G. sulfurreducens* to confirm purity of *P. shermanii.* Plates exhibited the characteristic morphology on anaerobically grown plates while an unidentified culture was observed on the aerobic plates from the MFC environment. As anaerobic conditions are necessary for power generation within the MFC, and with the inclusion of oxygen scavenger sodium thioglycolate, the purity within the MFC is probable however additional analysis of the microbial community should be completed in the future.

Gram stained slides were prepared at each time point sampled for the fermentations and MFCs. The slides that were prepared from the MFC at 67 h of operation provided confirmation of the presence of both species of bacteria via distinguishable colour difference of the two cultures. Despite vortexing the

samples, improved counting methods are needed due to non-uniform distribution on the slide and disparity of staining that occurs with cells at different stages of growth.

7.4 Conclusions

From the fermentations, production of propionic acid and the characteristic appearance of the red culture in the medium confirmed the presence and growth of both coculture strains. In addition, the MFC trials provided evidence of power generation accomplished by the novel coculture. An understanding of the contribution from each bacterium is necessary to improve the electrical output. For this reason, Chapter 8 will be devoted to a discussion about the tools and procedures needed to alleviate the issues encountered during this project with the aim of fully evaluating the viability of the cocatalyst.

Chapter 8 Experimental Design Optimization

This chapter serves to propose protocols and projects with the aim of ameliorating the performance and evaluation of the cocatalyst. Some of these ideas were investigated during experimentation while others were developed upon analysis of the cocatalyst results. The shortcomings that were observed in Chapter 7 will be addressed and potential solutions to advance the efficacy of the cocatalyst will be presented in this chapter.

8.1 Microbial community analysis

The gram stain and microscopy protocol developed for this study was designed to provide confirmation of the presence of both microbes in the coculture. Unfortunately the slide preparation method did not produce useful results therefore a more robust identification and quantification protocol should be used.

A more suitable option for this project would be qPCR, which is a widely used method to quantify diverse microbial consortia with accuracy and efficiency. This technique involves amplifying DNA to a detectable level to allow for quantification. Primers can be designed to anneal to a DNA sequence that is unique to a specific bacteria therefore amplifying genes that are exclusive to the microbe of interest. The standard curve method then employs a serial dilution of known template concentrations to establish a correlation between qPCR amplification and biomass concentration to attain quantitative results.

As this synthetic coculture does not exist in nature, an effort to understand and manage the cooperative effects of the interaction should also be investigated in the future.

A proof of concept experiment illustrating *Clostridium pseudomonas* as a viable sole electron acceptor in coculture with *G. sulfurreducens* employed qPCR technique to quantify the coculture growth and also to define the interactions between the species (Moscoviz et al. 2017). With biomass data gained from qPCR and by considering several assumptions, Moscoviz et al. 2017 managed to provide hypothetical carbon and electron balances to rationalize the formation of distinct metabolic shifts that occurred in the coculture environment. This analysis would be greatly beneficial to this current project to solidify the hypothesis that *G. sulfurreducens* is able to use *P. shermanii* as an electron acceptor and also to gain an understanding of the metabolic shifts that are occurring in the MFC and fermentation coculture environment. It is also interesting to note that out of 4 coculture replicates in Moscoviz et al.'s project, only 2 of them exhibited *G. sulfurreducens* growth. This lack of robust coculturing of *Clostridium pseudomonas* and *G. sulfurreducens* is similar to what was encountered in the cocatalyst trials in Chapter 7.

In addition to quantifying the microbial community present in the bulk anodic media, sampling the community present on anode would also help to generate a spatial understanding of the bacterial activity in the MFC environment. qPCR characterization of the relative amounts of bacteria in the bulk solution and at the anode surface during different stages of growth could determine the differences in microbial community. Finally, to determine the extent of biofilm formation on the anode, which is characteristic of *G.*

sulfurreducens, scanning electron microscopy could be used to image the biofilm attached to the anode.

Once primer design is achieved, the nest steps would be to find an effective DNA extraction protocol that would work for both microbes. As a starting point from literature, the Wizard® Genomic DNA Purification Kit and the Fast DNA Spin Kit have been used to extract genomic DNA form *G. sulfurreducens* and *G. metallireducens* respectively (Moscoviz et al. 2017; Xinyu Zhang et al. 2013).

8.2 Coculture growth optimization

The power density produced by the coculture was significantly less than that produced by the best performing pure cultures of *P. shermanii* and *G. sulfurreducens*. Due to this outcome, an effort should be made to fully explore the potential of the cocatalyst by employing systematic trials that can eliminate possible flaws of the cocatalyst design. In hopes to improve cocatalyst growth and consumption of both glucose and acetate, characterization and analysis improvements to enable a more confident assessment of the cocatalyst will be outlined in this section.

8.2.1 Purity

To verify that the MFC contains only the prescribed microbial strains in both cocatalyst and pure trials, a purity test beyond anaerobic plating *P. shermanii* and microscopy should be implemented. In Chapter 6, glucose consumption by a contaminant was evident in the MFC trial in which *G. sulfurreducens* was grown on glucose. To identify this contaminant and also to ensure that other trials are

pure, DNA sequencing could be employed to serve both of these purposes. Producing evidence of purity and also identifying any contaminants that are present would offer insight into whether exogenous microbes are causing any significant effect on the overall power generation.

8.2.2 Metabolite concentration

Despite the confirmation of sufficient acetate concentrations in the *P. shermanii* MFC trial, the observed variability characteristic of anaerobic *P. shermanii* growth contributed to some uncertainty surrounding the acetate production rate of each individual *P. shermanii* culture. This uncertainty was amplified since the HPLC apparatus was not operational during experimentation of the two coculture trials. Adjusting the inoculation time based on the HPLC result and adjusting the HPLC method to improve peak resolution of certain compounds was therefore not possible at the time of experimentation. The cause of dissimilar growth observed in the two coculture trials was also inconclusive due to the lack of bacterial growth information. To account for these uncertainties, acetate concentrations should be monitored during operation of each fuel cell, which could be achieved using a colorimetric acetate assay kit to provide timely results. This would ensure that *G. sulfurreducens* growth would not be limited by a lack of substrate at the time of inoculation. Timing of inoculation could also be adjusted according to the acetate concentration of each individual MFC. Furthermore, the consumption of acetate could continuously be observed throughout operation to allow the experiment to run based on substrate availability as opposed to terminating the experiment at a set time.

8.2.3 pH Analysis

A pH analysis could also provide insight into the growth thresholds for *P. shermanii* and *G. sulfurreducens*. While the consumption of glucose by *P. shermanii* strictly decreases the pH of the media resulting in an acidic environment, there is net proton consumption by *G. sulfurreducens* during acetate metabolism (Srinivasan and Mahadevan 2010). *G. sulfurreducens* therefore creates a more alkaline environment. This dynamic could be evaluated by conducting pH measurements throughout MFC operation of both pure and cocatalyst trials to visualize the effect that this syntropic relationship has on pH levels. This analysis could elucidate information regarding growth limits for both *P. shermanii* and *G. sulfurreducens* through observation of the relationship between pH level, substrate consumption and active growth.

The importance of pH monitoring was shown in an MFC study using *G. sulfurreducens* and *Clostridium cellulolyticum* as a cocatalyst whereby substrate consumption was inhibited by a drop in pH due to the accumulation of acidic fermentation products (Ren et al. 2007). With the addition of sterilized NaOH to an unproductive experiment at a pH of 5.2, the pH was increased to 7.0 and subsequently power production resumed (Ren et al. 2007). Once a full canvas of pH change during MFC operation is achieved, the need for additional buffering to increase substrate conversion in batch growth may be assessed.

8.2.4 Biofilm growth

Geobacter is well known for its biofilm formation as outlined in Chapter 2 therefore encouraging this phenomenon to occur in the MFC environment would be beneficial for power generation. Fe (III) can be used in pre-cultures of *G.*

sulfurreducens to encourage attachment to insoluble electron acceptors prior to inoculation to the fuel cell (Bond and Lovley 2003). Moreover, using a potentiostat to poise electrodes at +0.2 V versus an Ag/AgCl reference electrode has also been successful in encouraging biofilm formation in the MFC (Bond and Lovley 2003). The establishment of a robust biofilm of *Geobacter* would also allow for a continuous or self-cycling fermentation process to be considered in the future.

8.3 Use of *Geobacter metallireducens*

Upon initiation of this project, *G. metallireducens* was selected as the ideal cocatalyst for use with *P. shermanii* due to its ability to metabolize both acetate and propionate produced by *P. shermanii*. The proposed metabolism of propionate by *G. metallireducens* is shown in Figure 2-5 in Chapter 2.

From Figure 2-5, the consumption of propionate by *G. metallireducens* produces acetyl-coA and oxaloacetate, which are metabolites common to the Citric Acid Cycle (CAC). Since *P. shermanii* uses the same CAC pathway, these shared metabolites were likely also used by *P. shermanii* and would therefore result in an increase in electron production in the MFC. Based on the aforementioned propionate yields, it would be beneficial to investigate the use of *G. metallireducens* as its use could result in prolonged growth and power generation in the MFC. Additionally, the acetate consumption pathways also result in electron generation in addition to *G. metallireducens* cell growth in a similar fashion as *G. sulfurreducens.* However, an additional pathway that employs a acetyl-CoA synthetase reaction also exists and is unique to G. *metallireducens* (Aklujkar et al. 2009).

From Table 4-1 in Chapter 4, the yields of acetate and propionate demonstrate the potential to sustain the growth of *Geobacter* in a coculture fed with either glucose or glycerol as a substrate. Additionally, the propionate yields encourage and support the original proposal to employ *G. metallireducens* as the cocatalyst which would make use of both carbohydrate byproducts as opposed to *G. sulfurreducens* which is only able to metabolize acetate.

Chapter 9 Overall Conclusions

Performance of *P. shermanii* as a pure biocatalyst was improved using the air-cathode design. *G. sulfurreducens* grown on its preferred substrate of acetate produced the highest maximum power density of all experimental cases. The growth and power generating potential of the cocatalyst was confirmed in both fermentations and in the MFC. Specifically, the production of propionic acid, the characteristic appearance of a red culture in the fermentations and the increase in power generation following the addition of *G. sulfurreducens* in the MFC established the cocatalyst's viability. Gram staining in conjunction with microscopy was shown to be an ineffective quantification method for this technology.

Preliminary successes demonstrating the presence of syntropic interactions and illuminating the extent that anaerobic growth variability has on the cocatalyst's proliferation suggest that further development of this novel cocatalyst should be pursued. Gaining a more in depth understanding of the microbial community using qPCR would help to reveal pertinent interactions between the two bacteria. qPCR would also provide insight into the quantitative evolution of the cocatalyst in the media and at the anode surface. Once qPCR characterization is completed, efforts to optimize the growth and power generation of the cocatalyst will then be possible. Specifically, the timing of inoculation and *Geobacter* biofilm growth both have great potential to increase power generation in the MFC. Finally, *G. metallireducens* should be employed as the cocatalyst using either glucose or glycerol as a substrate to harness the electrogenic potential of metabolizing both acetate and propionate.

Chapter 10 References

Ahn, Youngho, and Bruce E. Logan. 2010. "Effectiveness of Domestic Wastewater Treatment Using Microbial Fuel Cells at Ambient and Mesophilic Temperatures." *Bioresource Technology* 101 (2): 469–475. https://doi.org/10.1016/j.biortech.2009.07.039.

Aklujkar, Muktak, Julia Krushkal, Genevieve DiBartolo, Alla Lapidus, Miriam L Land, and Derek R Lovley. 2009. "The Genome Sequence of Geobacter Metallireducens: Features of Metabolism, Physiology and Regulation Common and Dissimilar to Geobacter Sulfurreducens." *BMC Microbiology* 9 (1): 109. https://doi.org/10.1186/1471-2180-9-109.

Akob, D. M., H. J. Mills, T. M. Gihring, L. Kerkhof, J. W. Stucki, A. S. Anastacio, K.-J. Chin, et al. 2008. "Functional Diversity and Electron Donor Dependence of Microbial Populations Capable of U(VI) Reduction in Radionuclide-Contaminated Subsurface Sediments." *Applied and Environmental Microbiology* 74 (10): 3159–70. https://doi.org/10.1128/AEM.02881-07.

Althor, Glenn, James E. M. Watson, and Richard A. Fuller. 2016. "Global Mismatch between Greenhouse Gas Emissions and the Burden of Climate Change." *Scientific Reports* 6 (1). https://doi.org/10.1038/srep20281.

Alves, Mónica N., Ana P. Fernandes, Carlos A. Salgueiro, and Catarina M. Paquete. 2016. "Unraveling the Electron Transfer Processes of a Nanowire Protein from Geobacter Sulfurreducens." *Biochimica et Biophysica Acta (BBA) - Bioenergetics* 1857 (1): 7–13. https://doi.org/10.1016/j.bbabio.2015.09.010.

Bader, J., E. Mast-Gerlach, M.K. Popović, R. Bajpai, and U. Stahl. 2010. "Relevance of Microbial Coculture Fermentations in Biotechnology: Coculture Fermentations in Biotechnology." *Journal of Applied Microbiology* 109 (2): 371–87. https://doi.org/10.1111/j.1365-2672.2009.04659.x.

Biosciences, BD. 2018. "Animal Origin Peptones - BD Bionutrients Technical Manual." BD Biosciences. http://www.bdbiosciences.com/us/cell-culture/media-supplements/media-supplements/ao-animal-origin/bovine/trypticase-peptone/p/211921.

Bond, D. R. 2002. "Electrode-Reducing Microorganisms That Harvest Energy from Marine Sediments." *Science* 295 (5554): 483–85. https://doi.org/10.1126/science.1066771.

Bond, D. R., and D. R. Lovley. 2003. "Electricity Production by Geobacter Sulfurreducens Attached to Electrodes." *Applied and Environmental*

Microbiology 69 (3): 1548–55. https://doi.org/10.1128/AEM.69.3.1548-1555.2003.

Bond, Daniel R., Sarah M. Strycharz-Glaven, Leonard M. Tender, and César I. Torres. 2012. "On Electron Transport through Geobacter Biofilms." *ChemSusChem* 5 (6): 1099–1105. https://doi.org/10.1002/cssc.201100748.

Bourdakos, Nicholas, Enrico Marsili, and Radhakrishnan Mahadevan. 2014. "A Defined Co-Culture of Geobacter Sulfurreducens and Escherichia Coli in a Membrane-Less Microbial Fuel Cell." *Biotechnology and Bioengineering* 111 (4): 709–718.

Brendehaug, J., and T. Langsrud. 1985. "Amino Acid Metabolism in Propionibacteria: Resting Cells Experiments with Four Strains." *Journal of Dairy Science* 68 (2): 281–89. https://doi.org/10.3168/jds.S0022-0302(85)80823-7.

Champigneux, Pierre, Cyril Renault-Sentenac, David Bourrier, Carole Rossi, Marie-Line Delia, and Alain Bergel. 2018. "Effect of Surface Nano/Micro-Structuring on the Early Formation of Microbial Anodes with Geobacter Sulfurreducens : Experimental and Theoretical Approaches." *Bioelectrochemistry* 121 (June): 191–200. https://doi.org/10.1016/j.bioelechem.2018.02.005.

Dong, Heng, Hongbing Yu, Xin Wang, Qixing Zhou, and Junli Feng. 2012. "A Novel Structure of Scalable Air-Cathode without Nafion and Pt by Rolling Activated Carbon and PTFE as Catalyst Layer in Microbial Fuel Cells." *Water Research* 46 (17): 5777–87. https://doi.org/10.1016/j.watres.2012.08.005.

Dong, Kun, Boyang Jia, Chaoling Yu, Wenbo Dong, Fangzhou Du, and Hong Liu. 2013. "Microbial Fuel Cell as Power Supply for Implantable Medical Devices: A Novel Configuration Design for Simulating Colonic Environment." *Biosensors and Bioelectronics* 41 (March): 916–19. https://doi.org/10.1016/j.bios.2012.10.028.

Edwards, P.P., V.L. Kuznetsov, W.I.F. David, and N.P. Brandon. 2008. "Hydrogen and Fuel Cells: Towards a Sustainable Energy Future." *Energy Policy* 36 (12): 4356–62. https://doi.org/10.1016/j.enpol.2008.09.036.

Ehsani, Mehrdad, Yimin Gao, Stefano Longo, and Kambiz Ebrahimi. 2018. *Modern Electric, Hybrid Electric, and Fuel Cell Vehicles: Fundamentals, Theory, and Design*. http://public.ebookcentral.proquest.com/choice/publicfullrecord.aspx?p=5264494.

Feng, Yujie, Xin Wang, Bruce E. Logan, and He Lee. 2008. "Brewery Wastewater Treatment Using Air-Cathode Microbial Fuel Cells." *Applied Microbiology*

and Biotechnology 78 (5): 873–880. https://doi.org/10.1007/s00253-008-1360-2.

Galushko, Alexander S., and Bernhard Schink. 2000. "Oxidation of Acetate through Reactions of the Citric Acid Cycle by Geobacter Sulfurreducens in Pure Culture and in Syntrophic Coculture." *Archives of Microbiology* 174 (5): 314–21. https://doi.org/10.1007/s002030000208.

Goers, L., P. Freemont, and K. M. Polizzi. 2014. "Co-Culture Systems and Technologies: Taking Synthetic Biology to the next Level." *Journal of The Royal Society Interface* 11 (96): 20140065–20140065. https://doi.org/10.1098/rsif.2014.0065.

Gonzalez-Garcia, R., Tim McCubbin, Laura Navone, Chris Stowers, Lars Nielsen, and Esteban Marcellin. 2017. "Microbial Propionic Acid Production." *Fermentation* 3 (2): 21. https://doi.org/10.3390/fermentation3020021.

He, Weihua, Wulin Yang, Yushi Tian, Xiuping Zhu, Jia Liu, Yujie Feng, and Bruce E. Logan. 2016. "Pressurized Air Cathodes for Enhanced Stability and Power Generation by Microbial Fuel Cells." *Journal of Power Sources* 332 (November): 447–53. https://doi.org/10.1016/j.jpowsour.2016.09.112.

Hettinga, D. H., and G. W. Reinbold. 1972. "The Propionic Acid Bacteria - A Review" 35 (November).

Hu, Jianjun, Quanguo Zhang, Duu-Jong Lee, and Huu Hao Ngo. 2018. "Feasible Use of Microbial Fuel Cells for Pollution Treatment." *Renewable Energy* 129 (December): 824–29. https://doi.org/10.1016/j.renene.2017.02.001.

Huang, Liping, and Bruce E. Logan. 2008. "Electricity Generation and Treatment of Paper Recycling Wastewater Using a Microbial Fuel Cell." *Applied Microbiology and Biotechnology* 80 (2): 349–355. https://doi.org/10.1007/s00253-008-1546-7.

Javed, Muhammad Mohsin, Muhammad Azhar Nisar, Muhammad Usman Ahmad, Nighat Yasmeen, and Sana Zahoor. 2018. "Microbial Fuel Cells as an Alternative Energy Source: Current Status." *Biotechnology and Genetic Engineering Reviews*, June, 1–27. https://doi.org/10.1080/02648725.2018.1482108.

Kim, Mi-Sun, and Yu-jin Lee. 2010. "Optimization of Culture Conditions and Electricity Generation Using Geobacter Sulfurreducens in a Dual-Chambered Microbial Fuel-Cell." *International Journal of Hydrogen Energy* 35 (23): 13028–34. https://doi.org/10.1016/j.ijhydene.2010.04.061.

Kotloski, N. J., and J. A. Gralnick. 2013. "Flavin Electron Shuttles Dominate Extracellular Electron Transfer by Shewanella Oneidensis." *MBio* 4 (1): e00553-12-e00553-12. https://doi.org/10.1128/mBio.00553-12.

Kouzuma, Atsushi, Souichiro Kato, and Kazuya Watanabe. 2015. "Microbial Interspecies Interactions: Recent Findings in Syntrophic Consortia." *Frontiers in Microbiology* 6 (May). https://doi.org/10.3389/fmicb.2015.00477.

Kumar, Ravinder, Lakhveer Singh, and A.W. Zularisam. 2016. "Exoelectrogens: Recent Advances in Molecular Drivers Involved in Extracellular Electron Transfer and Strategies Used to Improve It for Microbial Fuel Cell Applications." *Renewable and Sustainable Energy Reviews* 56 (April): 1322–36. https://doi.org/10.1016/j.rser.2015.12.029.

Li, Wen-Wei, and Guo-Ping Sheng. 2011. "Microbial Fuel Cells in Power Generation and Extended Applications." In *Biotechnology in China III: Biofuels and Bioenergy*, edited by Feng-Wu Bai, Chen-Guang Liu, He Huang, and George T Tsao, 128:165–197. Berlin, Heidelberg: Springer Berlin Heidelberg. http://link.springer.com/10.1007/10_2011_125.

Lin, W. C., M. V. Coppi, and D. R. Lovley. 2004. "Geobacter Sulfurreducens Can Grow with Oxygen as a Terminal Electron Acceptor." *Applied and Environmental Microbiology* 70 (4): 2525–28. https://doi.org/10.1128/AEM.70.4.2525-2528.2004.

Liu, Hong, and Bruce E. Logan. 2004. "Electricity Generation Using an Air-Cathode Single Chamber Microbial Fuel Cell in the Presence and Absence of a Proton Exchange Membrane." *Environmental Science & Technology* 38 (14): 4040–46. https://doi.org/10.1021/es0499344.

Logan, Bruce E. 2008. *Microbial Fuel Cells*. John Wiley & Sons.

Logan, Bruce E., Bert Hamelers, René Rozendal, Uwe Schröder, Jürg Keller, Stefano Freguia, Peter Aelterman, Willy Verstraete, and Korneel Rabaey. 2006. "Microbial Fuel Cells: Methodology and Technology." *Environmental Science & Technology* 40 (17): 5181–5192.

Loginova, L. I., V. P. Manuilova, and V. P. Tolstikov. 1974. "Content of Free Amino Acids in Peptone and the Dynamics of Their Consumption in the Microbiological Synthesis of Dextran." *Pharmaceutical Chemistry Journal* 8 (4): 249–51. https://doi.org/10.1007/BF00777001.

Lovley, Derek R., Toshiyuki Ueki, Tian Zhang, Nikhil S. Malvankar, Pravin M. Shrestha, Kelly A. Flanagan, Muktak Aklujkar, et al. 2011. "Geobacter." In *Advances in Microbial Physiology*, 59:1–100. Elsevier. https://doi.org/10.1016/B978-0-12-387661-4.00004-5.

Malvankar, Nikhil S., and Derek R. Lovley. 2012. "Microbial Nanowires: A New Paradigm for Biological Electron Transfer and Bioelectronics." *ChemSusChem* 5 (6): 1039–46. https://doi.org/10.1002/cssc.201100733.

Malvankar, Nikhil S., Sibel Ebru Yalcin, Mark T. Tuominen, and Derek R. Lovley. 2014. "Visualization of Charge Propagation along Individual Pili Proteins

Using Ambient Electrostatic Force Microscopy." *Nature Nanotechnology* 9 (12): 1012–17. https://doi.org/10.1038/nnano.2014.236.
Mansoorian, Hossein Jafari, Amir Hossein Mahvi, Ahmad Jonidi Jafari, and Narges Khanjani. 2016. "Evaluation of Dairy Industry Wastewater Treatment and Simultaneous Bioelectricity Generation in a Catalyst-Less and Mediator-Less Membrane Microbial Fuel Cell." *Journal of Saudi Chemical Society* 20 (1): 88–100. https://doi.org/10.1016/j.jscs.2014.08.002.
Mehdinia, Ali, Minodokht Dejaloud, and Ali Jabbari. 2013. "Nanostructured Polyaniline-Coated Anode for Improving Microbial Fuel Cell Power Output." *Chemical Papers* 67 (8). https://doi.org/10.2478/s11696-013-0381-1.
Min, Booki, Shaoan Cheng, and Bruce E. Logan. 2005. "Electricity Generation Using Membrane and Salt Bridge Microbial Fuel Cells." *Water Research* 39 (9): 1675–86. https://doi.org/10.1016/j.watres.2005.02.002.
Moscoviz, Roman, Florence de Fouchécour, Gaëlle Santa-Catalina, Nicolas Bernet, and Eric Trably. 2017. "Cooperative Growth of Geobacter Sulfurreducens and Clostridium Pasteurianum with Subsequent Metabolic Shift in Glycerol Fermentation." *Scientific Reports* 7 (March): 44334. https://doi.org/10.1038/srep44334.
Oh, SangEun, Booki Min, and Bruce E. Logan. 2004. "Cathode Performance as a Factor in Electricity Generation in Microbial Fuel Cells." *Environmental Science & Technology* 38 (18): 4900–4904. https://doi.org/10.1021/es049422p.
Okamoto, Akihiro, Koichiro Saito, Kengo Inoue, Kenneth H. Nealson, Kazuhito Hashimoto, and Ryuhei Nakamura. 2014. "Uptake of Self-Secreted Flavins as Bound Cofactors for Extracellular Electron Transfer in *Geobacter* Species." *Energy Environ. Sci.* 7 (4): 1357–61. https://doi.org/10.1039/C3EE43674H.
Pant, Deepak, Gilbert Van Bogaert, Ludo Diels, and Karolien Vanbroekhoven. 2010. "A Review of the Substrates Used in Microbial Fuel Cells (MFCs) for Sustainable Energy Production." *Bioresource Technology* 101 (6): 1533–43. https://doi.org/10.1016/j.biortech.2009.10.017.
Pasternak, Grzegorz, John Greenman, and Ioannis Ieropoulos. 2016. "Regeneration of the Power Performance of Cathodes Affected by Biofouling." *Applied Energy* 173 (July): 431–37. https://doi.org/10.1016/j.apenergy.2016.04.009.
Piveteau, Pascal. 1999. "Metabolism of Lactate and Sugars by Dairy Propionibacteria: A Review." *Le Lait* 79 (1): 23–41.
Prokhorova, Anna, Katrin Sturm-Richter, Andreas Doetsch, and Johannes Gescher. 2017. "Resilience, Dynamics, and Interactions within a Model Multispecies Exoelectrogenic-Biofilm Community." Edited by Hideaki

Nojiri. *Applied and Environmental Microbiology* 83 (6): e03033-16. https://doi.org/10.1128/AEM.03033-16.
Qu, Youpeng, Yujie Feng, Xin Wang, and Bruce E. Logan. 2012. "Use of a Coculture To Enable Current Production by Geobacter Sulfurreducens." *Applied and Environmental Microbiology* 78 (9): 3484–87. https://doi.org/10.1128/AEM.00073-12.
Reguera, Gemma, Kevin D. McCarthy, Teena Mehta, Julie S. Nicoll, Mark T. Tuominen, and Derek R. Lovley. 2005. "Extracellular Electron Transfer via Microbial Nanowires." *Nature* 435 (7045): 1098–1101. https://doi.org/10.1038/nature03661.
Rehberger, Jill Louise. 1996. "Response of Propionibacterium to Acid and Low PH: Tolerance and Inhibition." http://lib.dr.iastate.edu/rtd/11395/.
Reiche, Alison. 2012. "Biocatalyst Selection for a Glycerol-Oxidizing Microbial Fuel Cell." University of Ottawa. http://www.ruor.uottawa.ca/handle/10393/22764.
Reiche, Alison, Jamie-lynn Sivell, and Kathlyn M. Kirkwood. 2015. "Electricity Generation by Propionibacterium Freudenreichii in a Mediatorless Microbial Fuel Cell." *Biotechnology Letters*, August. https://doi.org/10.1007/s10529-015-1944-8.
Ren, Zhiyong, Thomas E. Ward, and John M. Regan. 2007. "Electricity Production from Cellulose in a Microbial Fuel Cell Using a Defined Binary Culture." *Environmental Science & Technology* 41 (13): 4781–86. https://doi.org/10.1021/es070577h.
Sambrook, J., E. F. Fritsch, and T. Maniatis. 1989. *Molecular Cloning: A Laboratory Manual.* Cold Spring Harbor, NY: Cold Spring Harbor Laboratory Press.
Santoro, Carlo, Catia Arbizzani, Benjamin Erable, and Ioannis Ieropoulos. 2017. "Microbial Fuel Cells: From Fundamentals to Applications. A Review." *Journal of Power Sources* 356 (July): 225–44. https://doi.org/10.1016/j.jpowsour.2017.03.109.
Santoro, Carlo, Alexey Serov, Claudia W. Narvaez Villarrubia, Sarah Stariha, Sofia Babanova, Andrew J. Schuler, Kateryna Artyushkova, and Plamen Atanassov. 2015. "Double-Chamber Microbial Fuel Cell with a Non-Platinum-Group Metal Fe-N-C Cathode Catalyst." *ChemSusChem* 8 (5): 828–34. https://doi.org/10.1002/cssc.201402570.
Schröder, Uwe. 2007. "Anodic Electron Transfer Mechanisms in Microbial Fuel Cells and Their Energy Efficiency." *Phys. Chem. Chem. Phys.* 9 (21): 2619–29. https://doi.org/10.1039/B703627M.
Sherafatmand, Mohammad, and How Yong Ng. 2015. "Using Sediment Microbial Fuel Cells (SMFCs) for Bioremediation of Polycyclic Aromatic

Hydrocarbons (PAHs)." *Bioresource Technology* 195 (November): 122–130. https://doi.org/10.1016/j.biortech.2015.06.002.

Shrestha, Pravin Malla, Amelia-Elena Rotaru, Zarath M. Summers, Minita Shrestha, Fanghua Liu, and Derek R. Lovley. 2013. "Transcriptomic and Genetic Analysis of Direct Interspecies Electron Transfer." *Applied and Environmental Microbiology* 79 (7): 2397–2404. https://doi.org/10.1128/AEM.03837-12.

Sivell, Jamie-lynn. 2014. "Effect of Crude Glycerol from Biodiesel Production on the Performance and Anaerobic Metabolism of Catalysts in a Glycerol Oxidizing Microbial Fuel Cell." University of Ottawa. https://www.ruor.uottawa.ca/handle/10393/30919.

Snider, R. M., S. M. Strycharz-Glaven, S. D. Tsoi, J. S. Erickson, and L. M. Tender. 2012. "Long-Range Electron Transport in Geobacter Sulfurreducens Biofilms Is Redox Gradient-Driven." *Proceedings of the National Academy of Sciences* 109 (38): 15467–72. https://doi.org/10.1073/pnas.1209829109.

Speers, Allison M., and Gemma Reguera. 2012. "Electron Donors Supporting Growth and Electroactivity of Geobacter Sulfurreducens Anode Biofilms." *Applied and Environmental Microbiology* 78 (2): 437–44. https://doi.org/10.1128/AEM.06782-11.

Srinivasan, Karthikeyan, and Radhakrishnan Mahadevan. 2010. "Characterization of Proton Production and Consumption Associated with Microbial Metabolism." *BMC Biotechnology* 10 (1): 2. https://doi.org/10.1186/1472-6750-10-2.

Sun, Dan, Jie Chen, Haobin Huang, Weifeng Liu, Yaoli Ye, and Shaoan Cheng. 2016. "The Effect of Biofilm Thickness on Electrochemical Activity of Geobacter Sulfurreducens." *International Journal of Hydrogen Energy* 41 (37): 16523–28. https://doi.org/10.1016/j.ijhydene.2016.04.163.

Sund, Christian J., Sun McMasters, Scott R. Crittenden, Lee E. Harrell, and James J. Sumner. 2007. "Effect of Electron Mediators on Current Generation and Fermentation in a Microbial Fuel Cell." *Applied Microbiology and Biotechnology* 76 (3): 561–68. https://doi.org/10.1007/s00253-007-1038-1.

Tan, Yang, Ramesh Y. Adhikari, Nikhil S. Malvankar, Joy E. Ward, Trevor L. Woodard, Kelly P. Nevin, and Derek R. Lovley. 2017. "Expressing the *Geobacter Metallireducens* PilA in *Geobacter Sulfurreducens* Yields Pili with Exceptional Conductivity." Edited by Eleftherios T. Papoutsakis. *MBio* 8 (1): e02203-16. https://doi.org/10.1128/mBio.02203-16.

Thierry, Anne, Stéphanie-Marie Deutsch, Hélène Falentin, Marion Dalmasso, Fabien J. Cousin, and Gwenaël Jan. 2011. "New Insights into Physiology and Metabolism of Propionibacterium Freudenreichii." *International*

Journal of Food Microbiology 149 (1): 19–27. https://doi.org/10.1016/j.ijfoodmicro.2011.04.026.

Wang, Haiman, Youpeng Qu, Da Li, John J. Ambuchi, Weihua He, Xiangtong Zhou, Jia Liu, and Yujie Feng. 2016. "Cascade Degradation of Organic Matters in Brewery Wastewater Using a Continuous Stirred Microbial Electrochemical Reactor and Analysis of Microbial Communities." *Scientific Reports* 6 (1). https://doi.org/10.1038/srep27023.

Wang, Yung-Fu, Masaki Masuda, Seiya Tsujimura, and Kenji Kano. 2008. "Electrochemical Regulation of the End-Product Profile in *Propionibacterium Freudenreichii* ET-3 with an Endogenous Mediator." *Biotechnology and Bioengineering* 101 (3): 579–86. https://doi.org/10.1002/bit.21914.

Wang, Zhongqiang, and Shang-Tian Yang. 2013. "Propionic Acid Production in Glycerol/Glucose Co-Fermentation by Propionibacterium Freudenreichii Subsp. Shermanii." *Bioresource Technology* 137 (June): 116–23. https://doi.org/10.1016/j.biortech.2013.03.012.

Yang, Huijia, Minghua Zhou, Mengmeng Liu, Weilu Yang, and Tingyue Gu. 2015. "Microbial Fuel Cells for Biosensor Applications." *Biotechnology Letters* 37 (12): 2357–64. https://doi.org/10.1007/s10529-015-1929-7.

Yang, Tae Hoon, Maddalena V Coppi, Derek R Lovley, and Jun Sun. 2010. "Metabolic Response of Geobacter Sulfurreducens towards Electron Donor/Acceptor Variation." *Microbial Cell Factories* 9 (1): 90. https://doi.org/10.1186/1475-2859-9-90.

Yazdani, Syed Shams, and Ramon Gonzalez. 2007. "Anaerobic Fermentation of Glycerol: A Path to Economic Viability for the Biofuels Industry." *Current Opinion in Biotechnology* 18 (3): 213–19. https://doi.org/10.1016/j.copbio.2007.05.002.

Zhang, An, and Shang-Tian Yang. 2009. "Engineering *Propionibacterium Acidipropionici* for Enhanced Propionic Acid Tolerance and Fermentation." *Biotechnology and Bioengineering*, n/a-n/a. https://doi.org/10.1002/bit.22437.

Zhang, Xiaoyuan, Weihua He, Lijiao Ren, Jennifer Stager, Patrick J. Evans, and Bruce E. Logan. 2015. "COD Removal Characteristics in Air-Cathode Microbial Fuel Cells." *Bioresource Technology* 176 (January): 23–31. https://doi.org/10.1016/j.biortech.2014.11.001.

Zhang, Xinyu, Xiaofeng Ye, Kevin T. Finneran, Julie L. Zilles, and Eberhard Morgenroth. 2013. "Interactions between Clostridium Beijerinckii and Geobacter Metallireducens in Co-Culture Fermentation with Anthrahydroquinone-2, 6-Disulfonate (AH2QDS) for Enhanced Biohydrogen Production from Xylose." *Biotechnology and Bioengineering* 110 (1): 164–172.

Zhao, Feng, Robert C. T. Slade, and John R. Varcoe. 2009. "Techniques for the Study and Development of Microbial Fuel Cells: An Electrochemical Perspective." *Chemical Society Reviews* 38 (7): 1926. https://doi.org/10.1039/b819866g.

Zhou, Tuoyu, Huawen Han, Pu Liu, Jian Xiong, Fake Tian, and Xiangkai Li. 2017. "Microbial Fuels Cell-Based Biosensor for Toxicity Detection: A Review." *Sensors* 17 (10): 2230. https://doi.org/10.3390/s17102230.

Zielke, Eric A. n.d. "Thermodynamic Analysis of a Single Chamber Microbial Fuel Cell," 21.

Appendix A: Calculations

Glucose conversion (C_g)

Glucose conversion was calculated at the end of the fermentation time (f) unless otherwise specified.

$$C_g = g_0 - g_f \quad \textbf{Equation 9}$$

where, C_g is the glucose conversion in g/L

g_0 is the initial glucose concentration

g_f is the final glucose concentration

Product yield

The yield of fermentation products based on the amount of substrate consumed was calculated to normalize metabolic activity to substrate consumption.

$$y_{p/g} = \frac{p_2 - p_1}{g_2 - g_1} \quad \textbf{Equation 10}$$

Acetate threshold

The acetate threshold needed to support *G. sulfurreducens* growth in the coculture was based on *G. sulfurreducens*' ability to consume 20mM acetate in 60 h (Galushko and Schink 2000). *G. sulfurreducens* inoculation time was determined where *P. shermanii* had produced approximately 1.18 g/L acetate in the MFC.

$$0.02\ \frac{mol\ acetate}{L} \times 59.04 \frac{g\ acetate}{mol} = 1.18\ \frac{g\ acetate}{L}$$

MFC Calculations

Polarization and Power density

Polarization curves were generated using a potentiostat for each MFC. Potential was recorded as a function of current and this data was normalized using the surface area of the anode to find current density using Equation 11.

$$I_{An} = \frac{I}{A_{An}} \quad \textbf{Equation 11}$$

where,

I_{An} is the current density (mA/m^2)

I is the current (mA)

A_{An} is the area of the anode (m^2)

Power density was then calculated from each data point generated for the polarization curve using Equation 12.

$$P_{An} = \frac{IE}{A_{An}}\ 1000 \quad \textbf{Equation 12}$$

where, P_{An} is the power density in units of $mW\ m^{-2}$

E is the cell potential (V)

I is the current (A)

A_{An} is the anode surface area in units of m^2

Internal Resistance

Internal resistance is characterized by the portion of a polarization curve exhibiting a linear slope. The internal resistance was determined from the polarization curve attained by identifying data points encompassed in the slope

of the linear region. Equation 13 was the used to find the internal resistance value.

$$R_{int} = \frac{E_1 - E_2}{I_1 - I_2} \qquad \textbf{Equation 13}$$

R_{int} is the internal resistance of the MFC (Ω)

E_1 and I_1 are the potential (V) and current (A) of the first data point encompassed in the linear region of the polarization curve

E_2 and I_2 are the potential (V) and current (A) of the last data point encompassed in the linear region of the polarization curve

Electrochemical Efficiency (η)

The electrochemical efficiency (η) is determined using the theoretical maximum open circuit voltage (E°). The Gibbs energy for the reaction (G) must first be calculated.

Glucose oxidation

The overall fuel cell reaction assuming that all glucose is converted to carbon dioxide is:

$$C_6H_{12}O_6 + 6O_2 \rightarrow 6CO_2 + 6H_2O$$

G is calculated using standard enthalpies of formation (H_f^0) and entropies of formation (S_f^0) and accounting for the operating temperature of the fuel cell (T) of 30C or 303 K.

$$G_i = H_f^0 - T \times S_f^0 \quad \textbf{Equation 14}$$

For glucose: H_f^0 = - 1273.3 kJ/mol; S_f^0 = 212.1 J/molK

For carbon dioxide: H_f^0 = - 393.5 kJ/mol; S_f^0 = 213.6 J/molK

For water: H_f^0 = - 285.8 kJ/mol; S_f^0 = 69.9 J/molK

$$G° = \sum G_{products} - \sum G_{reactants} \quad \textbf{Equation 15}$$

Acetate oxidation

The overall fuel cell reaction assuming that all acetate is converted to carbon dioxide is:

$$CHCOO^- + 4CHO^{2-} + 2HO + H^+ \rightarrow 2CO + 4CHO^{2-}$$

From literature, $G°$ was found to be -249 kJ per mol acetate.

The theoretical maximum efficiency can then be calculated using Equation 16.

$$E^0 = \frac{-G°}{nF} \quad \textbf{Equation 16}$$

where,

n = 24 based on the number of electrons released from the complete oxidation of glucose to carbon dioxide.

Finally, electrochemical efficiency can be calculated using the experimental OCP and the theoretical maximum efficiency.

$$\eta = \frac{OCP}{E^0} \quad \textbf{Equation 17}$$

Appendix B: Standard Curves

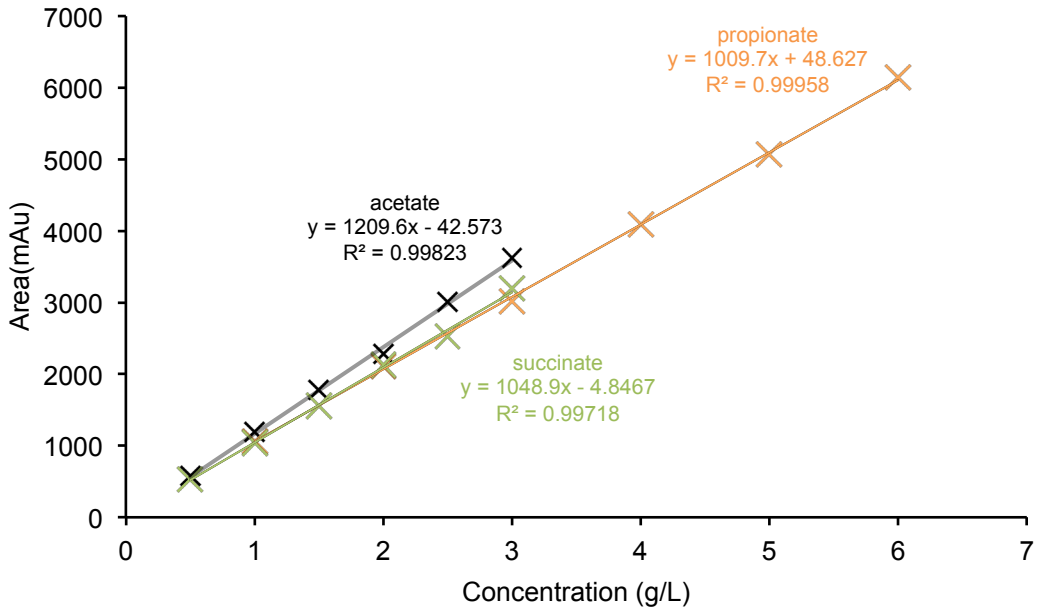

Figure 0-1 Standard curves for the quantification of metabolites by HPLC in Dr. Kirkwood lab.

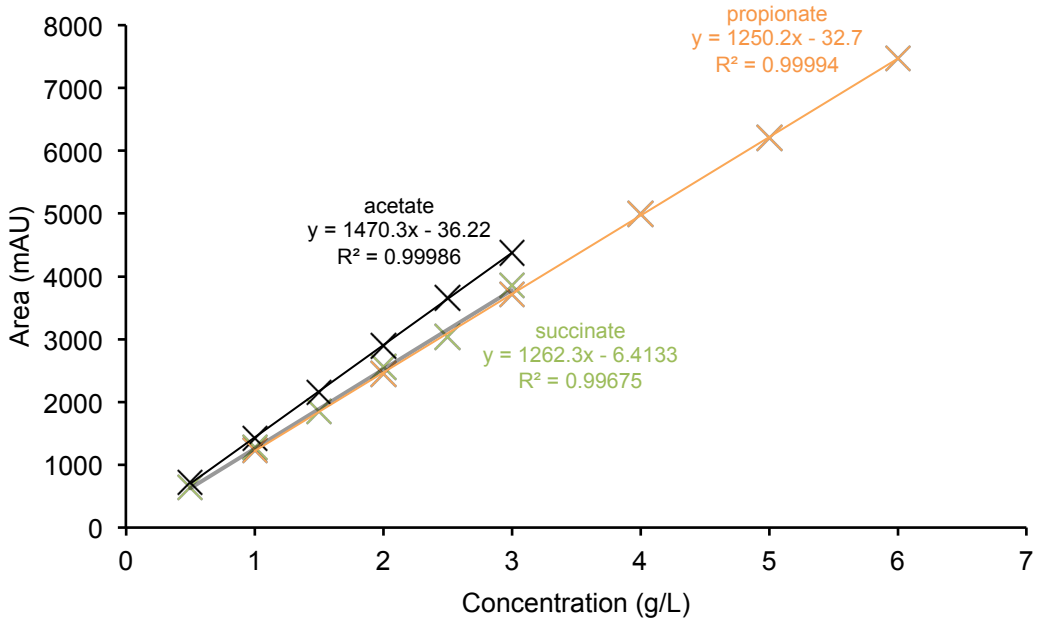

Figure 0-2 Standard curves for the quantification of metabolites by HPLC in Dr. Zhang lab.

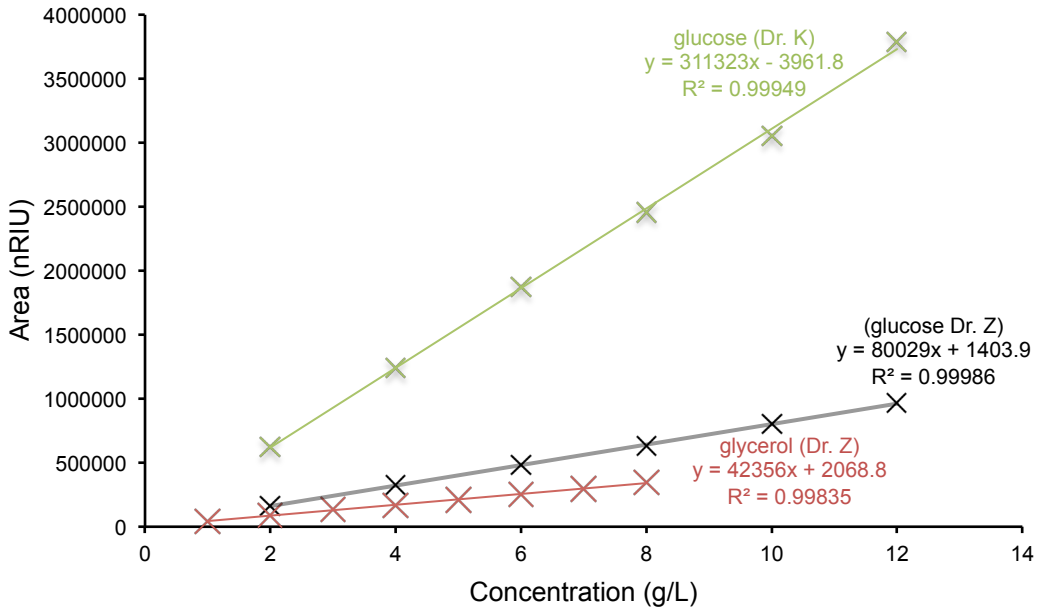

Figure 0-3 Standard curves for the quantification of glucose and glycerol by HPLC in Dr. Kirkwood lab and Dr. Zhang lab.